A THEORETICAL AND EXPERIMENTAL INVESTIGATION OF THE PARAMETRIC ACOUSTIC RECEIVING ARRAY

James J. Truchard

Texas University

Prepared for:

Naval Sea Systems Command

May 1974

UNCLASSIFIED

SECURITY CLASSIFICATION OF THIS PAGE (When Data Entered)

REPORT DOCUMENTATION PAGE

READ INSTRUCTIONS BEFORE COMPLETING FORM

1. REPORT NUMBER: ARL-TR-74-17	2. GOVT ACCESSION NO.
3. RECIPIENT'S CATALOG NUMBER: AD-783099	
4. TITLE (and Subtitle): A THEORETICAL AND EXPERIMENTAL INVESTIGATION OF THE PARAMETRIC ACOUSTIC RECEIVING ARRAY	5. TYPE OF REPORT & PERIOD COVERED: technical report
	6. PERFORMING ORG. REPORT NUMBER
7. AUTHOR(s): James J. Truchard	8. CONTRACT OR GRANT NUMBER(s): N00024-73-C-1127
9. PERFORMING ORGANIZATION NAME AND ADDRESS: Applied Research Laboratories, The University of Texas at Austin, Austin, Texas 78712	10. PROGRAM ELEMENT, PROJECT, TASK AREA & WORK UNIT NUMBERS
11. CONTROLLING OFFICE NAME AND ADDRESS: Naval Sea Systems Command, Department of the Navy, Washington, D. C. 20362	12. REPORT DATE: May 1974
	13. NUMBER OF PAGES: 149
14. MONITORING AGENCY NAME & ADDRESS(if different from Controlling Office): ---	15. SECURITY CLASS. (of this report): UNCLASSIFIED
	15a. DECLASSIFICATION/DOWNGRADING SCHEDULE: ---

16. DISTRIBUTION STATEMENT (of this Report)

Approved for public release; distribution unlimited.

17. DISTRIBUTION STATEMENT (of the abstract entered in Block 20, if different from Report)

---

18. SUPPLEMENTARY NOTES

---

19. KEY WORDS (Continue on reverse side if necessary and identify by block number)

Parametric Reception
Nonlinear Acoustics
Second-Order Wave Equation
Beam patterns
Computer Program

20. ABSTRACT (Continue on reverse side if necessary and identify by block number)

The parametric reception of a low frequency plane wave by the use of nonlinear interactions between acoustic waves is examined both theoretically and experimentally. The parametric reception of a low frequency wave is accomplished by the use of a high frequency acoustic pump wave which interacts with the low frequency signal wave to produce sound waves at the sum and difference frequencies. These sound waves are received by a second transducer placed on the axis of the pump transducer. This type of parametric array allows for the

DD FORM 1 JAN 73 1473 EDITION OF 1 NOV 65 IS OBSOLETE S/N 0102-014-6601

UNCLASSIFIED

SECURITY CLASSIFICATION OF THIS PAGE (When Data Entered)

20.

possibility of narrowbeam detection of a low frequency acoustic signal wave.

The interaction of two plane waves is examined theoretically in a manner similar to that considered by Westervelt. Of particular interest is the case in which the pump wave is assumed to be a plane wave originating at and propagating perpendicular to some planar boundary. The low frequency signal wave is assumed to be present over all space. The interaction of two plane waves is of interest for two reasons.

(1) This interaction produces a truncated end-fire array (i.e., the parametric receiving array) with a length equal to the spacing between the planar boundary and the observer, and (2) this interaction relates directly to the problem of sound scattered by sound as formulated by Westervelt.

Next, the solution for the interaction of a high frequency spherical wave from a point source and a low frequency plane wave is obtained theoretically using a two-dimensional stationary phase solution of Westervelt's scattering integral. The point source solution is in turn used to generate the solution for parametric receiving arrays with various pump transducers including a truncated line source transducer, a rectangular piston transducer, and a circular piston transducer. In each case, the observer is assumed to be in the farfield of the pump transducer. However, the result includes the effects of interaction in the nearfield of the pump transducer. The solution of the parametric receiving array with a point source pump and a truncated line receiver is also found. The theoretical solutions also include the effects of misalignment of either the pump or receiving transducer. With either the pump transducer or the receiver misaligned, the difference frequency beam pattern is an asymmetrical beam pattern and is the mirror image of the sum frequency beam pattern. This property is examined in detail in terms of the problem of two sound waves interacting at nonzero angles.

A series of experiments were conducted with a 48 ft parametric receiving array with a pump frequency of 90 kHz. In the experiments, an omnidirectional transducer was used with either a rectangular piston transducer or a square piston transducer. Each transducer could be used as either the pump transducer or the receiver so that a variety of parametric receiving array configurations could be realized. A small rotator was used to allow independent rotation of the piston transducer for measurement of the effects of misalignment of the piston transducer. Theoretical and experimental results are compared for the parametric receiving array with several transducer arrangements. The agreement between the theory and the experiment was excellent.

ARL-TR-74-17
May 1974

A THEORETICAL AND EXPERIMENTAL INVESTIGATION OF THE PARAMETRIC ACOUSTIC RECEIVING ARRAY

James J. Truchard

NAVAL SEA SYSTEMS COMMAND
Contract N00024-73-C-1127

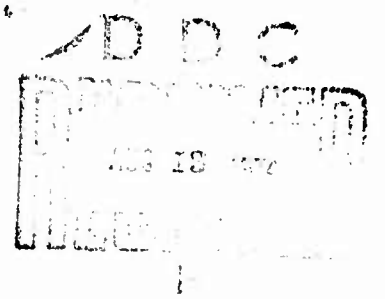

APPLIED RESEARCH LABORATORIES
THE UNIVERSITY OF TEXAS AT AUSTIN
AUSTIN, TEXAS 78712

ABSTRACT

The parametric reception of a low frequency plane wave by the use of nonlinear interactions between acoustic waves is examined both theoretically and experimentally. The parametric reception of a low frequency wave is accomplished by the use of a high frequency acoustic pump wave which interacts with the low frequency signal wave to produce sound waves at the sum and difference frequencies. These sound waves are received by a second transducer placed on the axis of the pump transducer. This type of parametric array allows for the possibility of narrowbeam detection of a low frequency acoustic signal wave.

The interaction of two plane waves is examined theoretically in a manner similar to that considered by Westervelt. Of particular interest is the case in which the pump wave is assumed to be a plane wave originating at and propagating perpendicular to some planar boundary. The low frequency signal wave is assumed to be present over all space. The interaction of two plane waves is of interest for two reasons.

(1) This interaction produces a truncated end-fire array (i.e., the parametric receiving array) with a length equal to the spacing between the planar boundary and the observer, and (2) this interaction relates directly to the problem of sound scattered by sound as formulated by Westervelt.

Next, the solution for the interaction of a high frequency spherical wave from a point source and a low frequency plane wave is obtained theoretically using a two-dimensional stationary phase solution

of Westervelt's scattering integral. The point source solution is in turn used to generate the solution for parametric receiving arrays with various pump transducers including a truncated line source transducer, a rectangular piston transducer, and a circular piston transducer. In each case, the observer is assumed to be in the farfield of the pump transducer. However, the result includes the effects of interaction in the nearfield of the pump transducer. The solution of the parametric receiving array with a point source pump and a truncated line receiver is also found. The theoretical solutions also include the effects of misalignment of either the pump or receiving transducer. With either the pump transducer or the receiver misaligned, the difference frequency beam pattern is an asymetrical beam pattern and is the mirror image of the sum frequency beam pattern. This property is examined in detail in terms of the problem of two sound waves interacting at nonzero angles.

A series of experiments were conducted with a 48 ft parametric receiving array with a pump frequency of 90 kHz. In the experiments, an omnidirectional transducer was used with either a rectangular piston transducer or a square piston transducer. Each transducer could be used as either the pump transducer or the receiver so that a variety of parametric receiving array configurations could be realized. A small rotator was used to allow independent rotation of the piston transducer for measurement of the effects of misalignment of the piston transducer. Theoretical and experimental results are compared for the parametric receiving array with several transducer arrangements. The agreement between the theory and the experiment was excellent.

TABLE OF CONTENTS

TABLE OF CONTENTS (Cont'd)

LIST OF FIGURES

LIST OF FIGURES (Cont'd)

LIST OF FIGURES (Cont'd)

LIST OF SYMBOLS

I. Latin Symbols

a 1/2 the length of a line transducer

a 1/2 the length of a rectangular aperture for a transducer

a radius of a circular piston transducer

A argument for the description of the angular response of the second-order sound field (Chapter IV)

b 1/2 the height of a rectangular aperture for a transducer

B argument for the description of the angular response of line receiver (Chapter IV)

c_o small signal sound speed

$g(\vec{r}|\vec{r}_o)$ freefield Green's Function

i $\sqrt{-1}$

$\vec{i}$ basis vector in the x direction

$\vec{j}$ basis vector in the y direction

$J_m(\cdot)$ Mth order Bessel Function with argument $(\cdot)$

k_1, k_2 the acoustic wave number, $\frac{2\Pi f_1}{c_o}$ and $\frac{2\Pi f_2}{c_o}$, respectively

$k_\pm$ wave number at the sum or difference frequency (the upper sign corresponds to the sum frequency and the lower sign corresponds to the difference frequency)

$\vec{k}$ basis vector in the z direction

ℓ distance from the center of a line source or receiver to an arbitrary point on the line source or receiver

C argument for the description of the angular response of the second-order sound field (Chapter IV)

C_i the cosine integral

D argument for the description of the angular response of a line receiver (Chapter IV)

D_{ij} components of the viscous stress tensor

E voltage from hydrophone in a parametric receiving array

F an auxiliary function for the description of the interaction of two plane sound waves

$F(\rho_T)$ functional relationship for pressure and density for an isentropic fluid

$F(\rho_T,S)$ functional relationship between pressure, density, and entropy

L separation distance between the two transducers for the parametric receiving array

M argument for the description of the angular response of a parametric receiving array

M_c receiving sensitivity for a hydrophone

p total acoustic pressure

p_o static or undisturbed pressure

p_1 first-order acoustic pressure

p_2 second-order acoustic pressure

P peak amplitude of a sinusoidal pressure

$\vec{r}$ vector from the origin to the point of interaction

$\vec{r}_o$ vector from the origin to the observer point

$\vec{\underline{r}}$ the vector $\vec{r}$ after rotation and translation into a new coordinate system

R distance from an element on a line transducer to an observer

S(y,z) slowly varying term in the integral and in a double integral

t time

$\bar{\underline{T}}$ a tensor

u particle velocity

x	x-axis coordinate
y	y-axis coordinate
z	z-axis coordinate

II. Greek Symbols

α	small signal attenuation coefficient
β	$1 + \frac{1}{2}\frac{B}{A}$
∇	differential operator
η	coefficient of bulk viscosity
λ	acoustic signal wavelength
μ	coefficient of shear viscosity
$\phi_{\pm}$	a solution to the homogeneous wave equation
ϕ	angle between pump axis and position vector of an observer
ρ_T	total density
ρ_o	static density
ρ_1	first-order density
ρ_2	second-order density
θ	angular coordinate of the direction of propagation of the low frequency signal
ω_1	angular frequency
$\omega_{\pm}$	angular frequency $\omega_1 \pm \omega_2$

I. INTRODUCTION

It is well known that a finite amplitude sound wave will distort as it propagates.[1-8] This nonlinear propagation or self-interaction occurs because the phase velocity is a function of the instantaneous amplitude of the particle velocity. It would also be expected that two sound waves of frequencies f_1 and f_2 present simultaneously in a medium would generate sum and difference frequencies, $f_1 \pm f_2$. A spurious difference frequency tone was observed by a German organist, Sorge, in 1745, and later in 1754 by an Italian violinist, Tartini.[9] These spurious frequency components have been known to musicians ever since and are referred to as "combination tones." In 1875, Helmholtz[10] predicted that a sum frequency tone should also exist. With the use of a Helmholtz resonator, Helmholtz showed that the difference frequency tone was generated by such instruments as the harmonium when two high frequency tones were played simultaneously. Helmholtz suggested that this tone was generated in the air within the instrument. On the other hand, the presence of two notes from a pipe organ had little effect on a resonator. In this case, Helmholtz concluded that the difference frequency was either subjective or generated within the ear. The existence of the sum frequency was a matter of debate until 1895 when Rücker and Edser[11] observed its effect on a tuning fork of the same frequency. Rayleigh[12] discussed the subject in his book The Theory of Sound in 1910. Lamb[13] used Airy's[2] method of successive approximations to demonstrate the existence of sum and difference frequency components. The existence of sum and difference frequency

components in the throat of a horn was considered by Rocard[14] in 1933 and by Thuras, Jenkins, and O'Neil[4] in 1935. Thuras, Jenkins, and O'Neil measured the sum and difference frequency components experimentally using a long tube.

The interaction of two sound waves in a bounded region was considered again in 1956 by Ingard and Pridmore-Brown.[15] In 1957, Westervelt[16,17] generated a solution for the interaction of two infinite plane waves with no boundaries present.

Despite this activity, the interaction of sound waves did not receive widespread attention until the early 1960's when Westervelt[18] proposed the nonlinear or parametric acoustic array for the transmission or detection of a low frequency acoustic wave. He showed that a highly directional, low frequency sound beam could be generated with a small transducer by the use of the interaction of two high frequency carrier sound beams. This parametric transmitting array has been demonstrated experimentally by Bellin and Beyer[19], Hobaek,[20] Zverev and Kalachev,[21] Muir and Blue,[22] Smith,[23] Merklinger,[24] Truchard and Willette,[25] among others.[26-28]

The parametric reception of a low frequency wave, also proposed by Westervelt,[18] is accomplished by the use of a high frequency acoustic pump wave which interacts with the low frequency signal wave to produce sound waves at the sum and difference frequencies. These sound waves are received by a second transducer placed on the axis of the pump transducer. The parametric receiving array was first studied by Berktay[29,30] and later by Tjotta.[31] An experiment was conducted by Berktay and Al-Temimi[32,33] that demonstrated the existence of the parametric receiving array and,

furthermore, showed that the array had a directivity function which is very similar to that of a conventional end-fire array with a length equal to the distance between the two transducers. Similar experiments have been conducted by Barnard et al.,[34] Konrad et al.,[35] Muir and Berktay,[36] Zverev and Kalachev,[37] and Date and Tozuka.[38]

Most of the experimenters developed a theoretical model designed to correspond to the conditions of the particular experiment. The experiments conducted by Berktay and Al-Temimi were primarily done in the nearfield of the transducer. Consequently, the theory was appropriately designed for consideration of interaction in the nearfield of the pump transducer. On the other hand, the numerical solution by Barnard et al. assumed that the interaction occurred only in the farfield of the pump transducer. The theory used by Muir and Berktay for the analysis of a single parametric array is described fully in a paper by Berktay and Shooter.[39] A closed form solution was found for the sum and difference frequency sound field for the parametric receiving array in the farfield of the narrowbeam pump transducer. The theoretical approach of Zverev and Kalachev and of Date and Tozuka does not use Westervelt's perturbation procedure for finding the value of the sum and difference frequency sound pressure. Instead, the modulation of the high frequency pump wave by the low frequency signal wave is considered in terms of the phase modulation of the pump wave caused by the time varying change in the sound speed due to the presence of the signal wave. Recently, Rogers et al.[40] obtained a solution for the parametric receiving array in the nearfield of a small narrowbeam pump transducer.

In each of the models described above, the effects of shadowing of the signal wave by the pump transducer were neglected. These effects were considered by Al-Temimi[41] and were found to reduce the directivity of the parametric receiving array when the pump transducer was large compared to the signal frequency wavelength.

The possibility for utilizing an arrangement similar to the parametric receiving array for the construction of a traveling wave parametric amplifier was proposed by Tucker,[42] Stepanov,[43] and Berktay.[30] However, each researcher concluded that amplification of the signal wave is not possible unless the sum frequency wave is suppressed or the medium is dispersive. Such amplification in a dispersive waveguide is predicted by Ostrovskii and Papilova.[44]

Berktay and Al-Temimi[45] have recently related the parametric receiving array to the problem of sound scattered by sound. This relationship is an interesting one and deserves attention because it has continually been debated since Ingard and Pridmore-Brown first studied the problem.[15] Ingard and Pridmore-Brown predicted that a scattered sound field would propagate outside the interaction region common to the two primary waves. Their experimental measurement seemed to verify the predictions. However, later attempts at verifying these predictions have proved unsuccessful.[46,47,48] In 1957, Westervelt[16,17] considered the nonlinear interaction of two infinite plane waves intersecting at nonzero angles and found that the scattered pressure was related only to the value of the primary sound wave amplitude at the observer point. This solution did not include the effects of boundaries or absorption. Consequently, the solution had a singularity when the primary sound waves were

propagating in the same direction. This result was consistent with previous predictions by Lord Rayleigh[12] and Lamb[13] which had been verified experimentally by Thuras, Jenkins, and O'Neil,[4] provided we assume that the interaction occurs over an infinite distance. Furthermore, Westervelt predicted that no scattered sound exists outside the region of interaction. Various magnitudes of scattered sound pressure outside the region of interaction have been predicted by Dean,[49] Lauvstad and Tjötta,[50] and Al-Temimi.[47]

In 1972,[51] Westervelt recast the 1957 result into a form which permitted the singularity to be removed. He furthermore related this new solution to the truncated end-fire array, i.e., the parametric receiving array for the case when the frequency of one wave was considerably higher than the other.

The present study includes theoretical analysis and experimental investigation of the parametric receiving array. The investigation of the parametric receiving array is extended to include omnidirectional pump transducers and pump transducers which have one dimension up to one wavelength or more at the signal frequency and two dimensions which are small compared to the signal frequency wavelength in order to minimize the effects of acoustic shadowing. A closed form solution of Westervelt's scattering integral for an omnidirectional pump transducer will be found and, in turn, used to obtain the solution for a line pump transducer. The theory is based on Westervelt's quasilinear solution in which only second-order interactions are considered. The effects of absorption are ignored in the derivation of the basic second-order wave equation. However, the attenuation of the first- and second-order sound waves due to absorption

is included in the description of these sound waves in a manner similar to that used by Westervelt. Westervelt's solution for the problem of sound scattered by sound is analyzed and related to the parametric receiving array for two plane waves. An end-fire array function is generated from this solution. The parametric receiving array offers an excellent opportunity to study the scattering of sound by sound since interaction occurs at nonzero angles between the direction of propagation of the two waves. In a manner similar to that used by Westervelt in 1972, the singularity is removed from the 1957 result by the addition of a solution of the homogeneous wave equation, thereby placing a boundary condition on the second-order pressure. The second-order sound field is shown to be nonzero even when the two sound waves are not propagating in the same direction. In Chapter III, the significant features of this solution are interpreted in terms of the properties of the parametric receiving array.

Also in Chapter III, the solution for the interaction of a spherical wave from a point source and a plane wave is found using Westervelt's scattering integral. The second-order sound pressure is found by integrating the freefield Green's function over the volume distribution of sources to form the scattering integral. This scattering integral is in turn used to find the second-order sum and difference frequency sound pressure. The integral is evaluated using a two-dimensional stationary phase integral solution technique which has been used to solve certain optics problems. This solution is found to have the same end-fire array properties as the solution for the interaction of two plane waves.

In Chapter IV, the point source solution is used as a starting point to solve for the second-order sound field generated by a truncated line source and a plane wave; the line source was chosen because the experimental and theoretical models can be made to coincide most easily. The effects of acoustic shadowing of the low frequency plane wave are minimized even when the pump has one dimension on the order of a wavelength at the signal frequency. The large dimension for the pump allows the study of the effects of pump size on array beamwidth and sensitivity. Using the large pump, the scattering of sound by sound can also be investigated.

Lastly, Chapter IV considers the interaction of plane sound waves and waves produced by a pump transducer that is small in all three dimensions compared to a wavelength at the signal frequency. Again, the point source solution is used.

In Chapter V, the experimental arrangement is described. The experiments were conducted aboard the STEP Barge at ARL's Lake Travis Test Station. The geometry for the theoretical and experimental studies was such that the results could be readily compared. Several types of transducers were used to reproduce the geometries prescribed by the theoretical models. The arrangement of electronic equipment is essentially the same as that used by the author and described in a paper by Barnard et al.[34]

Chapter VI includes a comparison of experimental and theoretical results. Beam patterns with the pump aligned and misaligned are compared in the same coordinate systems. Sound pressure level predictions are compared with the experimental results. The agreement between the theory

and the experiment was excellent. The results are discussed in light of the problem of sound scattered by sound.

In the final chapter, a summary of the theoretical and experimental results of the present study is given.

II. THE EQUATIONS OF HYDRODYNAMICS FOR THREE-DIMENSIONAL WAVE MOTION IN A LOSSLESS FLUID

In elementary treatments of acoustic wave propagation it is usually assumed that waves of infinitesimal amplitude are being modeled so that the intrinsically nonlinear acoustic equations can be linearized. Using this assumption, acoustic wave propagation without distortion is predicted. Likewise, if acoustic waves with two or more frequencies are present, no intermodulation is predicted for the propagation of these waves. If the nonlinearity of the acoustic equations is taken into account, an originally sinusoidal waveform will indeed distort as it propagates or, if two waves are present, intermodulation products will be predicted. These intermodulation products will be present whether the amplitude of the two waves is large or small. The ability to detect these intermodulation products will depend on whether the amplitude is large enough to be detected in the presence of the background noise. In order to account for this intermodulation, the elementary wave equation must be modified to take into account higher order terms present in the propagation of a wave.

A perturbation method used by Eckart,[52] and later by Lighthill[53,54] and Westervelt,[16,17] can be used to obtain a wave equation which includes second-order components to provide a better model for the propagation of a finite amplitude sound wave. In this theory, sometimes referred to as small-signal nonlinear theory or quasilinear theory, only the first modulation product terms are considered with a second-order wave equation which has source terms proportional to the time derivative of the square

of the first-order sound pressure. If two sound fields with two different frequencies are present, a source term is predicted that is proportional to the time derivative of the cross product of the two first-order sound pressures. In this manner, either of the two sound fields can be a superposition of several waves each having the same frequency. It must be noted that this model is valid only if the two waves have amplitudes small enough that the higher order terms can be ignored. In other words, if excess attenuation or amplitude loss is present due to finite amplitude effects this model will no longer be valid. However, a large number of problems concerning the parametric receiving array can be solved by using the second-order or quasilinear solution.

The properties of a fluid can be described in either Eulerian or Lagrangian coordinates.[55] The relationship of these two coordinate systems with real sources present has been studied by Kline.[56] In the present study, the Eulerian coordinate system is used throughout. Whenever necessary, the boundary conditions will be simplified so that the boundary conditions can be expressed in Eulerian coordinates without difficulty.

We shall derive a second-order wave equation in a manner similar to that used by Westervelt.[57] The equations for the conservation of mass and momentum will be given with real sources and viscosity included. However, absorption and real sources will be ignored in the derivation of the wave equation. The effects of absorption will be included in an "ad hoc" manner in the solution of the second-order wave equation in Chapter III. If the effects of real sources are to be included, the first-order substitution into the second-order wave equation must include these sources. The equation of state will be that of an isentropic fluid.

In Eulerian coordinates, the equations of the conservation of mass and momentum with sources present can be expressed as follows:[58]

Conservation of Mass

$$\frac{\partial \rho_T}{\partial t} + \vec{\nabla} \cdot \rho_T u = Q \tag{2.1}$$

Conservation of Momentum

$$\frac{\partial \rho_T \vec{u}}{\partial t} + \vec{\nabla} \cdot \overline{T} = \vec{F} \tag{2.2}$$

where ρ_T is the total density, $\vec{u}$ is the particle velocity, ρ_o is the ambient or undisturbed density, Q is the rate of introduction of new fluid mass into a unit volume, $\overline{T}$ is a tensor such that $\overline{T}$ is the sum of $\overline{T}_S$, the stress tensor, and $\overline{T}_M$, the momentum flux tensor, and F is the external force per unit volume.

The momentum flux tensor can be expressed as

$$\overline{T}_M = \begin{pmatrix} \rho_T u_x u_x & \rho_T u_x u_y & \rho_T u_x u_z \\ \rho u_y u_x & \rho u_y u_y & \rho u_y u_z \\ \rho u_z u_x & \rho u_z u_y & \rho u_z u_z \end{pmatrix} \tag{2.3}$$

where u_x, u_y, and u_z are the three components of $\vec{u}$.

The stress tensor can be expressed as

$$\overline{T}_S = \begin{pmatrix} p & o & o \\ o & p & o \\ o & o & p \end{pmatrix} + \begin{pmatrix} D_{xx} & D_{xy} & D_{xz} \\ D_{yx} & D_{yy} & D_{yz} \\ D_{zx} & D_{zy} & D_{zz} \end{pmatrix} \tag{2.4}$$

where p is the total pressure and

$$D_{ii} = -(\eta - \frac{2\mu}{3})\,\vec{\nabla}\cdot\vec{u} - 2\mu\,\frac{\partial u_i}{\partial x_i}$$

$$D_{ij} = -\mu\left(\frac{\partial u_i}{\partial x_j} + \frac{\partial u_j}{\partial x_i}\right) \qquad i \neq j \tag{2.5}$$

where μ is the coefficient of shear viscosity and η is the coefficient of bulk viscosity.

For inviscid fluids, the tensor $\bar{\bar{T}}_S$ is a simple one with p on the main diagonal and zeroes elsewhere. In this case, $\vec{\nabla}\cdot\bar{\bar{T}}_S$ is simply $\vec{\nabla}p$. To obtain the expression for $\vec{\nabla}\cdot\bar{\bar{T}}_M$, we consider the x component such that

$$(\vec{\nabla}\cdot\bar{\bar{T}}_M)_x = u_x\,\frac{\partial(\rho_T u_x)}{\partial x} + u_x\,\frac{\partial(\rho_T u_y)}{\partial y} + u_x\,\frac{\partial(\rho_T u_z)}{\partial z} + \rho_T u_x\,\frac{\partial u_x}{\partial x}$$

$$+ \rho_T u_y\,\frac{\partial u_x}{\partial x} + \rho_T u_z\,\frac{\partial u_x}{\partial z} = \vec{u}_x\,\vec{\nabla}\cdot(\rho_T\vec{u}) + \rho_T(\vec{u}\cdot\vec{\nabla})\,u_x \quad . \tag{2.6}$$

Then we have

$$\vec{\nabla}\cdot\bar{\bar{T}}_M = \vec{u}\vec{\nabla}\cdot(\rho_T\vec{u}) + \rho_T(\vec{u}\cdot\vec{\nabla})\vec{u} \quad . \tag{2.7}$$

The momentum equation for an inviscid fluid now can be expressed as

$$\frac{\partial\rho_T\vec{u}}{\partial t} + \vec{\nabla}p + \vec{u}\,\vec{\nabla}\cdot(\rho_T\vec{u}) + \rho_T(\vec{u}\cdot\vec{\nabla})\vec{u} = \vec{F} \tag{2.8}$$

The acoustic pressure can be related to the density through the equation of state:

$$p = F(\rho_T, S) \quad , \tag{2.9}$$

where S is the entropy.

For an isentropic fluid we have

$$p = F(\rho_T) \quad . \tag{2.10}$$

We shall use a perturbation procedure similar to that used by Eckart,[52] Lighthill,[53] and Westervelt.[16,17] The field variables $\vec{u}$, ρ_T, and p can be expanded in series such that:

$$\begin{aligned} \vec{u} &= \lambda\vec{u}_1 + \lambda^2\vec{u}_2 + \ldots, \\ \rho_T &= \rho_o + \lambda\rho_1 + \lambda^2\rho_2 + \ldots, \text{ and} \\ p &= p_o + \lambda p_1 + \lambda^2 p_2, \end{aligned} \tag{2.11}$$

where λ is a nondimensional mathematical parameter introduced for convenience and p_o is the ambient pressure. We have assumed that $\vec{u}_o=0$. An approximate equation of state for an isentropic fluid can be obtained by expanding p in a Taylor series and keeping only the first two terms such that

$$p = p_o + \left(\frac{\partial p}{\partial \rho_T}\right)_{S,0} (\rho_T-\rho_o) + \frac{1}{2}\left(\frac{\partial^2 p}{\partial \rho_T{}^2}\right)_{S,0} (\rho_T-\rho_o)^2 \tag{2.12}$$

where S is the entropy.

The infinitesimal sound speed c_o is defined by

$$\left(\frac{\partial p}{\partial \rho_T}\right)_{S,0} = c_o{}^2 \quad . \tag{2.13}$$

The pressure can also be expressed as

$$p = p_o + c_o{}^2 (\rho_T-\rho_o) + \frac{1}{2}\frac{c_o{}^2}{\rho_o}\left(\frac{B}{A}\right)(\rho_T-\rho_o)^2 \quad , \tag{2.14}$$

where

$$B/A = \rho_o/c_o{}^2(\partial^2 p/\partial \rho_T{}^2)_{S,0} \quad . \tag{2.15}$$

By substituting Equation (2.11) into Equation (2.14) and assembling like

powers of λ, we get

$$p_1 = c_o^2 \rho_1 \tag{2.16}$$

and

$$\begin{aligned} p_2 &= c_o^2 \rho_2 + \left(\frac{B}{2A}\right) \frac{c_o^2}{\rho_o} \rho_1^2 \\ &= c_o^2 \rho_2 + \left(\frac{B}{2A}\right) \frac{(p_1)^2}{\rho_o c_o^2} \end{aligned} \tag{2.17}$$

If we assume that the source terms in Equations (2.1) and (2.8) are first-order functions, we can obtain the first-order equations by substituting Equations (2.11) into (2.1) and (2.8), keeping terms with first powers of λ. We have the following equations:

Conservation of Mass

$$\frac{\partial \rho_1}{\partial t} + \rho_o \vec{\nabla} \cdot \vec{u}_1 = Q \tag{2.18}$$

Conservation of Momentum

$$\rho_o \frac{\partial \vec{u}_1}{\partial t} + \vec{\nabla} p_1 = \vec{F} \tag{2.19}$$

Wave Equation for ρ_1, p_1, and $\vec{u}$

$$\frac{\partial^2 \rho_1}{\partial t^2} - c_o^2 \nabla^2 \rho_1 = \rho_o \frac{\partial q}{\partial t} - \vec{\nabla} \cdot \vec{F}$$

$$\text{or } \nabla^2 p_1 - \frac{1}{c_o^2} \frac{\partial^2 p_1}{\partial t^2} = \Box^2 p_1 = -\rho_o \frac{\partial q}{\partial t} + \vec{\nabla} \cdot \vec{F} \quad , \tag{2.20}$$

where $\Box^2 = \nabla^2 - \frac{1}{c_o^2} \frac{\partial^2}{\partial t^2}$ is the wave operator,

and $\Box^2\vec{u}_1 = -\frac{1}{\rho_o c_o^2}\frac{\partial\vec{F}}{\partial t} + \frac{\vec{\nabla}Q}{\rho_o}$.

Likewise, the second-order equations can be obtained by equating terms containing λ^2 to obtain the following second order equation.

Conservation of Mass

$$\frac{\partial\rho_2}{\partial t} + \rho_o\vec{\nabla}\cdot\vec{u}_2 + \vec{\nabla}\cdot\rho_1\vec{u}_1 = 0 \tag{2.21}$$

Conservation of Momentum

$$\rho_o\frac{\partial\vec{u}_2}{\partial t} + \frac{\partial\rho_1\vec{u}_1}{\partial t} + \rho_o\vec{u}_1(\vec{\nabla}\cdot\vec{u}_1) + \rho_o(\vec{u}_1\cdot\vec{\nabla})\vec{u}_1 + \vec{\nabla}p_2 = 0 \tag{2.22}$$

Wave Equation

$$\frac{\partial^2\rho_2}{\partial t^2} - c_o^2\nabla^2\rho_2 = \vec{\nabla}\cdot\left[\rho_o\vec{u}_1(\vec{\nabla}\cdot\vec{u}_1) + \rho_o(\vec{u}_1\cdot\vec{\nabla})\vec{u}_1\right] + \nabla^2(p_2 - c_o^2\rho_2) \tag{2.23}$$

$$\text{or}\left[\nabla^2 - \frac{1}{c_o^2}\frac{\partial^2}{\partial t^2}\right]p_2 = \Box^2 p_2 = -\rho_o\vec{\nabla}\cdot\left[u_1(\vec{\nabla}\cdot\vec{u}_1) + (\vec{u}_1\cdot\vec{\nabla})u_1\right] - \frac{1}{2\rho_o c_o^4}\left(\frac{B}{A}\right)\frac{\partial^2(p_1)^2}{\partial t^2} \quad . \tag{2.24}$$

If we assume $\vec{u}$ is irrotational, we can find a scalar ϕ such that we have $\vec{u}=\vec{\nabla}\phi$. We shall denote single time derivatives with a dot above the parameter and double time derivatives with two dots. If we furthermore assume that no real sources are present, the second order wave equation can be expressed as

$$\Box^2 p_2 = -\rho_o\left[(\vec{\nabla}\cdot\vec{\nabla}\phi_1)^2 + (\vec{\nabla}\phi_1)\cdot\nabla^2(\vec{\nabla}\phi_1) + \frac{1}{2}\nabla^2(\vec{\nabla}\phi_1\cdot\vec{\nabla}\phi_1)\right]$$

$$- \frac{1}{2\rho_o c_o^4}\left(\frac{B}{A}\right)\frac{\partial^2 (p_1)^2}{\partial t^2}$$

$$= -\rho_o\left[\frac{1}{\rho_o^2 c_o^4}(\dot{p}_1)^2 + \vec{\nabla}\phi_1(\nabla^2\vec{\nabla}\phi) + \frac{1}{2}\Box^2(\vec{\nabla}\phi_1\cdot\vec{\nabla}\phi_1)\right.$$

$$\left. + \frac{1}{2c_o^2}\frac{\partial^2}{\partial t^2}(\vec{\nabla}\phi_1\cdot\vec{\nabla}\phi_1)\right] \qquad (2.25)$$

$$- \frac{1}{2\rho_o c_o^4}\left(\frac{B}{A}\right)\frac{\partial^2 (p_1)^2}{\partial t^2} \quad .$$

We can use the following identities to simplify the wave equation:

$$\frac{1}{2}\frac{\partial^2}{\partial t^2}(\vec{\nabla}\phi_1\cdot\vec{\nabla}\phi_1) = \left(\frac{\partial\vec{\nabla}\phi_1}{\partial t}\right)\cdot\frac{\partial\vec{\nabla}\phi_1}{\partial t} + (\vec{\nabla}\phi_1)\cdot\left(\frac{\partial^2(\vec{\nabla}\phi_1)}{\partial t^2}\right)$$

$$= \frac{1}{\rho_o^2}\vec{\nabla}p_1\cdot\vec{\nabla}p_1 - \frac{\vec{\nabla}\phi_1\cdot\vec{\nabla}\dot{p}_1}{\rho_o} \qquad (2.26)$$

$$(\vec{\nabla}\phi_1)\cdot(\nabla^2\vec{\nabla}\phi_1) = \frac{1}{c_o^2}\vec{\nabla}\phi_1\cdot\frac{\partial^2\vec{\nabla}\phi_1}{\partial t^2} = \frac{(\vec{\nabla}\phi_1)}{\rho_o c_o^2}\cdot\vec{\nabla}\dot{p}_1 \qquad (2.27)$$

$$\Box^2(\dot{p}\phi_1) = 2(\vec{\nabla}\dot{p}_1)\cdot\vec{\nabla}\phi_1 - \frac{2}{c_o^2}\ddot{p}_1\dot{\phi}_1 \qquad (2.28)$$

and

$$\Box^2 p_1^2 = -\frac{2}{c_o^2}(\dot{p}_1)^2 + 2\vec{\nabla}p_1\cdot\vec{\nabla}p_1 \quad . \qquad (2.29)$$

Then the wave equation for p_2 is:

$$\Box^2 p_2 = -\frac{1}{\rho_o c_o^4}\left(\frac{B}{2A}\right)\frac{\partial^2(p_1^2)}{\partial t^2} \tag{2.30}$$

$$-\rho_o\left[\frac{1}{\rho_o^2 c_o^4}(\dot{p}_1)^2 + \frac{1}{c_o^2}\left(\frac{1}{\rho_o^2}\vec{\nabla}p_1\cdot\vec{\nabla}p_1 - \frac{\vec{\nabla}\phi_1\cdot\vec{\nabla}\dot{p}_1}{\rho_o}\right)\right.$$

$$\left. - \frac{1}{\rho_o c_o^2}(\vec{\nabla}\phi_1)\frac{\partial(\vec{\nabla}p_1)}{\partial t} + \frac{1}{2}\Box^2(\vec{\nabla}\phi_1\cdot\vec{\nabla}\phi_1)\right]$$

$$= -\frac{1}{\rho_o c_o^4}\left(\frac{B}{2A}\right)\frac{\partial^2(p_1^2)}{\partial t^2}$$

$$-\rho_o\left[\frac{2}{\rho_o^2 c_o^4}(\dot{p}_1)^2 + \frac{2}{\rho_o^2 c_o^4}\frac{\partial^2(p_1^2)}{\partial t^2}\right.$$

$$\left. + \frac{\Box^2}{\rho_o}\left(\frac{\dot{p}_1\phi_1}{c_o^2} - \frac{p_1^2}{2\rho_o c_o^2} - \frac{\rho_o}{2}\vec{\nabla}\phi_1\cdot\vec{\nabla}\phi_1\right)\right]$$

or

$$\Box^2 p_2 = -\frac{1}{\rho_o c_o^4}\left(1 + \frac{B}{2A}\right)\frac{\partial^2 p_1^2}{\partial t^2} \tag{2.31}$$

$$+\Box^2\left[\frac{1}{c_o^2}\phi_1\dot{p}_1 - \frac{1}{2\rho_o c_o^2}p_1^2 - \frac{1}{2}\rho_o\,\vec{u}_1\cdot\vec{u}_1\right]$$

The second-order wave equation can alternatively be expressed in the following form:

$$\Box^2 p_2 = -\rho_o\left[\frac{1}{c_o^2}\frac{\partial^2(\vec{u}_1\cdot\vec{u}_1)}{\partial t^2}\right] - \frac{1}{\rho_o c_o^4}\left(\frac{B}{2A}\right)\frac{\partial^2(p_1)^2}{\partial t^2} \tag{2.32}$$

$$+\Box^2\left[\frac{p_1^2}{2\rho_o c_o^2} - \rho_o\frac{\vec{u}_1\cdot\vec{u}_1}{2}\right]$$

The first two terms on the right-hand side of Equations (2.31) and (2.32) are the source terms for the second-order pressure. The first term in each expression is present whether or not the fluid is nonlinear. The second term is due to the nonlinearity of the fluid. The term $\Box^2(\cdot)$ on the right-hand side of Equations (2.31) and (2.32) is also present whether or not the fluid is nonlinear. The term $\Box^2(\cdot)$ is ignored by Westervelt[57] in the derivation of the second-order wave equation since the term yields a local pressure. Therefore, it is not cumulative and does not propagate outside the interaction region. For the parametric transmitter, the low frequency sound wave generated by the interaction of two high frequency waves will propagate outside the region of interaction and the term can usually be ignored. For the parametric receiving array, the observer is in the region of interaction; therefore, the term can only be ignored if it is small compared to the first two terms. The physical significance of Equation (2.32) can be more readily understood if we obtain an expression for the second-order pressure in terms of the second-order scalar potential ϕ_2. We can obtain such an expression by integrating the second-order momentum equation over space and using the appropriate first-order relations to obtain:

$$p_2 = -\rho_o \frac{\partial \phi_2}{\partial t} - \frac{1}{2}\left(\rho_o \vec{u}_1 \cdot \vec{u}_1 - \frac{p_1^2}{\rho_o c_o^2}\right) \tag{2.33}$$

where $-\frac{1}{2}\left(\rho_o \vec{u}_1 \cdot \vec{u}_1 - \frac{p_1^2}{\rho_o c_o^2}\right)$ is a local pressure due to the presence of the first-order sound field. The second wave equation (Equation 2.32) includes this pressure in a simple form.

In Chapter III we shall solve the second-order wave equation (Equation 2.31 or Equation 2.32) for several configurations of the first-order sound field. The first of these configurations will be two infinite plane waves and then two plane waves present over a half space. We shall show that Equations (2.31) and (2.32) are equivalent for a first-order field consisting of two plane waves. We shall also use a Green's function solution of Equation (2.31) to solve for the second-order pressure generated by the interaction of a spherically spreading wave and a plane wave. For this solution we shall only consider the source term,

$-\frac{1}{\rho_o c_o^4}\left(1+\frac{B}{2A}\right)\frac{\partial^2 p_1^2}{\partial t^2}$, in a manner similar to that suggested by Westervelt.[55]

III. SOLUTION OF THE SECOND-ORDER WAVE EQUATION

In the last chapter, we derived the second-order wave equation with a source function which is quadratic in the first-order field variables. For the parametric receiving array, we are interested in the sum and difference frequency sound pressures which are generated by the cross-product terms in the source function.

In Section A, we present a simple means to generate the source function for the sum and difference sound pressures by the use of complex numbers.

In Section B, we consider the interaction of two plane waves with an angle θ between their directions of propagation. The interaction of two infinite plane waves is of interest because the problem relates directly to the problem of the scattering of sound by sound as first formulated by Westervelt. For the lossless case, the source function is equal to the D'Alembertian of a function of the first-order sound fields. Hence, the value of the second-order sound pressure is dependent only on the local sound pressure unless the two first-order sound waves are propagating in the same direction. In the case of collinear waves, the predicted value for the sound pressure for the sum and difference frequency components is infinite as would be expected if no boundaries, absorption, or finite amplitude effects are present. This result led Westervelt to predict that no scattering of sound by sound would exist if the two sound waves were not propagating in the same direction. In the last part of Section B, we shall consider the interaction of one sound

field present over all space and a second present over one-half space starting at some planar boundary and propagating away from and perpendicular to this boundary. To solve this problem, we add a homogeneous solution of the wave equation to the solution obtained in the first part of Section B. In this derivation, we shall neglect the effects of real sources that would be necessary to generate the first-order fields. In fact, we shall place the second-order pressure equal to the local pressure expressed in Equation (2.33) at the planar boundary. If we observe the second-order pressure at some distance from the boundary, we find that this pressure is cumulative and propagates in a direction different from the direction of either of the primary waves. The dependence of the pressure amplitude on the angle between the propagation vectors of the two primary waves is very similar to the directivity function of the parametric receiving array as found by Berktay.

For two plane waves we have no difficulty in solving the wave equation directly. However, in general, we will find it necessary to formulate the solution in terms of an integral of a Green's function. A description of the Green's function solution is given in Section C.

In order to solve the problem of a parametric receiving array with an arbitrarily shaped planar piston pump, we shall find a solution which can be used as a starting point for solving more complex problems. The most obvious solution is the solution of a high frequency point source pump and a plane wave low frequency signal. If we have the solution for an omnidirectional pump transducer, the solution for virtually any other type of two- or three-dimensional pump transducer can be obtained by summing this solution over the active face or volume of the transducer.

It is in this light that we shall generate the solution for the interaction of a spherical wave from a point source and a plane wave. We shall use the Green's function integral solution for the second-order wave equation with a first-order sound field consisting of a spherical source and a plane wave. This solution yields a rather unwieldy integral which does not succumb to simple integration techniques. This integral can be solved using a two-dimensional stationary phase technique similar to one used in optics. We shall ignore the effects of real sources and the local pressure. In reality, the second-order pressure contribution at the source and receiver may not be negligible for a particular application of the parametric receiving array since we may desire to use the properties of the directivity function, particularly in the nearfield of the parametric array, to eliminate an undesired noise source. If an additional pressure term is present due to the pump source or the local pressure, the performance of the parametric receiving array may be degraded for an application requiring a very high rejection of a target at an undesired bearing. In order to analyze the effects of the real sources and the local pressure terms, a thorough analysis of the particular type of transducer is needed. Since the transducers are designed to operate at the carrier frequency, the transducer's properties at the low frequency may be such that the transducer actually moves with the low frequency fluid particle displacement. This condition could significantly change the way the parametric array would perform as compared to its performance under the assumption that the transducer's position remains fixed. In this study, this particular problem will not be considered; however, it does appear to be worthy of further investigation.

A. Use of Complex Numbers

In Equation (2.31), we can see that the sum and difference frequency source terms are generated by cross-products of each of the two first-order sound fields. It is convenient to use complex numbers to represent the oscillatory part of the various functions. The real physical variable is equated to the real part of the complex variable. In the case where quadratic terms are encountered, special care must be taken in their calculation. For two complex numbers M and N

$$\mathrm{Re}[M]\cdot\mathrm{Re}[N] = \frac{1}{2}\,\mathrm{Re}\; M[N+N^*]$$

where Re[M] represents the real part of the complex variable and the asterisk denotes the complex conjugate. The transformation

$$MN \Rightarrow \frac{1}{2}\,MN + \frac{1}{2}\,MN^*$$

will be used to generate the quadratic terms when complex variables are used.

For example, consider the case of two plane waves with wave vectors intersecting at angle θ. The first-order pressure is

$$p_1 = P_{11}e^{j(\vec{k}_1\cdot\vec{r}-\omega_1 t)} + P_{12}e^{j(\vec{k}_2\cdot\vec{r}-\omega_2 t)}$$

$$= p_{11} + p_{12}$$

where P_{11} and P_{12} are the peak amplitudes of the two sound waves, $j=\sqrt{-1}$,

$\vec{k}_1$ and $\vec{k}_2$ are the propagation vectors,

$\vec{r}$ is the vector from the origin, and

ω_1 and ω_2 are the angular frequencies of the two waves.

Then we have

$$(p_1)^2 = p_{11}^2 + 2p_{11}p_{12} + p_{12}^2 \quad .$$

The desired sum and difference frequency components can be obtained by using

$$(p_1^2)_+ + (p_1^2)_- = \frac{2}{2} p_{11}p_{12} + \frac{2}{2} p_{11}p_{12}^*$$

$$= P_{11}P_{12}e^{j\left[(\vec{k}_1+\vec{k}_2)\cdot\vec{r} - (\omega_1+\omega_2)t\right]}$$

$$+ P_{11}P_{12}e^{j\left[(\vec{k}_1-\vec{k}_2)\cdot\vec{r} - (\omega_1-\omega_2)t\right]}$$

where the + and - subscript denotes the sum and difference frequencies. In order to simplify the notation, we shall use the subscript (±) on (p_1^2), ω, k, and the absorption coefficient (α) to denote either the sum or difference frequency term. The upper subscript denotes sum frequency and the lower subscript denotes the difference frequency.

B. Solution of the Second-Order Wave Equation for Two Plane Waves

We shall now consider the interaction of two plane waves propagating with an angle θ between their directions of propagation. For the parametric receiving array, we shall assume that the first plane wave is the high frequency pump wave and the second plane wave is the low frequency signal wave. We shall ignore the effects of absorption. The first-order sound field is then given by

$$p_1 = p_{11} + p_{12} \qquad (3.1)$$

$$= P_{11}e^{j(\vec{k}_1\cdot\vec{r}-\omega_1 t)} + P_{12}e^{j(\vec{k}_2\cdot\vec{r}-\omega_2 t)} \quad .$$

The desired sum and difference frequency components of p_1^2 then are

$$(p_1^2)_\pm = P_{11}P_{12}e^{j\left[(\vec{k}_1 \pm \vec{k}_2)\cdot\vec{r} - (\omega_1 \pm \omega_2)t\right]} \quad . \tag{3.2}$$

Following the procedures of Westervelt,[16,17] we find:

$\Box^2 (p_1^2)_\pm$ to be

$$\Box^2 (p_1^2)_\pm = \nabla^2 (p_1^2)_\pm - \frac{1}{c_o^2}\frac{\partial^2 (p_1^2)_\pm}{\partial t^2} = \tag{3.3}$$

$$\left[\frac{(\omega_1 \pm \omega_2)^2}{c_o^2} - |\vec{k}_1 \pm \vec{k}_2|^2\right](p_1^2)_\pm$$

$$= \pm 2(k_1 k_2 - \vec{k}_1 \cdot \vec{k}_2)(p_1^2)_\pm \quad .$$

We can solve for (p_1^2) to get

$$(p_1^2)_\pm = \frac{\pm \Box^2 (p_1^2)_\pm}{2(k_1 k_2 - \vec{k}_1 \cdot \vec{k}_2)} \tag{3.4}$$

for $k_1 k_2 \neq \vec{k}_1 \cdot \vec{k}_2$.

The time derivative of $(p_1^2)_\pm$ is

$$\frac{\partial^2 (p_1^2)_\pm}{\partial t^2} = \mp \frac{\omega_\pm^2 \Box^2 (p_1^2)_\pm}{2(k_1 k_2 - \vec{k}_1 \cdot \vec{k}_2)} \tag{3.5}$$

and the wave equation (Equation 2.31) is

$$\Box^2 p_2 = \Box^2 \left[\pm \frac{\omega_\pm^2 (p_1^2)_\pm \left(1+\frac{B}{2A}\right)}{2(k_1 k_2 - \vec{k}_1 \cdot \vec{k}_2)\rho_o c_o^4} + \frac{(\phi_1 \dot{p}_1)_\pm}{c_o^2} - \frac{1}{2\rho_o c_o^2}(p_1^2)_\pm - \frac{1}{2}\rho_o (\vec{u}_1 \cdot \vec{u}_1)_\pm \right] . \tag{3.6}$$

Since p_1 can be expressed as

$$p_1 = P_{11} e^{j(\vec{k}_1 \cdot \vec{r} - \omega_1 t)} + P_{12} e^{j(\vec{k}_2 \cdot \vec{r} - \omega_2 t)} ,$$

we have the following first-order relationships

$$\phi_1 = -\frac{1}{\rho_o} \int p_1 \, dt , \tag{3.7}$$

$$\rho_o \phi_1 = j \left[\frac{P_{11}}{\omega_1} e^{j(\vec{k}_1 \cdot \vec{r} - \omega_1 t)} + \frac{P_{12}}{\omega_2} e^{j(\vec{k}_2 \cdot \vec{r} - \omega_2 t)} \right] , \tag{3.8}$$

$$\vec{u}_1 = \vec{\nabla}\phi_1$$

$$= \frac{P_{11}\vec{k}_1}{\rho_o \omega_1} e^{j(\vec{k}_1 \cdot \vec{r} - \omega_1 t)} + \frac{P_{12}\vec{k}_2}{\rho_o \omega_2} e^{j(\vec{k}_2 \cdot \vec{r} - \omega_2 t)} , \tag{3.9}$$

and

$$\dot{p}_1 = -j\omega_1 P_{11} e^{j(\vec{k}_1 \cdot \vec{r} - \omega_1 t)} - j\omega_2 P_{12} e^{j(\vec{k}_2 \cdot \vec{r} - \omega_2 t)} . \tag{3.10}$$

Then the appropriate sum and difference frequency terms can be expressed as

$$\frac{1}{c_o^2}(\phi_1 \dot{p}_1)_\pm = \pm \frac{1}{2}\left(\frac{\omega_1}{\omega_2} + \frac{\omega_2}{\omega_1}\right) \frac{P_{11} P_{12}}{\rho_o c_o^2} e^{j(\vec{k}_\pm \cdot \vec{r} - \omega_\pm t)} , \tag{3.11}$$

$$-\frac{1}{2\rho_o c_o^2}(p_1^2)_\pm = \frac{-P_{11} P_{12}}{2\rho_o c_o^2} e^{j(\vec{k}_\pm \cdot \vec{r} - \omega_\pm t)} , \tag{3.12}$$

$$-\frac{1}{2}\rho_o(\vec{u}_1\cdot\vec{u}_1)_{\pm} = \frac{-P_{11}P_{12}(\vec{k}_1\cdot\vec{k}_2)}{\rho_o\omega_1\omega_2}\, e^{j(\vec{k}_{\pm}\cdot\vec{r}-\omega_{\pm}t)} \quad . \tag{3.13}$$

By substituting Equations (3.11), (3.12), and (3.13) into Equation (3.6), we get

$$\Box^2 p_2 = \Box^2\left\{\left[\frac{\pm\omega_{\pm}^2(k_1k_2)(1+\frac{B}{2A})}{2\omega_1\omega_2(k_1k_2-\vec{k}_1\cdot\vec{k}_2)} \pm \frac{1}{2}\left(\frac{\omega_1^2+\omega_2^2}{\omega_1\omega_2}\right) - \left(\frac{1}{2}+\frac{\vec{k}_1\cdot\vec{k}_2}{k_1k_2}\right)\right]\frac{(p_1^2)_{\pm}}{\rho_o c_o^2}\right\} \tag{3.14}$$

or

$$\Box^2 p_2 = \Box^2\left\{\left[\pm\frac{\omega_{\pm}^2(\vec{k}_1\cdot\vec{k}_2)}{2\omega_1\omega_2(k_1k_2-\vec{k}_1\cdot\vec{k}_2)} \pm \frac{\omega_{\pm}^2(k_1k_2)}{2\omega_1\omega_2(k_1k_2-\vec{k}_1\cdot\vec{k}_2)}\left(\frac{B}{2A}\right) - \left(\frac{1}{2}-\frac{1}{2}\frac{\vec{k}_1\cdot\vec{k}_2}{k_1k_2}\right)\right]\frac{(p_1^2)_{\pm}}{\rho_o c_o^2}\right\} \quad . \tag{3.15}$$

Equation (3.15) has the same form as we would have obtained if we had used Equation (2.32) instead of Equation (2.31) as the starting point for the derivation. Hence, for two plane waves Equation (2.31) and Equation (2.32) are equivalent. The second-order pressure is then found to be

$$p_2 = \frac{\pm\omega_{\pm}^2\left[\vec{k}_1\cdot\vec{k}_2 + \left(\frac{B}{2A}\right)k_1k_2\right](p_1^2)_{\pm}}{2\omega_1\omega_2(k_1k_2-\vec{k}_1\cdot\vec{k}_2)} - \left(\frac{1}{2}-\frac{1}{2}\frac{\vec{k}_1\cdot\vec{k}_2}{k_1k_2}\right)\frac{(p_1^2)_{\pm}}{\rho_o c_o^2} \quad . \tag{3.16}$$

This solution corresponds to the solution for plane waves of infinite extent with no absorption or finite amplitude effects present. As can be seen, the second-order sound pressure is proportional to the local value of (p_1^2) except when $k_1k_2=\vec{k}_1\cdot\vec{k}_2$. This result led Westervelt to conclude that no scattering of sound by sound existed when two sound waves were not propagating in the same direction. A conclusion based on Equation (3.16) is subject to the conditions that

1) no absorption is present, and

2) the plane waves are of infinite extent.

Strictly speaking, conclusions about the scattering of sound by sound outside the region of interaction cannot be made since the plane waves are assumed to be present over all space.

If one plane wave is present over all space and the second present only in the half space $x \geq 0$ and propagates in the $+x$ direction, then we have

$$p_{11} = P_{11} e^{j(k_1 x - \omega_1 t)} \quad , \quad x \geq 0. \tag{3.17}$$

We assume that the second wave propagates with an angle θ with respect to the direction of propagation of the first wave such that we have

$$p_{12} = P_{12} e^{j(\vec{k}_2 \cdot \vec{r} - \omega_1 t)} \quad . \tag{3.18}$$

If we neglect the effects of the real source at $x = 0$, the pressure at $x = 0$ must be equal to the local pressure, the second term in Equation (3.16). Any solution which satisfies the second-order homogeneous wave equation

$$\Box^2 \Phi = 0 \tag{3.19}$$

can be added to the solution to satisfy the boundary conditions. One such solution is a plane wave such that

$$\Phi_{\pm} = \frac{\mp \omega_{\pm}^2 \left(\frac{\vec{k}_1 \cdot \vec{k}_2}{k_1 k_2} + \frac{B}{2A} \right) P_{11} P_{12} \exp \left\{ j \left[(k_1 \pm k_2) \left(\sqrt{1 - \frac{k_{2y}^2}{(k_1 \pm k_2)^2}}\ \vec{i} \pm \frac{k_{2y}}{(k_1 \pm k_2)} \vec{j} \right) \cdot \vec{r} - \omega_{\pm} t \right] \right\}}{2(k_1 k_2 - \vec{k}_1 \cdot \vec{k}_2)\ \rho_o c_o^4} \tag{3.20}$$

where $\vec{i}$ is unit vector in the x direction,

$\vec{j}$ is a unit vector in the y direction, and

k_{2y} is the component of the k_2 wave vector in the y direction.

This solution represents a plane wave of frequency

$$\frac{(k_1 \pm k_2)c_o}{2\pi} \tag{3.21}$$

with a wave vector

$$(k_1 \pm k_2)\left(\sqrt{1 - \frac{k_{2y}^2}{(k_1 \pm k_2)^2}}\ \vec{i} \pm \frac{k_{2y}}{(k_1 \pm k_2)}\ \vec{j}\right) \quad . \tag{3.22}$$

We can express this solution as

$$\Phi_{\pm} = F p_2' \tag{3.23}$$

where

$$F = - \exp\left\{ j\left[(k_1 \pm k_2)\ x \sqrt{1 - \frac{k_2^2 \sin^2\theta}{(k_1 \pm k_2)^2}} \pm k_{2y} \sin\theta - \vec{r}\cdot(\vec{k}_1 \pm \vec{k}_2) \right] \right\} \tag{3.24}$$

$$= - \exp\left\{ j\left[(k_1 \pm k_2)\ x \sqrt{1 - \frac{k_2^2 \sin^2\theta}{(k_1 \pm k_2)^2}} - k_1 x \mp k_2 \cos\theta \right] \right\}$$

and

$$p_2' = \frac{\pm\omega_{\pm}^2 \left(\frac{\vec{k}_1 \cdot \vec{k}_2}{k_1 k_2} + \frac{B}{2A} \right) P_{11} P_{12} \exp\left[j(\vec{k}_1 \pm \vec{k}_2)\cdot r - \omega_{\pm} t \right]}{2(k_1 k_2 - \vec{k}_1 \cdot \vec{k}_2)\ \rho_o c_o^4} \tag{3.25}$$

where $\vec{k}_2 = k_2 \cos\theta\ \vec{i} + k_2 \sin\theta\ \vec{j}$, and

$$\vec{r} = x\vec{i} + y\vec{j} \quad .$$

If $k_1 \gg k_2$, we can approximate F as

$$F \cong - \exp\left\{ j\left[(k_1 \pm k_2)\ x \left(1 - \frac{1}{2} \frac{k_2^2 \sin^2\theta}{(k_1 \pm k_2)^2} \right) - k_1 x \mp k_2 \cos\theta \right] \right\} \tag{3.26}$$

$$= - \exp\left\{ j\left[\pm k_2\ x\ (1 - \cos\theta) - \frac{1}{2} \frac{k_2^2 \sin^2\theta}{(k_1 \pm k_2)} \right] \right\} \quad .$$

The second-order pressure at (x,0) can be expressed as

$$p_2'' = (1+F)\, p_2' \tag{3.27}$$

$$= \left\{ 1 - \exp\left\{ j\left[(k_1 \pm k_2)\, x \sqrt{1 - \frac{k_2^2 \sin^2\theta}{(k_1 \pm k_2)^2}} - k_1 x \mp k_2 \cos\theta \right] \right\} \right\}$$

$$\cdot \frac{\left(\pm\omega_\pm^2\right)\left(\frac{\vec{k}_1 \cdot \vec{k}_2}{k_1 k_2} + \frac{B}{2A}\right) P_{11} P_{12} \exp\left\{ j\left[(\vec{k}_1 \pm \vec{k}_2)\cdot\vec{r} - \omega_\pm t \right] \right\}}{2(k_1 k_2 - \vec{k}_1 \cdot \vec{k}_2)\, \rho_o c_o^4} .$$

If $k_1 \gg k_2$, we have

$$p_2'' = \left\{ 1 - \exp\left\{ j\left[\pm k_2 x(1-\cos\theta) - \frac{k_2^2 \sin^2\theta}{2(k_1 \pm k_2)} \right] \right\} \right\}$$

$$\cdot \frac{\left(\pm\omega_\pm^2\right)\left(\frac{\vec{k}_1 \cdot \vec{k}_2}{k_1 k_2} + \frac{B}{2A}\right) P_{11} P_{12} \exp\left[j\left(\vec{k}_1 x \pm k_2 x \cos\theta \pm k_{2y} \sin\theta - \omega_\pm t \right) \right]}{2(k_1 k_2 - \vec{k}_1 \cdot \vec{k}_2 \cos\theta)\, \rho_o c_o^4} \tag{3.28}$$

$$= \frac{j(\omega_\pm^2)(\cos\theta + \frac{B}{2A}) x P_{11} P_{12}}{2k_1 \rho_o c_o^4} \cdot \frac{\sin\left[k_2 x(1-\cos\theta) \mp \frac{k_2^2 x \sin^2\theta}{4(k_1 \pm k_2)} \right]}{\frac{k_2 x(1-\cos\theta)}{2}}$$

$$\cdot \exp\left[j(k_1 \pm k_2)x \mp k_2 x(1-\cos\theta) - \frac{k_2^2 x \sin^2\theta}{4(k_1 \pm k_2)} \pm k_{2y} \sin\theta - \omega_\pm t \right]$$

$$\cong \frac{j(\omega_\pm)(\cos\theta + \frac{B}{2A}) P_{11} P_{12} x}{2\rho_o c_o^3} \cdot \frac{\sin\left[k_2 \frac{x(1-\cos\theta)}{2} \right]}{\frac{k_2 x(1-\cos\theta)}{2}}$$

$$\cdot \exp j\left[(k_1 \pm k_2)x \mp k_2 x(1-\cos\theta) - \frac{k_2^2 x \sin^2\theta}{4(k_1 \pm k_2)} \pm k_{2y} \sin\theta - \omega_\pm t \right] . \tag{3.29}$$

The solution in Equation (3.27) gives the second-order pressure for two plane waves interacting over a half space. The plane wave with frequency f_1 propagates in the x direction from x = 0.

The function (1 + F) has a zero for $\theta = 0$ which cancels the singularity in p_2'.

The pressure in Equation (3.29) has an amplitude which is proportional to x when $\theta = 0$. This result is consistent with the result predicted by Lamb,[13] Berktay,[30] and Lauvstad and Tjötta.[50] The directivity function is the same as found by Berktay for a parametric receiving array with a well collimated pump wave. For a given value of x the pressure has a phase dependence on y of $\pm k_{2y} \sin \theta$.

The second-order pressure is seen to be cumulative even when $\theta \neq 0$. Therefore, we see that cumulative interaction does exist for an arbitrary angle of θ.

C. Solution of the Second-Order Wave Equation Using the Freefield Green's Functions

Since all of the problems of interest for parametric arrays do not have the simple geometries of plane waves, it is necessary to find a more generally applicable solution for the second-order wave equation. We can integrate the freefield Green's function over the volume distribution of the source. The freefield Green's function is a solution for an unbounded medium of the equation[58]

$$\Box\, g(\vec{r}_o|r) = -\,\delta(\vec{r}_o - \vec{r}) \tag{3.30}$$

where $\vec{r}_o = (x_o, y_o, z_o)$ is the observer point,

$r = (x, y, z)$ is the source point, and

$\delta(\vec{r}_o-\vec{r}) = \delta(x_o-x)\ \delta(y_o-y)\ \delta(z_o-z)$ is the delta function for three dimensions. Thus, $g(\vec{r}_o|\vec{r})$ is the spatial solution for a simple harmonic point source at r and has the form

$$g(\vec{r}_o|\vec{r}) = \frac{e^{ikR}}{4\pi R} \tag{3.31}$$

where $R = |\vec{r}_o-\vec{r}|$.

When absorption is present, the solution for Equation (3.30) can be modified by making the wave number complex. We then have a freefield Green's function of the form

$$g(\vec{r}_o|\vec{r}) = \frac{e^{(j\frac{\omega}{c}-\alpha)R}}{4\pi R} \tag{3.32}$$

where α is the absorption coefficient.

A particular solution for the equation

$$\Box^2 p_2 = \frac{-1}{\rho_o c_o^4}\left(1+\frac{B}{2A}\right)\frac{\partial^2 p_1^2}{\partial t^2} \tag{3.33}$$

can be expressed in terms of the Green's function and has the form

$$p_2(\vec{r},t) = \frac{-(1+\frac{B}{2A})}{4\pi\rho_o c_o^4}\int_V \frac{\partial^2 p_1^2}{\partial t^2}\ \frac{\exp i\left[k_\pm|\vec{r}_o-\vec{r}|-\alpha_\pm|\vec{r}_o-\vec{r}|\right]}{|\vec{r}_o-\vec{r}|}\,dv \tag{3.34}$$

where V is the volume of integration,

$\vec{r}_o$ is a vector from the origin to the observation point, and

$\vec{r}$ is a vector from the origin to the point of interaction.

D. A Solution for An Omnidirectional Pump Transducer

The geometry used for the solution for an omnidirectional pump transducer is shown in Fig. 3.1. The signal source is assumed to be far from the parametric receiver so that the low frequency wave approximates

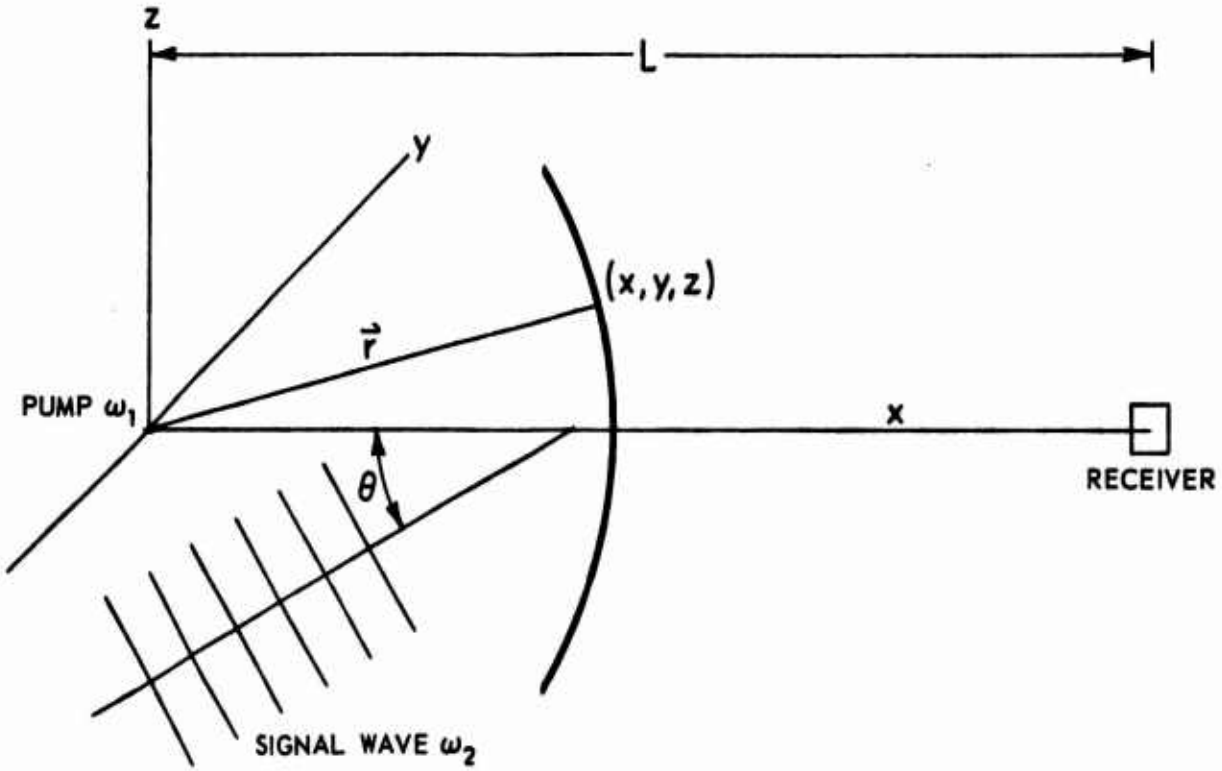

FIGURE 3.1
A PARAMETRIC RECEIVING ARRAY
WITH A POINT SOURCE PUMP

a plane wave in the vicinity of the receiver. Then at the point (x, y, z) and a time t the sound waves can be represented in complex form as

$$p_1 = j \frac{P_{11} \exp\left[-(\alpha_1 - jk_1)\sqrt{x^2+y^2+z^2} - j\omega_1 t\right]}{\sqrt{x^2+y^2+z^2}} \tag{3.35}$$

and

$$p_2 = P_{12} \exp\left[-(\alpha_2 - jk_2)(\cos\theta x + \sin\theta y) - j\omega_2 t\right] \tag{3.36}$$

where α_1, α_2 and k_1, k_2 are the absorption coefficients and the wave numbers at the frequencies ω_1 and ω_2,

P_{11} is the amplitude of the pump pressure referred to 1 meter, and

P_{12} is the amplitude of the plane wave signal.

The direction of propagation of the signal wave is assumed to be parallel to the (x, y) plane.

We find the sum and difference frequency components of p_1^2 to be

$$(p_1^2)_{\pm} = j \frac{P_{11}P_{12} \exp\left[-\alpha_1\sqrt{x^2+y^2+z^2} - \alpha_2(x\cos\theta + y\sin\theta)\right]}{\sqrt{x^2+y^2+z^2}} \tag{3.37}$$

$$\cdot \exp\left[j(k_1\sqrt{x^2+y^2+z^2} \pm k_2 x\cos\theta \pm k_{2y}\sin\theta) - j(\omega_1 \pm \omega_2)t\right] .$$

The source term is then given by

$$-\frac{(1+\frac{B}{2A})}{\rho_o c_o^4}\frac{\partial^2 p_1^2}{\partial t^2} = j(\omega_1 \pm \omega_2)^2 \frac{(1+\frac{B}{2A})}{\rho_o c_o^4} \frac{P_{11}P_{12}\exp\left(-\alpha_1\sqrt{x^2+y^2+z^2}\right)}{\sqrt{x^2+y^2+z^2}} \tag{3.38}$$

$$\cdot \exp\left[-\alpha_2(x\cos\theta + y\sin\theta)\right]$$

$$\cdot \exp\left[j(k_1\sqrt{x^2+y^2+z^2} \pm k_2 x\cos\theta \pm k_2 y\sin\theta)\right]$$

$$\cdot \exp\left[-j(\omega_1 \pm \omega_2)t\right] .$$

The integral Green's function solution for the second-order wave equation is then

$$p_2 = \frac{j(\omega_1 \pm \omega_2)^2 (1+\frac{B}{2A})\, P_{11} P_{12}}{4\pi \rho_o c_o^4} \cdot \iiint_{-\infty}^{\infty} \frac{\exp\left[-\alpha_1 \sqrt{x^2+y^2+z^2} - \alpha_2 (x \cos\theta + y \sin\theta)\right]}{\sqrt{x^2+y^2+z^2}\ \sqrt{(x_o-x)^2+y^2+z^2}} \tag{3.39}$$

$$\cdot \exp\left[-\alpha_{\pm} \sqrt{(x_o-x)^2+y^2+z^2} + j(k_1 \sqrt{x^2+y^2+z^2} \pm k_2 x \cos\theta \pm y \sin\theta)\right]$$

$$\cdot \exp\left[+ j(k_1 \pm k_2) \sqrt{(x_o-x)^2+y^2+z^2} - j(\omega_1 \pm \omega_2)t\right] dx\,dy\,dz$$

where $\alpha_{\pm}$ is the absorption of the sum or difference frequency wave, and

x_o is the position of the observer.

This rather complicated integral does not lend itself to direct integration. For its evaluation we shall use an alternate method, commonly used in optics, which is known as the method of stationary phase. Single integrals are frequently evaluated using this integral technique; however, double integrals can also be evaluated by the method of stationary phase.[59]

The solution for the integral in Equation (3.39) is given in Appendix I. To the author's knowledge, this use of a two-dimensional stationary phase solution is the first for a nonlinear acoustics problem. Thus, the integral over y and z can be expressed in the following form

$$\iint S(y,z)\, e^{j\, k\, f(y,z)}\, dy\,dz \quad . \tag{3.40}$$

This integral can be evaluated by the method of stationary phase provided $S(y,z)$ is a slowly varying function of y and z, and $k\, f(y,z)$ is a rapidly

varying function of y and z. The contributions to the asymtotic expansion of the integral come only from certain critical points.[59] The critical point of interest for us is the one within the region of integration where

$$\frac{\partial f}{\partial y} = \frac{\partial f}{\partial z} = 0 \quad . \tag{3.41}$$

This point represents the point on the wavefront of the second-order pressure at the interaction region which will eventually strike the receiver. From Appendix A, we find that

$$\frac{\partial f}{\partial z} = 0 \text{ for } z = 0 \tag{3.42}$$

and

$$\frac{\partial f}{\partial y} = 0 \text{ for } y \cong \frac{\mp k_2 \sin\theta\,(x)(x_o-x)}{k_1(x_o) \pm k_2(x_o-x)}$$

where we have assumed that $k_1 \gg k_2$. We see that the coordinate of the critical point varies as a function of x.

The second-order pressure is found to be

$$p_2 = \frac{-(\omega_1 \pm \omega_2)\,(1+\frac{B}{2A})\,P_{11}P_{12}}{2\rho_o c_o^3} \exp(jk_{\pm}x_o - j\omega_{\pm}t)$$

$$\int_{-\infty}^{\infty} \frac{\exp\left[-\alpha_1 x - \alpha_1 (x\cos\theta) - \alpha_1 (x_o-x)\right]}{x(x_o-x)\left[\frac{k_1}{(k_1 \pm k_2)x} + \frac{1}{(x_o-x)}\right]}$$

$$\cdot \exp\left[\mp jk_2(1-\cos\theta)x + j\frac{k_2^2 \sin^2\theta}{(k_1 \pm k_2)}\left(\frac{x^2}{x_o} - x\right)\right] dx \tag{3.43}$$

If we assume that $\alpha_2 x(\cos\theta) \cong \alpha_2 x$ and that the contributions from $x = -\infty$ to $x = 0$ and $x = x_o$ to ∞ are negligible, we have

$$p_2 \cong -(\omega_\pm)\left(1+\frac{B}{2A}\right)\frac{P_{11}P_{12}}{\rho_o c_o^3}\,\frac{\exp\left[-(\alpha_\pm - j\,k_\pm)\,x_o - j\,\omega_\pm t\right]}{x_o} \tag{3.44}$$

$$\int_o^{x_o} \exp\left\{j\left[\mp k_2\, x(1-\cos\theta) + \frac{1}{2}\frac{k_2^2\sin^2\theta}{(k_1 \pm k_2)}\left(\frac{x^2}{x_o} - x\right)\right]\right\} dx$$

or

$$p_2 \cong -(\omega_\pm)\left(1+\frac{B}{2A}\right)\frac{P_{11}P_{12}\exp\left[-(\alpha_\pm - j\,k_\pm)\,x_o - j\,\omega_\pm t\right]}{2\rho_o c_o^3 x_o}$$

$$\int_o^{x_o} \exp\left\{j\left[\mp k_2\, x(1-\cos\theta)\right]\right\} dx \tag{3.45}$$

$$= -(\omega_\pm)\left(1+\frac{B}{2A}\right)\frac{P_{11}P_{12}\exp\left[-(\alpha_\pm - j\,k_\pm)\,x_o - j\,\omega_\pm t\right]}{2\rho_o c_o^3}$$

$$\cdot\left[\frac{\exp\left[\mp k_2\, x_o(1-\cos\theta)\right] - 1}{\mp k_2\, x_o(1-\cos\theta)}\right]$$

$$= \frac{-(\omega_\pm)\left(1+\frac{B}{2A}\right)P_{11}P_{12}\exp\left[-(\alpha_\pm - j\,k_\pm)\,x_o \mp j\,\frac{k_2\, x_o(1-\cos\theta)}{2} - j\,\omega_\pm t\right]}{2\rho_o c_o^3} \tag{3.46}$$

$$\cdot\,\frac{\sin\left[\frac{k_2\, x_o(1-\cos\theta)}{2}\right]}{\frac{k_2\, x_o(1-\cos\theta)}{2}} \quad .$$

In the derivation of Equation (3.45), we have neglected the phase term

$$\frac{1}{2}\frac{k_2^2 \sin^2\theta}{(k_1 \pm k_2)}\left(\frac{x^2}{x_o} - x\right) \quad . \tag{3.47}$$

This term has a maximum magnitude of

$$\frac{1}{8}\frac{k_2^2 \sin^2\theta}{(k_1 \pm k_2)} x_o \quad \text{at } x = \frac{x_o}{2} \quad . \tag{3.48}$$

If we restrict the maximum allowed phase error to $\frac{\pi}{4}$, we have

$$\frac{k_2^2 x_o \sin^2\theta}{(k_1 \pm k_2)} < 2\pi \quad . \tag{3.49}$$

This assumption could be removed from the integral answer by completing the square in the exponent for x^2 and x and making a change of variables. The result would be in the form of a Fresnel integral which is tabulated. This solution will not be included in the present analysis since the assumption in Equation (3.49) will usually be valid for the cases of interest to us.

The second-order pressure in Equation (3.46) has a magnitude of

$$\hat{p} = \frac{(\omega_\pm)\left(1+\frac{B}{2A}\right) P_{11} P_{12} \exp\left[-(\alpha_\pm) x_o\right]}{2\rho_o c_o^3} \tag{3.50}$$

and a directivity function

$$D(\theta) = \frac{\sin\left[\frac{k_2 x_o(1 - \cos\theta)}{2}\right]}{\frac{k_2 x_o(1 - \cos\theta)}{2}} \quad . \tag{3.51}$$

Except for absorption, the amplitude is independent of range. The directivity function is the same as that found by Berktay.

IV. THE SECOND-ORDER SOUND FIELD FOR SEVERAL CONFIGURATIONS OF THE PARAMETRIC RECEIVING ARRAY

We shall now find the second-order sound pressure for some simple pump configurations using the point-source solution found in Chapter III. Since we are treating "small signal nonlinear" or "quasilinear" interactions, we can use the principle of superposition on either of the first-order sound fields. In this case, we consider the interactions of a plane wave with an infinite number of spherical waves from point sources summed over the surface or volume of the pump source. Using this procedure, we have a simple means to solve parametric receiving array problems for a wide variety of geometrical configurations. We shall only consider the case when the low frequency wave is a plane wave. Other studies by Berktay and Shooter,[39] and Rogers et al.,[40] have considered cases in which the wavefront of the low frequency wave is spherical, because the signal source is placed a finite distance from the parametric receiving array. In this analysis, we shall study only planar signal sound waves.

We shall first consider a finite length line source pump transducer. Two dimensions of the line source are small compared to the signal wavelength, and the other dimension is on the order of a signal wavelength. The theoretical and experimental results can be easily compared because the effects of shadowing of the low frequency signal wave by the pump transducer are minimized. A coordinate system which is the same as that used in the following chapters for experimental work will be used. We shall also investigate the effects of misalignment of the line

source transducer on the parametric receiving beam patterns. This analysis will also enable us to investigate the problem of the scattering of sound by sound. We will be able to investigate the directional properties of the second-order sound waves. This geometry will provide us with a means to observe the so-called "doppler angles" of the propagation of the sum and difference frequency sound waves.

In Section B, we shall consider the use of a line hydrophone to receive the second-order pressure wave generated by a point source and a plane wave. The line hydrophone will have one dimension which is on the order of a wavelength at the signal frequency and two dimensions which are small compared to the signal frequency wavelength. In fact, for the experimental work, the line transducer used for the hydrophone will be the same one which is used as a pump in the line source pump experiment. Again, this geometry will enable us to study the effects of a misaligned receiver, and also to observe the properties of the second-order sound field. We can observe the "doppler angles" of the sum and difference frequency waves. Again we shall use a geometry which coincides with the geometry used for experiments. In each of the solutions in Sections A and B, the effects of the interactions at the real source are not included. We simply use the scattering integral solution over the volume of interaction. We shall likewise ignore the local pressure at the receiver.

In Section C, the interaction of a plane wave and a pump wave generated by a pump transducer which has all three dimensions, which are small compared to the signal wavelength, will be considered. We shall not, however, restrict ourselves to the consideration of pump transducers with beam patterns small compared to the desired parametric receiving array

beamwidth. The small pump transducer is of interest to us because such a pump transducer would be used in most practical applications. With a small pump transducer, the ratio of array length to pump transducer size is maximized. The solution obtained will be valid for a range of pump transducers, varying from very narrow beam to very broad beam. In each case, the observer is assumed to be in the farfield of the pump transducer. However, the second-order pressure generated in the nearfield region of the transducer will be included in our solution. Likewise, the solution for a finite length line receiver will be valid only when the omnidirectional pump transducer is in the farfield of the receiving transducer. A solution could be generated for the nearfield of the pump or receiving transducer using techniques similar to those used by Stenzel,[60] Freedman,[61] and others.[62]

A. Solution for a Line Pump Source

The solution for a line source is obtained by integration of the point source solution over the length of the line. The geometry used for this solution is shown in Fig. 4.1. The line of length 2a is assumed to lie in the (x,y) plane. The propagation vector for the low frequency wave is also in the (x,y) plane.

Then the first-order sound field at ω_1 due to an elemental length $\delta\ell$ at $\vec{r}=\vec{\ell}$ of the line source can be expressed as

$$\delta p_1(\vec{\ell}) = \frac{jP_{11}}{R}\frac{\delta\ell}{2a}\exp\left[-(\alpha_1 R - jk_1 R) + j\omega_1 t\right] \qquad (4.1)$$

where P_{11} is the axial farfield pressure referred to 1 meter due to the line source. Along the x axis, the signal wave can be expressed as

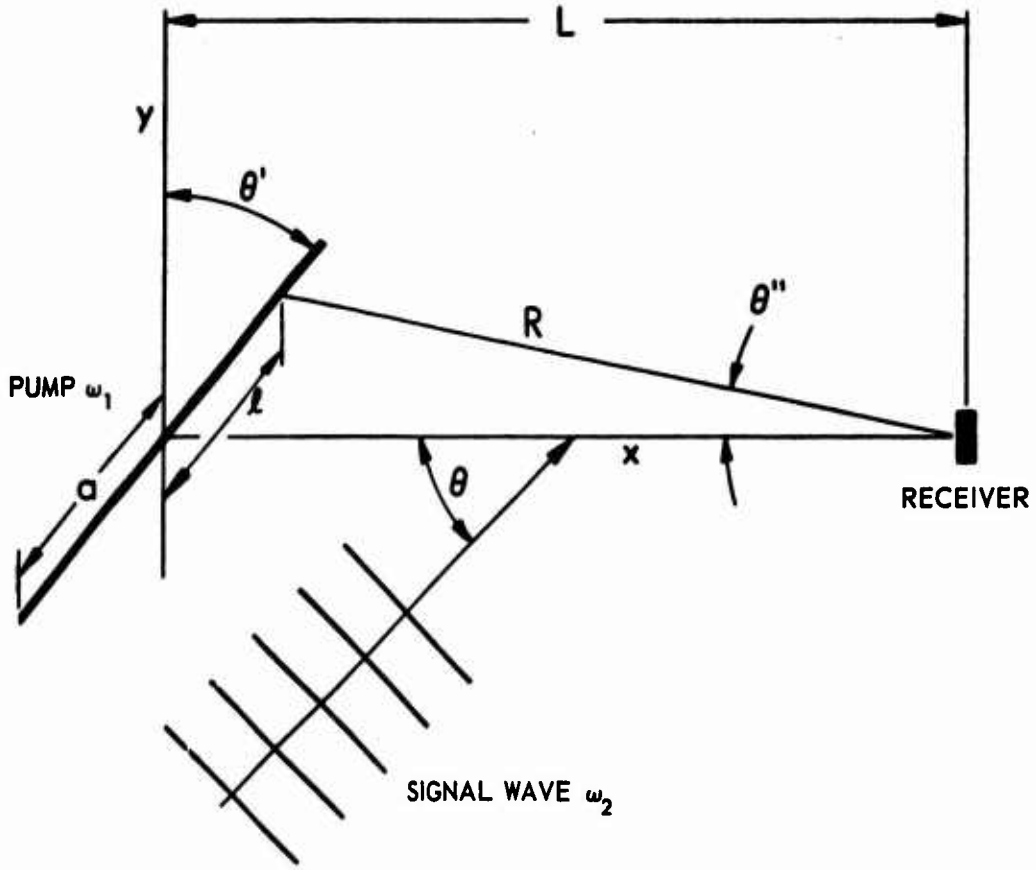

FIGURE 4.1
A PARAMETRIC RECEIVING ARRAY
WITH A LINE SOURCE PUMP

$$p_2 = P_{12} \exp\left[-(\alpha_2 - jk_2)r \cos\theta + j\omega_2 t\right] \tag{4.2}$$

This plane wave must be expressed in terms of the new coordinate system $(\underline{r},\underline{\theta})$ which is rotated by θ'' and translated by (ℓ,θ'). The position vector in the new coordinate system is

$$\begin{aligned}\vec{\underline{r}} = &[\cos\theta''\ (x-\ell\sin\theta') - \sin\theta''\ (y-\ell\cos\theta')]\vec{\underline{i}} \\ &+[\sin\theta''\ (x-\ell\sin\theta') + \cos\theta''\ (y-\ell\cos\theta')]\vec{\underline{j}}\end{aligned} \tag{4.3}$$

where $\vec{\underline{i}}$ and $\vec{\underline{j}}$ are the basis vectors for the new coordinate system. The plane wave vector in the new coordinate system is

$$\vec{\underline{k}}_2 = k_2 \cos(\theta''+\theta)\vec{\underline{i}} + k_2 \sin(\theta''+\theta)\vec{\underline{j}} \tag{4.4}$$

and then $\vec{\underline{k}}_2 \cdot \vec{\underline{r}}$ is given by

$$\vec{\underline{k}}_2 \cdot \vec{\underline{r}} = \vec{k}_2 \cdot \vec{r} - k_2\ell \sin(\theta+\theta') \quad . \tag{4.5}$$

The plane wave pressure expressed in terms of $\underline{r},\theta,\theta'$, and θ'' is

$$p_2 = P_{12} \exp\left\{-(\alpha_2 - jk_2)[\underline{r}\cos(\theta+\theta'') + \ell\sin(\theta+\theta')]\right\} \quad . \tag{4.6}$$

Then from Equation (3.46) the sum and difference frequency sound pressure at L is

$$\begin{aligned}\delta p(L,\theta,\theta',\theta'') = &-\frac{(\omega_1 \pm \omega_2)\beta P_{11} P_{12}}{2a(2\rho_o c_o^3)}\,\delta\ell \exp\left\{-\alpha_2\ell\sin(\theta+\theta') - (\alpha_\pm - jk_\pm)R\right\} \quad . \\ &\cdot \exp\left[\pm jk_2\ell\sin(\theta+\theta') \mp j\frac{k_2R}{2}(1-\cos(\theta+\theta''))\right] \\ &\cdot \frac{\sin\left[\frac{k_2R}{2}(1-\cos(\theta+\theta''))\right]}{\frac{k_2R}{2}(1-\cos(\theta+\theta''))}\end{aligned} \tag{4.7}$$

where $\beta = 1 + \frac{B}{2A}$.

Using the farfield approximation for a line source, we have

$$R = \frac{L-\ell \sin\theta'}{\cos\theta''} \cong L - \ell \sin\theta' \tag{4.8}$$

for the phase and amplitude terms of the elemental pressure. Then the elemental pressure can be shown to be

$$\delta p(L,\theta,\theta') = \frac{-(\omega_1 \pm \omega_2)\beta P_{11} P_{12} \delta\ell}{2a(2\rho_o c_o^3)} \cdot \exp\left[-(\alpha_\pm - jk_\pm)L\right]\exp\left[\mp jM + jA\ell - j\omega_\pm t\right] \frac{\sin(M+\ell C)}{M+\ell C} \tag{4.9}$$

where

$$A = \pm \frac{k_2}{2} \sin(\theta+\theta') \pm \frac{k_2}{2} \sin\theta' - k_\pm \sin\theta' \quad , \tag{4.10}$$

$$C = \frac{k_2}{2} [-\sin\theta' + \sin(\theta+\theta')] \quad , \text{ and} \tag{4.11}$$

$$M = \frac{k_2}{2} [L(1 - \cos\theta)] \quad . \tag{4.12}$$

The total pressure can be obtained by integrating over ℓ such that

$$p(L,\theta,\theta') = \frac{-(\omega_1 \pm \omega_2)\beta P_{11} P_{12}}{2\rho_o c_o^3} \exp\left[-(\alpha_\pm - jk_\pm)L\right] \cdot \frac{1}{2a} \int_{-a}^{a} \exp[\mp jM + jA\ell] \frac{\sin(M+\ell C)}{M+\ell C} \, d\ell \quad . \tag{4.13}$$

If we assume that $\sin(M+\ell C)/M+\ell C$ is a slowly varying function of ℓ,

$$p(L,\theta,\theta') \cong \frac{-(\omega_1 \pm \omega_2)\beta P_{11} P_{12}}{2\rho_o c_o^3} \exp\left[-(\alpha_\pm - jk_\pm)L \mp jM - j\omega_\pm t\right] \frac{\sin aA}{aA} \frac{\sin M}{M} \quad . \tag{4.14}$$

The maximum amplitude for $\theta=0$ is

$$\hat{p} = \frac{-(\omega_1 \pm \omega_2)\beta P_{11} P_{12}}{2\rho_o c_o^3} \exp[-(\alpha_\pm L)] \quad . \tag{4.15}$$

The approximation used in Equation (4.14) can be eliminated by direct integration of Equation (4.13).

The pressure can be expressed as

$$p = \frac{\hat{p}}{2a} \exp\left[+jk_\pm L \mp jM - j\omega_\pm t\right] \cdot \int_{-a}^{a} \exp[jA\ell] \quad . \tag{4.16}$$

$$\frac{\left[\exp[j(M+C\ell)] - \exp[-j(M+C\ell)]\right]}{2j(M+C\ell)} \delta\ell \quad ,$$

and with a change of variables, we have

$$p = \frac{\hat{p}}{(2a)(2C)} \exp\left[+jk_\pm L \mp jM - \frac{jMA}{C}\right] \left\{ \int_{y_1}^{y_2} \frac{\exp(jy)}{2jy}\, dy - \int_{y_3}^{y_4} \frac{\exp(jy)}{2jy}\, dy \right\}$$

$$= \frac{\hat{p}}{(2a)(2C)} \exp\left[+jk_\pm L \mp jM - \frac{jMA}{C}\right] \left\{ -j\left[Ci(y_2) - Ci(y_1) - Ci(y_4) + Ci(y_3)\right] \right.$$

$$\left. + \left[Si(y_2) - Si(y_1) - Si(y_4) + Si(y_3)\right] \right\} \tag{4.17}$$

where $Ci(y)$ is the cosine integral, $Si(y)$ is the sine integral,

$$\begin{aligned} y_1 &= \frac{(A+C)}{C}(M-aC) \quad , \\ y_2 &= \frac{(A+C)}{C}(M+aC) \quad , \\ y_3 &= \frac{(A-C)}{C}(M-aC) \quad , \text{ and} \\ y_4 &= \frac{(A-C)}{C}(M+aC) \quad . \end{aligned} \tag{4.18}$$

In order to evaluate the cosine integral in the case when a pair of the y_i's are zero, the limit as each y_i approaches zero must be taken in order to obtain a solution. Likewise, if any y equals 0 over the range of integration, Cauchy's integral formula must be used to obtain the value of the integral.

Computed results using Equation (4.17) will be presented in Chapter VI. The basic properties of a parametric receiving array using a line source pump can best be seen by an examination of Equation (4.14). The amplitude is seen to be independent of range except for absorption. This result is subject to the condition that we are in the farfield of the pump transducer. However, the interaction from the nearfield region of the transducer is included in the result.

Further examination of the expression for the second-order pressure indicates that we have a directivity function which is a product of two functions; one function is $\frac{\sin M}{M}$, where $M = \frac{k_2}{2} L(1 - \cos\theta)$, which is the directivity function of an end-fire array of length L. This function is the same as the directivity function for two plane waves interacting over some distance L. The second function $\frac{\sin aA}{aA}$, where

$$A = \pm \frac{k_2}{2} \sin(\theta+\theta') \pm \frac{k_2}{2} \sin\theta' - k_{\pm} \sin\theta' \quad ,$$

is an interesting one because this function includes both θ and θ'. For the case when $\theta = 0$ the dependence of the directivity function on θ' is the same as that of the original pump wave. This result does not agree with the results of a previous investigation by Rogers et al., in which the second-order sound field was predicted to have the properties of the pump wave as if it were operated at the sum or difference frequency. We

shall examine this result further in Chapter VI when it is compared to experimental data. With further examination of the expression for A we see that the array directivity function as the angle θ is changed will be modified for various values of θ'. This result is also in conflict with the result predicted by Rogers et al. This result will also be compared extensively with experimental data since it allows us to examine the problem of scattering of sound by sound when the two waves are propagating at nonzero angles.

When θ' is zero, we observe that the low frequency directivity of the parametric receiving array will be modified slightly by the expression

$$\frac{\sin aA}{aA} \quad .$$

This modification is less than one might intuitively expect. The reduction in the side lobes is less than that produced by taking the product of the directivity function of the end-fire array and directivity function of the pump at the signal frequency.

B. Solution for a Line Hydrophone and a Point Source Pump

As in the previous example, we shall use the point source solution as a starting point. In the solution for the point source pump, a small point receiver is assumed. Using the geometry shown in Fig. 4.2, we shall consider response of a line hydrophone of length 2a consisting of an infinite number of point receivers lying in the (x,y) plane. The propagation vector for the low frequency wave is also in the (x,y) plane.

The receiving sensitivity due to an elemental length $\delta\ell$ at $\vec{r}$ is

$$\delta M_c(\omega) = \frac{M_c(\omega)\delta\ell}{2a} \qquad (4.19)$$

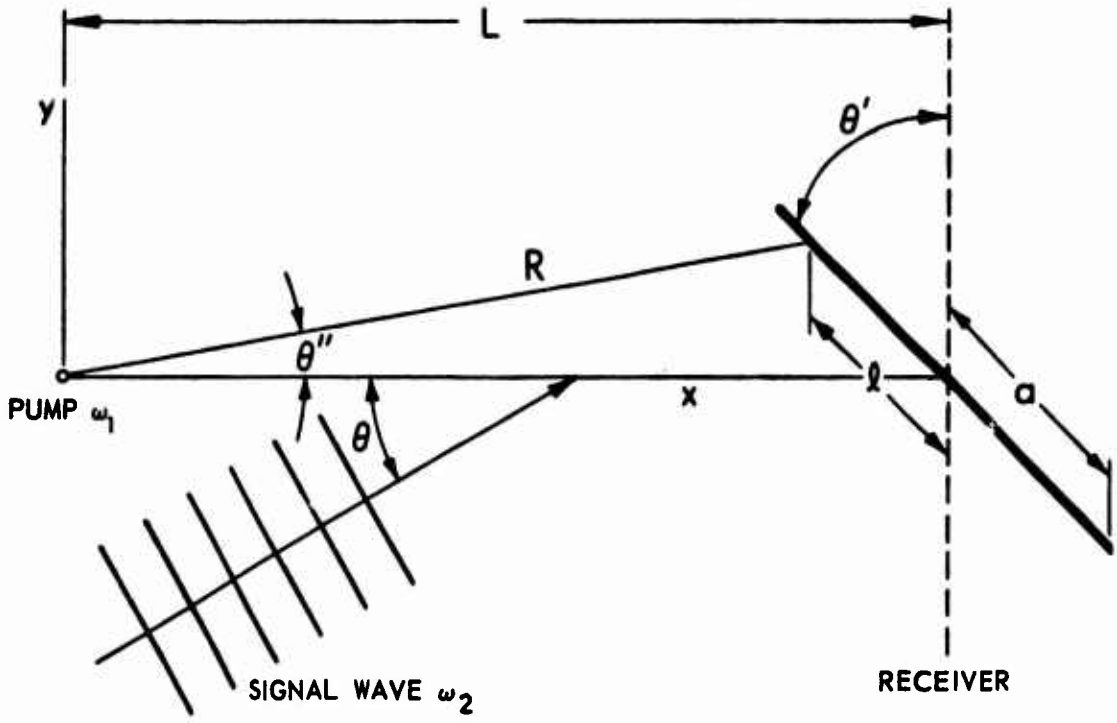

FIGURE 4.2
A PARAMETRIC RECEIVING ARRAY
WITH A LINE RECEIVER

where $M_c(\omega)$ is the receiving response of the line in volts per micropascal to a plane wave of frequency ω propagating in a direction perpendicular to the line.

The high frequency pump wave has the form

$$p_{11} = j \frac{P_{11}}{R} \exp[-(\alpha_1 R - jk_1 R) - j\omega_1 t] \tag{4.20}$$

where P_{11} is the farfield pressure referred to 1 meter. The signal wave at $(r,\theta")$ can be expressed as

$$p_{12} = P_{12} \exp[-(\alpha_2 - jk_2) r \cos(\theta - \theta") - j\omega_2 t] \quad . \tag{4.21}$$

The second-order pressure at $(r,\theta")$ is

$$p_2(R,\theta") = \frac{(\omega_1 \pm \omega_2)}{2\rho_o c_o^2} \beta P_{11} P_{12}$$

$$\cdot \exp\left\{-(\alpha_\pm - jk_\pm) R \pm jk_2 R \frac{(1 - \cos(\theta - \theta"))}{2} - j\omega_\pm t\right\} \tag{4.22}$$

$$\cdot \frac{\sin\left[k_2 R \left(\frac{1 \cos(\theta - \theta")}{2}\right)\right]}{k_2 R \left(\frac{1 - \cos(\theta - \theta")}{2}\right)} \quad .$$

Again using the farfield approximation, we have

$$R = \frac{L - \ell \sin\theta'}{\cos\theta'} \cong L - \ell \sin\theta' \tag{4.23}$$

for the phase and amplitude term. The elemental voltage generated by the second-order sound pressure is

$$\delta E = - \frac{M_c \delta \ell}{2a} \frac{(\omega_1 \pm \omega_2)\beta P_{11} P_{12}}{2\rho_o c_o^2} \tag{4.24}$$

$$\cdot \exp\left[-(\alpha_\pm - jk_\pm) L - j\omega t\right]$$

$$\cdot \exp\left[\mp j \frac{k_2}{2} [L(1 - \cos\theta)] + jB\ell\right] \cdot \frac{\sin(M + \ell D)}{M + \ell D}$$

where

$$B = \pm \frac{jk_2}{2} \sin(\theta-\theta') \pm jk_2 \frac{\sin\theta'}{2} - k_\pm \sin\theta' \quad , \tag{4.25}$$

$$D = [-\sin\theta' + \sin(\theta-\theta')] \quad , \text{ and} \tag{4.26}$$

$$M = \frac{k_2}{2}[L(1 - \cos\theta)] \quad . \tag{4.27}$$

The total voltage can be obtained by integrating over ℓ, yielding

$$E = -\frac{(\omega_1 \pm \omega_2)\beta P_{11} P_{12}}{2\rho_o c_o^3} M_c \exp\left[-(\alpha_\pm - jk_\pm)L - j\omega_\pm t\right]$$

$$\cdot \frac{1}{2a} \int_{-a}^{a} \exp[jM + jB\ell] \frac{\sin(M+\ell D)}{(M+\ell D)} d\ell \quad . \tag{4.28}$$

If we assume that $\frac{\sin(M+\ell D)}{M+\ell D}$ is a slowly varying function of ℓ, we have

$$E \cong -\frac{(\omega_1 \pm \omega_2)\beta P_{11} P_{12} M_c}{2\rho_o c_o^3} \exp\left[-(\alpha_\pm - jk_\pm)L \mp jM - j\omega_\pm t\right]$$

$$\cdot \frac{\sin aB}{aB} \frac{\sin M}{M} \quad . \tag{4.29}$$

The maximum amplitude for $\theta = 0$ is

$$E_{max} = -\frac{(\omega_1 \pm \omega_2)\beta P_{11} P_{12} M_c}{\rho_o c_o^3} \exp[-\alpha_\pm L] \quad . \tag{4.30}$$

The approximation used in Equation (4.29) can be eliminated by direct integration of Equation (4.28).

The received voltage can be expressed as

$$E = \frac{E_{max}}{2a} \exp\left[+jk_{\pm}L \mp jM - j\omega_{\pm}t\right] \tag{4.31}$$

$$\cdot \int_{-a}^{a} \exp[jB\ell]\left\{\frac{\exp[j(M+D\ell)] - \exp[-j(M+D\ell)]}{2j(M+D\ell)}\right\}\delta\ell$$

and with a change of variables we have

$$E = \frac{E_{max}}{2a(2D)} \exp\left[+jk_{\pm}L \mp jM + j\,\frac{MB}{D} - j\omega_{\pm}t\right] \tag{4.32}$$

$$- j[Ci(y_2) - Ci(y_1) - Ci(y_4) + Ci(y_3)]$$

$$+ [Si(y_2) - Si(y_1) - Si(y_4) + Si(y_3)]$$

where Ci(y) is the cosine integral, Si(y) is the sine integral,

$$\begin{aligned} y_1 &= \frac{(B+D)}{D}(M-aD) \quad , \\ y_2 &= \frac{(B+D)}{D}(M+aD) \quad , \\ y_3 &= \frac{(B-D)}{D}(M-aD) \quad , \text{ and} \\ y_4 &= \frac{(B-D)}{D}(M+aD) \quad . \end{aligned} \tag{4.33}$$

The solution for a line receiver is very similar to the solution for the line pump. However, upon examination of Equation (4.29), we note that there is an important difference. The beam pattern obtained by varying θ' with $\theta = 0$ is the same as that obtained by the line receiver at the sum or difference frequency. When θ' is equal to 0, the parametric receiving array beam pattern is the same as that found for a line source pump. These properties will be demonstrated in Chapter VI when we compare the experimental and theoretical results.

C. Solutions for the Parametric Receiving Array for Pump Source with Two Finite Dimensions

We shall now consider the interaction of a pump wave produced by a rectangular piston with one dimension which is small compared to signal frequency wavelength, and a second dimension which can be a wavelength or more at the signal frequency. The planar radiator with dimensions 2a and 2b is assumed to have an angle θ' with respect to the plane x = 0 as shown in Fig. 4.3. The observer is in the plane z = 0. From Equation (4.17), the solution for an elemental area of length 2a and height δz for z = 0 is

$$\delta p = \frac{\delta M \hat{p}}{(2b)\ 2a\ 2C} \left| \exp\left[-(\alpha_1 - jk_\pm)\ L \mp jM - \frac{jMA}{C} - j\omega_\pm t\right] \right| \cdot \left| -j[Ci(y_2) - Ci(y_1) - Ci(y_4) + Ci(y_3)] + [Si(y_2) - Si(y_1) - Si(y_4) + Si(y_3)] \right| \quad (4.34)$$

where y_i is as defined in Equation (4.18).

If 2b is small compared to wavelength, the contributions from the various elemental areas 2a δM will be equal for a given δM in the farfield of the radiator since R' $\cong$ L and $\theta''' \cong 0$ for small values of M.

The total pressure is the same as that found in Equation (4.17). If 2a is small compared to the signal frequency wavelength,

$$p = -\frac{(\omega_1 \pm \omega_2)\beta P_{11} P_{12}}{2\rho_o c_o^3} \exp\left[-(\alpha_\pm - jk_\pm)\ L \mp jM - j\omega_\pm t\right] \cdot \frac{\sin aA}{aA} \frac{\sin M}{M} \quad . \quad (4.35)$$

We shall now consider a circular piston pump transducer with a radius which is small compared to a signal frequency wavelength. The geometry for this solution is shown in Fig. 4.4. Again we shall use the

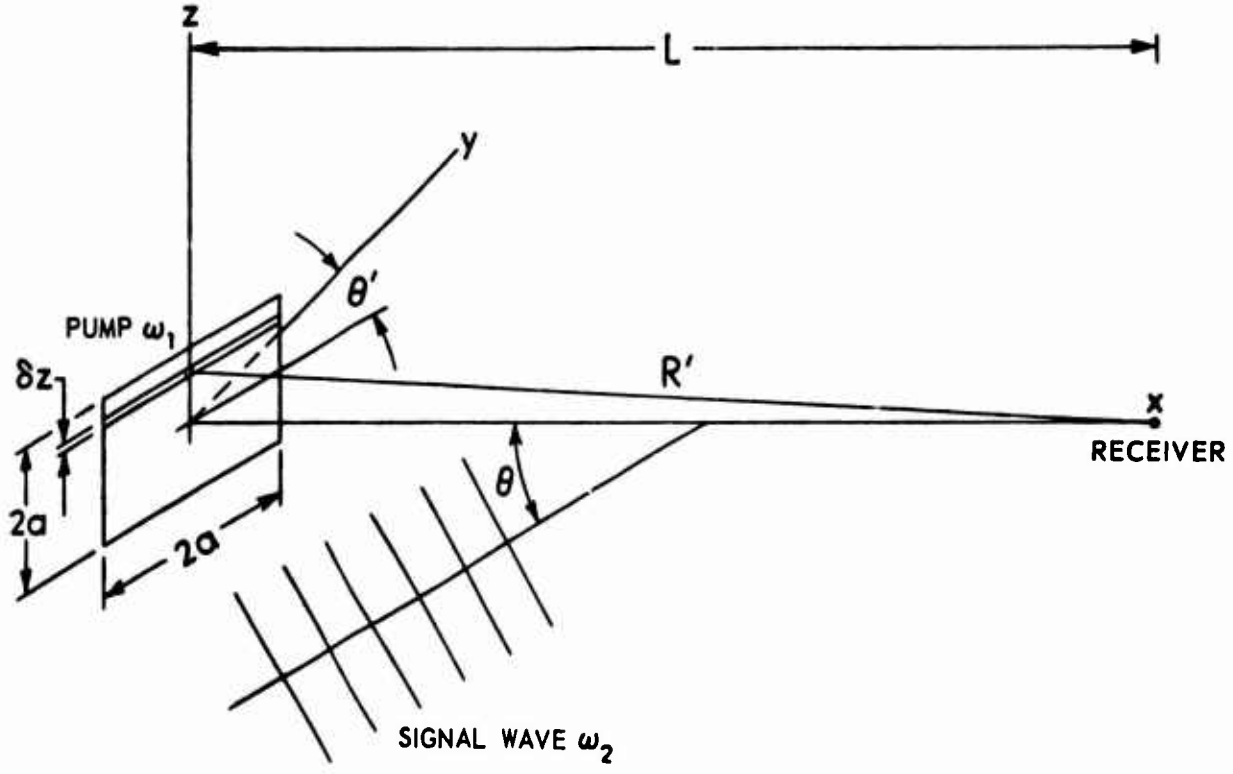

FIGURE 4.3
A PARAMETRIC RECEIVING ARRAY
WITH A SMALL PISTON PUMP

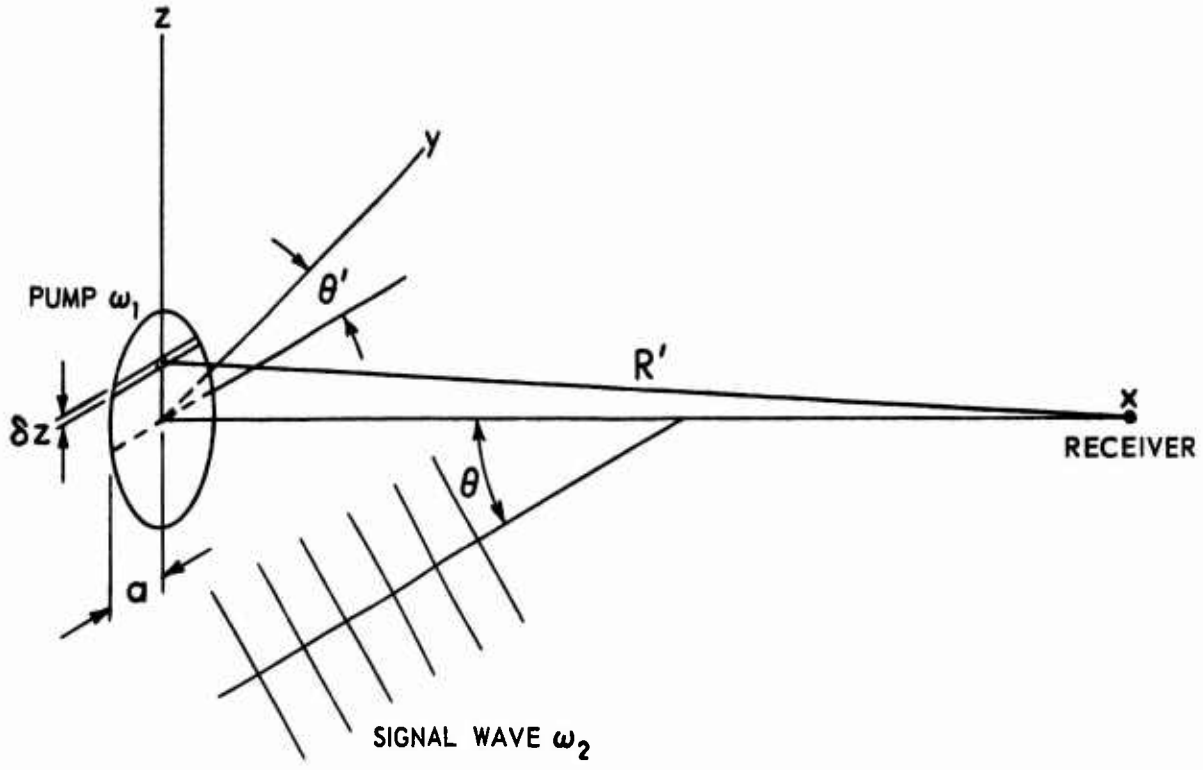

FIGURE 4.4
A PARAMETRIC RECEIVING ARRAY
WITH A CIRCULAR PISTON PUMP

solution for a line source as a starting point. In the farfield R' is approximately equal to L, and the pressure contribution from a line source of length $\sqrt{a^2-z^2}$ and width of δz is given by

$$\delta p = - \frac{(\omega_1 \pm \omega_2)\beta P_{11} P_{12}}{2\rho_o c_o^3} \left(2 \frac{\sqrt{a^2 - z^2}}{\Pi a^2} \right) \cdot \exp\left[-(\alpha_\pm - jk_\pm L \mp jM - j\omega_\pm t) \cdot \frac{\sin M}{M} \cdot \frac{\sin \sqrt{a - z^2}\, A}{\sqrt{a^2 - z^2}\, A} \right] \delta z \tag{4.36}$$

where $\left(2 \frac{\sqrt{a^2 - z^2}}{\Pi a^2} \right)$ is the normalization for the area found by integrating the incremental area over $\delta \ell$ such that we have

$$\int_{-a}^{a} \int_{\frac{\delta z \ \delta \ell}{\sqrt{a^2 - z^2}}}^{\sqrt{a^2 - z^2}} = 2 \int_{-a}^{a} \frac{\sqrt{a^2 - z^2}}{\Pi a^2} \, dz \quad . \tag{4.37}$$

We now consider the integral

$$\int_{-a}^{a} \frac{2 \sin \sqrt{a^2 - z^2}\, A}{A \Pi a^2} \, dz \quad .$$

With a change of variables, this integral is

$$4 \int_0^1 \frac{t \sin (t\, a\, A)\, dt}{a \Pi A \sqrt{1 - t^2}} \quad .$$

This integral can be evaluated using Sonine's integral described by Watson.[63] This integral is a definition of a Bessel function of order m and has the form

$$J_m(x) = \frac{2x^{m-n}}{2^{m-n}\Gamma(M-n)} \int_0^1 J_n (xt)\, t^{n+1} (1-t^2)^{m-n-1} \, dt \tag{4.38}$$

where $J_m(x)$ is a Bessel function of order M,

Γ is the Gamma function, and

$J_n(xt)$ is a Bessel function of order n.

For $n = \frac{1}{2}$ and M = 1, this integral has the form

$$J_1(x) = \frac{2}{\pi} \int_0^1 \frac{t \sin(xt)}{\sqrt{(1-t^2)}}\, dt \quad . \tag{4.39}$$

Using Equation (4.39), we have

$$\frac{4}{(aA)\pi} \int_0^1 \frac{t \sin(taA)}{\sqrt{1-t^2}}\, dt = \frac{2\, J_1(aA)}{aA} \quad . \tag{4.40}$$

The second-order pressure for a circular pump source is then found to be

$$p = - \frac{(\omega_1 \pm \omega_2)\beta P_{11} P_{12}}{2\rho_o c_o^3} \exp\left[-(\alpha_\pm - jk_\pm L) \mp jM - j\omega_\pm t\right] \tag{4.41}$$

$$\cdot \frac{\sin M}{M} \frac{2\, J_1(aA)}{aA} \quad .$$

The amplitude of the pressure expressed in Equation (4.41) is the same as that found for a rectangular piston transducer. The directivity function is a product of the end-fire array function and the function $\frac{2\, J_1(aA)}{2A}$. The function $\frac{2\, J_1(aA)}{2A}$ resembles the directivity function for a circular piston found in linear theory. For the second-order sound pressure, A replaces the expression $k_1 \sin \theta'$. The properties of the parametric array receiving with a circular piston pump for various θ and θ' are seen to be very similar to these properties of a parametric receiving array with a square piston pump if we take into account the difference in the shape of each aperture.

V. EXPERIMENTAL APPARATUS

The experimental study of the parametric receiving array was conducted aboard the STEP Barge at the Applied Research Laboratories Lake Travis Test Station. This barge, designed for testing large sonar transducers, has heavy handling equipment available for moving and rotating large transducer arrays and electronic instrumentation to do acoustical and electrical performance testing on these transducers.

The STEP Barge is moored in 100 ft of water on Lake Travis, a fresh water lake about 25 miles west of Austin, Texas.

The mechanical and electrical apparatus used for the parametric receiving array experiments is described in the following two sections.

A. Mechanical Apparatus

An overall view of the parametric receiving array is shown in Fig. 5.1. The parametric receiving array was suspended below the STEP Barge using an aluminum I-beam attached to a column which could be rotated. The low frequency source used to generate the signal wave was located on a second barge some 325 ft away from the center of the parametric receiving array.

In Fig. 5.2, we see a close-up of the parametric receiving array. The beam used for supporting the two transducers was constructed so that the two ends could be lifted for removal or replacement of the transducers with the column in place in the water. Support brackets were mounted on either end of the I-beam for the placement of the two transducers. The separation distance between the two transducers was

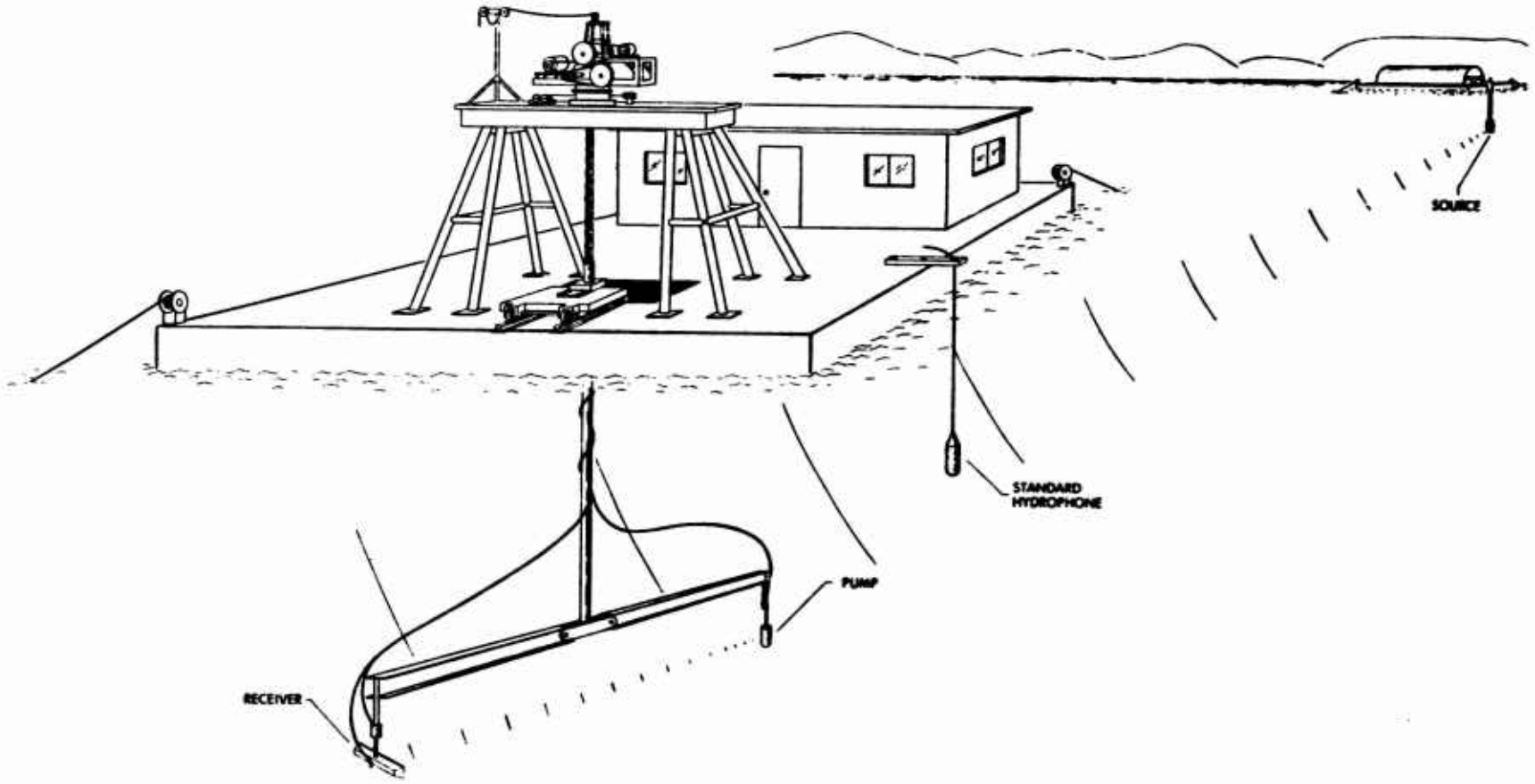

FIGURE 5.1
NONLINEAR PARAMETRIC RECEIVING ARRAY EXPERIMENT

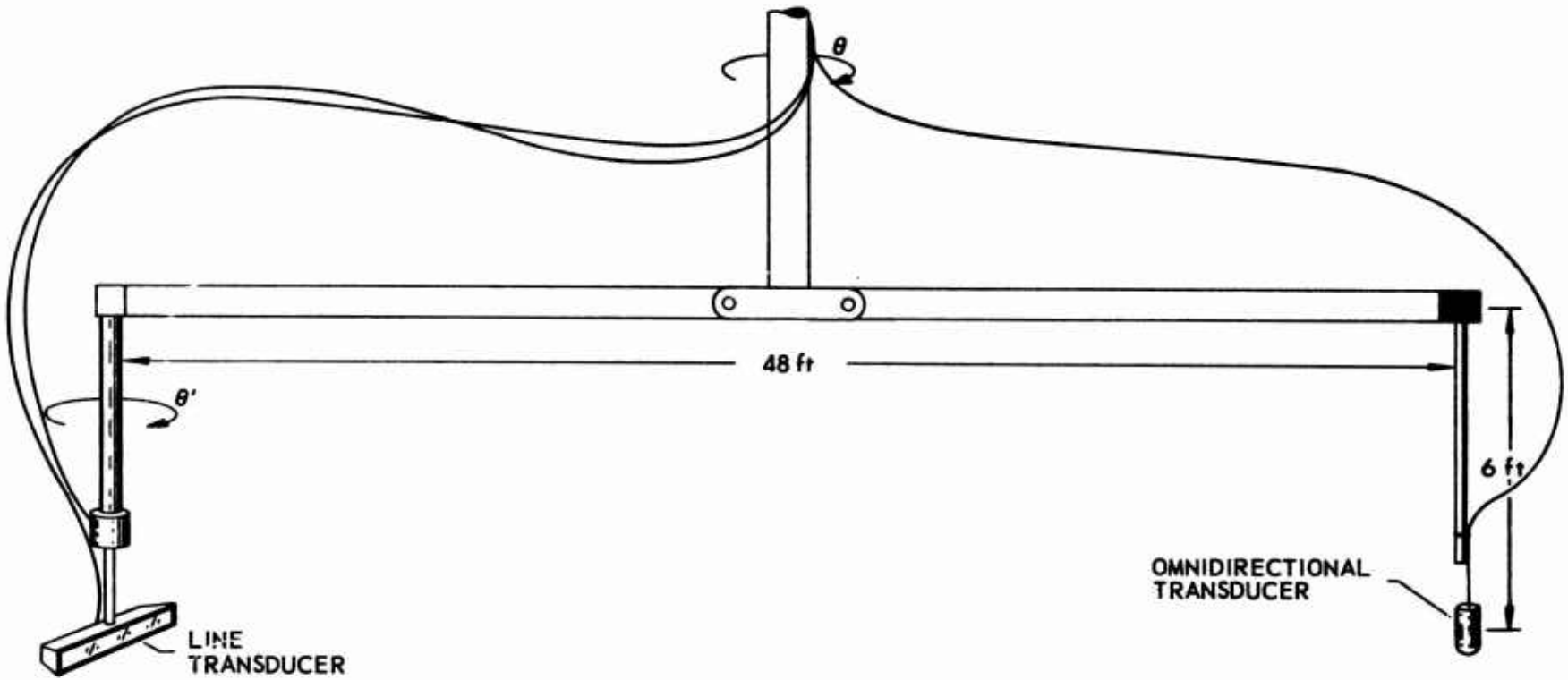

FIGURE 5.2
DETAILED VIEW OF THE PARAMETRIC RECEIVING ARRAY

adjustable. For the experiments described in the next chapter, the transducers were placed a fixed 48 ft distance apart and equidistant from the support column. The support on one end of the beam had a small rotator. The angle of rotation of the transducer mounted on this end corresponded to θ' in the theoretical model. The I-beam was rotated by the column mechanically coupled to a synchro. The angle measured by this synchro corresponded to the angle θ in the theoretical model. The two transducers for the parametric receiving array were mounted 6 ft below the I-beam in order to minimize the effects of acoustical reflections. The I-beam was supported 27 ft below the water surface, so that the parametric receiving array was 33 ft below the water surface.

B. The Measurement System for the Parametric Receiving Array

An overall block diagram for the system used for the parametric receiving array experiments is shown in Fig. 5.3. The pump transducer was driven by a power amplifier with a CW signal generated by a precision crystal oscillator. The pump frequency remained fixed at 90 kHz throughout all of the experiments conducted in this study. Special care was taken to ensure that the side band noise level generated by the power amplifier was low in order to achieve a good signal-to-noise ratio at the side band frequencies. Figure 5.4 gives a breakdown of the receiving subsystem for the parametric receiving array. The signal from the hydrophone was fed directly into a crystal notch filter providing an 80 dB rejection of the carrier signal. The signal was then amplified and fed into a second crystal filter to further remove the carrier frequency. Two passive bandpass filters were used to select either of the side bands at the sum or difference frequency. A sampling digital voltmeter measured the rms

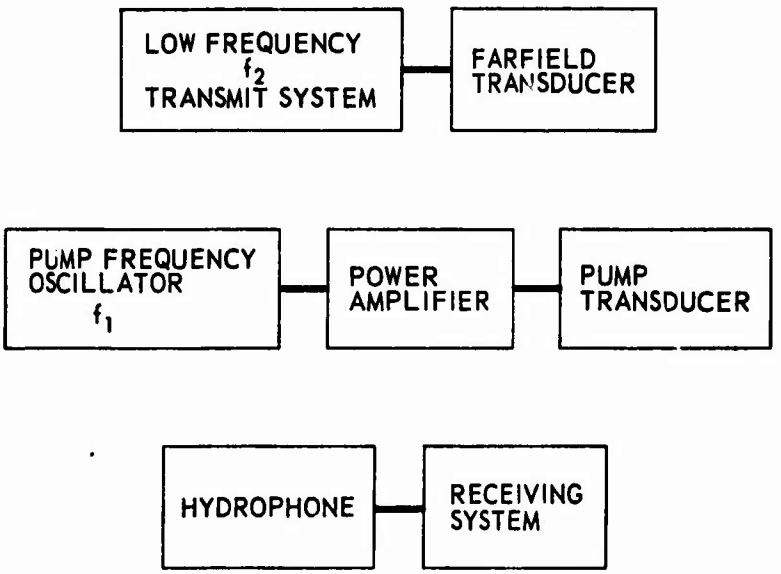

FIGURE 5.3
PARAMETRIC RECEIVING ARRAY BLOCK DIAGRAM

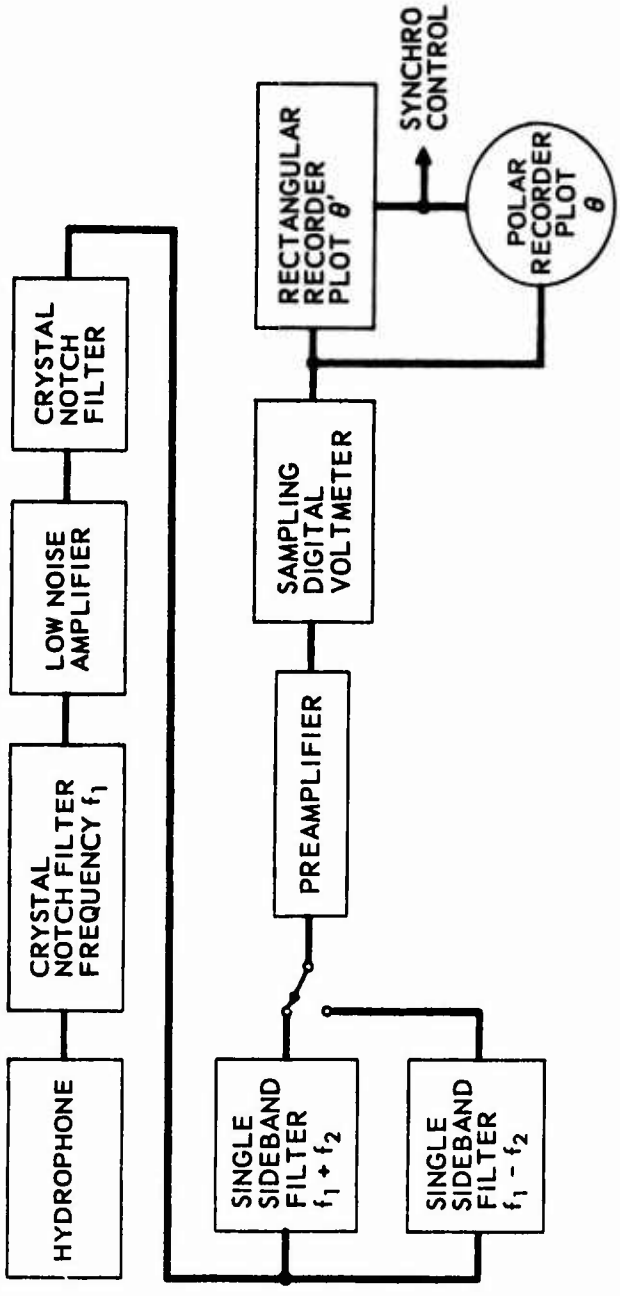

FIGURE 5.4
RECEIVING SUBSYSTEM FOR THE PARAMETRIC RECEIVING ARRAY

value of the side band signal at a specified time. For the calibration of the parametric receiving array, the voltage was read directly from the digital readout. Beam patterns were plotted on either a polar or rectangular plotter using the dc output of the sampling digital voltmeter. The dc output was also used with a portable voltohmmeter for the alignment of the various transducers during the experiments.

A block diagram of the low frequency source subsystem is shown in Fig. 5.5. A gated sine wave at the signal frequency was used to drive the farfield transducers. Special low pass filters were used on the input and output of the power amplifier, thereby eliminating noise at the side band frequencies of the parametric receiving array. The calibration of the parametric receiving array was achieved in several steps. First, the transducers used for absolute sound pressure level measurements were calibrated using the 3-transducer reciprocity calibration procedure described by Bobber.[64] A block diagram for the system used for this calibration is shown in Fig. 5.6. The calibration of the transducers was made with the transducers in place in order to minimize the errors caused by transducer misalignment. Two additional transducers were used to assist in the calibration: one was mounted on a movable trolley and the second was suspended by its cable at the center of the array. Since the crystal filter was coupled directly to the hydrophone, a second calibration was necessary to correct for the loading by the crystal filter. This calibration was accomplished using the comparison method. First, the open circuit voltage of the hydrophone was measured for a given acoustic pressure; then, the output voltage of the hydrophone, filter, and amplifier combination was measured at the various side band frequencies.

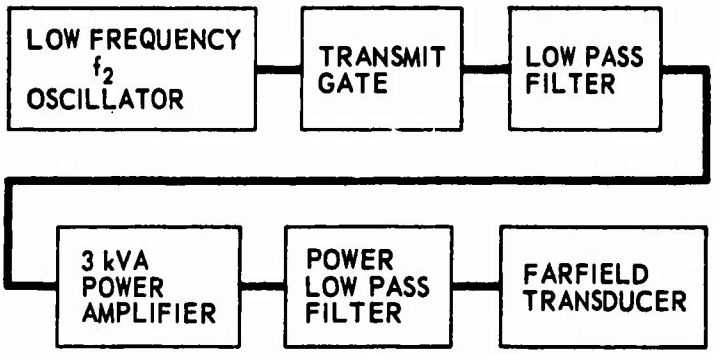

FIGURE 5.5
SIGNAL SOURCE TRANSMIT SUBSYSTEM

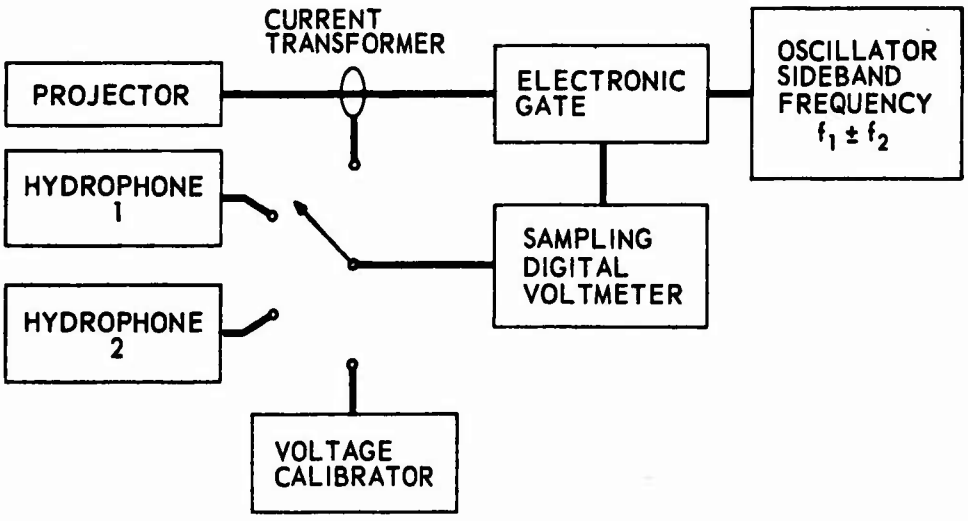

FIGURE 5.6
HYDROPHONE CALIBRATION SYSTEM

The low frequency signal pressure amplitude was measured using a low frequency standard hydrophone, also calibrated using the reciprocity calibration procedure. The low frequency signal had to be measured with great care because the signal propagated over a long distance to the parametric receiving array, and had to be measured early in the pulse before reflections from the surface arrived. On the other hand, the mechanical Q of the source transducer increased the rise time of the signal to several periods. Consequently, the number of cycles available for making a measurement was small. To ensure a good measurement of the low frequency signal, the sampling digital voltmeter was used in the PER INTEGRAL RMS mode. This mode makes the sample time an integral number of periods at the signal frequency. The timing for this measurement is derived from a reference signal from the low frequency oscillator. The low frequency standard hydrophone was placed immediately in front of the parametric receiving array as is illustrated in the overall system diagram (Fig. 5.1).

While great care was used to make the acoustical measurements, it should be mentioned that errors as great as ±2 dB could occur on any particular measurement because of uncertainties in the conditions in the medium. In our experiments, an attempt to improve this accuracy to better than ±2 dB was made by calibrating the various transducers in situ and by measuring the rms value of the signals in integral number of cycles using a sampling digital voltmeter with a measurement resolution of ±0.1 dB. These precautions still do not preclude the possibility of irregularities in the propagation medium.

Five types of transducers were used for the parametric receiving array experiments. They are as follows.

1. A rectangular transducer 18 in. long and 3 in. high for a pump and a receiver transducer.
2. A small standard transducer with an omnidirectional transducer beam pattern for a pump and receiver transducer.
3. A low frequency standard transducer.
4. A 4 in. piston transducer for a pump and a receiver transducer.
5. A broadband standard hydrophone.

An additional description of these transducers is given in Appendix B.

VI. COMPARISON OF THEORETICAL AND EXPERIMENTAL RESULTS FOR THE PARAMETRIC RECEIVING ARRAY

We shall now examine the theoretical results of Chapters III and IV in light of some experiments on the parametric receiving array. The parametric receiving array for these experiments had a fixed length of 48 ft, a limitation which was minimized by using various signal frequencies and various transducers for our experiments.

Unfortunately, one cannot measure the interaction of two infinite plane waves experimentally to compare to the theoretical model of Chapter III. We can, however, observe experimentally a spherically spreading wave generated by a point source interacting with a plane wave. Perhaps this case represents the physical situation in which the theory might best predict the experimental results. We shall likewise examine the performance of the parametric array with a rectangular piston pump with one dimension on the order of a wavelength at the signal frequency and one dimension that was small compared to a wavelength at the signal frequency. This case is interesting because it allows us to look at the preferred angle of propagation of the second-order sound field as predicted by t theory. The properties of a parametric receiving array using a line receiver were measured. A small piston pump was also examined to compare to the theory presented in Chapter IV. In each of these cases, the geometries of the theory and experiment were made to coincide, thereby facilitating comparison between the theory and experiment. These geometries are shown in Fig. 6.1.

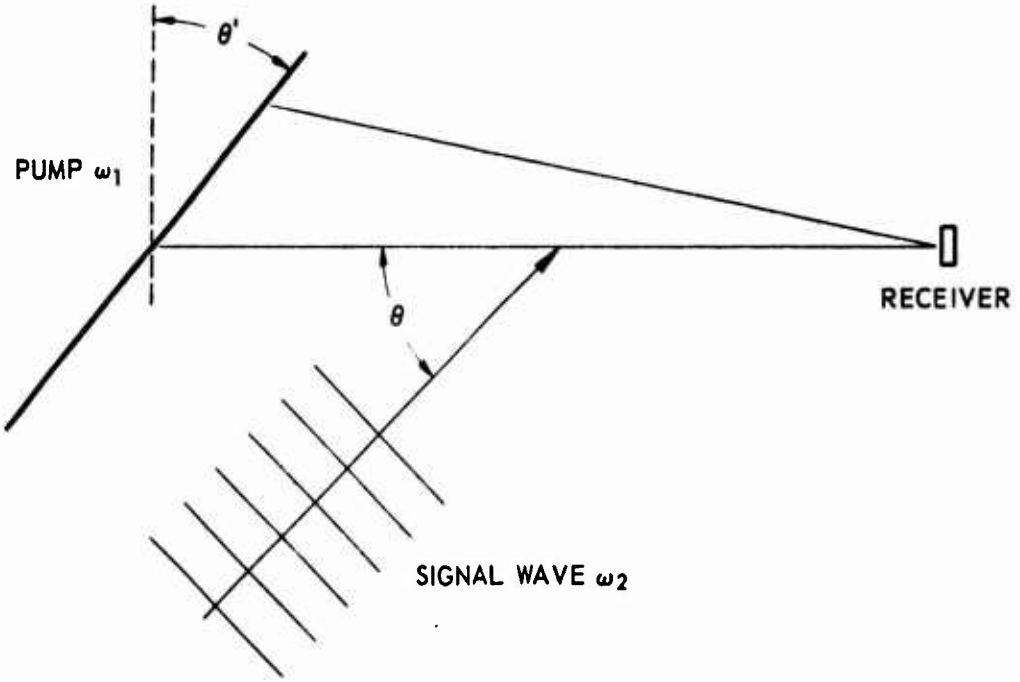

(a) A PARAMETRIC RECEIVING ARRAY
WITH A LINE SOURCE PUMP

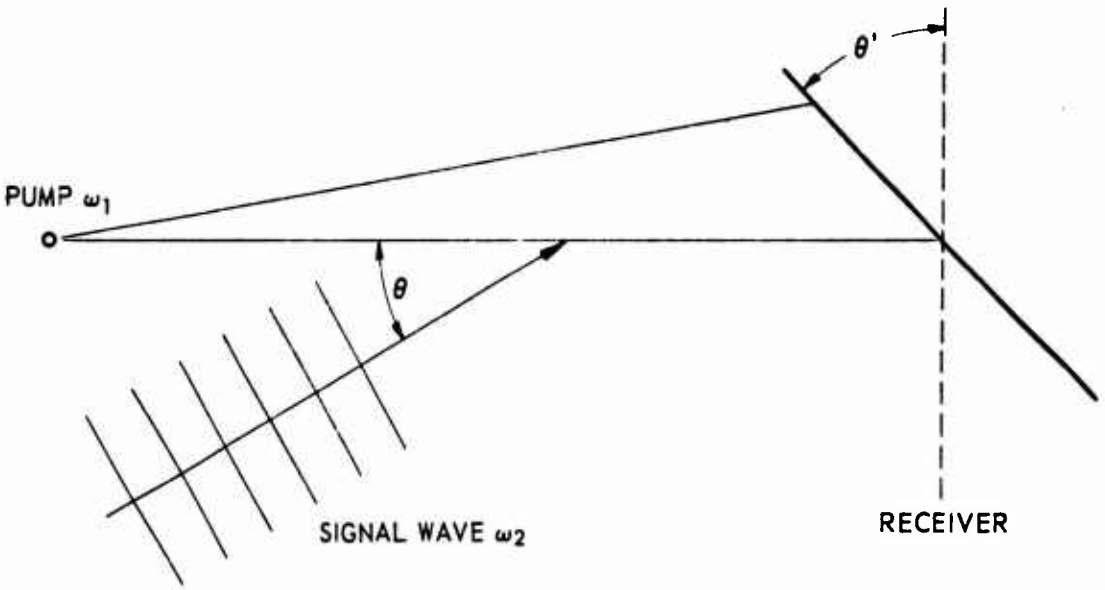

(b) A PARAMETRIC RECEIVING ARRAY
WITH A LINE RECEIVER

FIGURE 6.1
GEOMETRIES FOR THE PARAMETRIC
RECEIVING ARRAY EXPERIMENTS

A. Experiments Using a Point Source Pump

A small transducer which was omnidirectional in the horizontal plane was mounted rigidly 6 ft below one end of the parametric receiving array I-beam. On the opposing end of the I-beam, an assortment of transducers were mounted. These transducers included an omnidirectional transducer, a small piston transducer, and the rectangular transducer. Parametric receiving array beam patterns at 5 kHz for the omnidirectional pump transducer are shown in Fig. 6.2. These beam patterns were made using the 4 in. square piston transducer as the receiver. Additional beam patterns using the line transducer as a receiver, with the omnidirectional pump transducer, will be shown in Section VI.C. since our theoretical result showed that a large receiving transducer would modify the beam pattern.

The result from Equation (3.46) was used to calculate the theoretical beam pattern, and an HP 9830 computer program was written to plot this result. This program, listed in Appendix C, was also used to plot the theoretical beam patterns for the rectangular pump transducers. As can be seen, the theoretical model does predict the correct beam pattern for the parametric receiving array. The major lobe width and side lobe height and bearing were very close to that predicted by the theoretical model. This remarkable agreement between the theory and experiment leaves little doubt that this model is accurate for predicting the performance with an omnidirectional pump. However, the expression for the phase of the omnidirectional pump would not necessarily be verified by the excellent agreement of the amplitude. Amplitude measurements were made for the omnidirectional transducer using the procedures

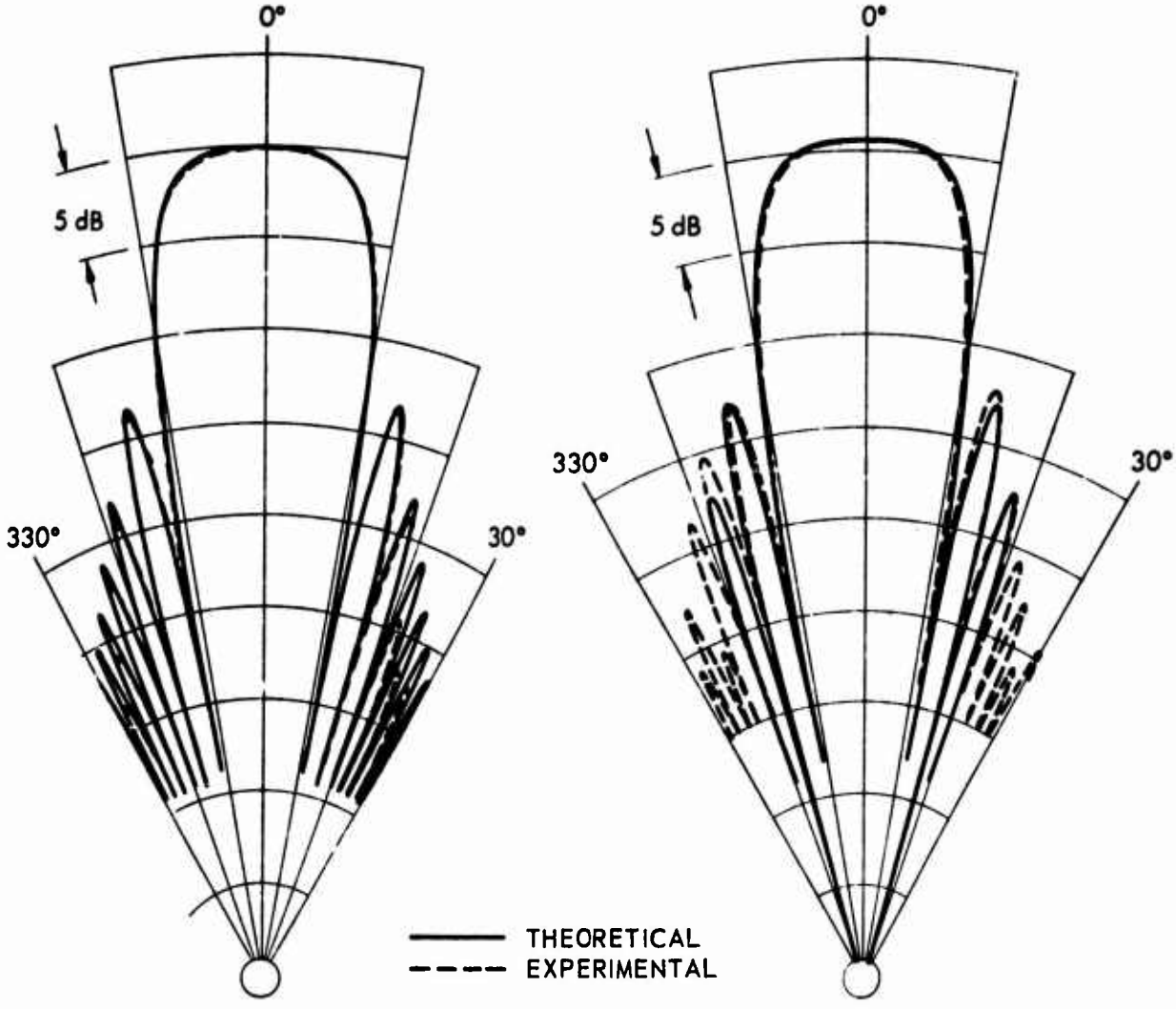

(a) SUM FREQUENCY

(b) DIFFERENCE FREQUENCY

FIGURE 6.2
PARAMETRIC RECEIVING ARRAY BEAM PATTERNS
USING AN OMNIDIRECTIONAL PUMP AT 5 kHz

described in Chapter V. Experimental measurements were also made using an omnidirectional receiver. The 3 dB beamwidth was found to be equal to that of the theoretical result. However, the signal-to-noise ratio was too low to measure the side lobe levels.

The sum frequency sound pressure level as a function of frequency is shown in Fig. 6.3. The sound pressure level has been normalized to the level for sound pressure levels of 0 dB re 1 μPa at 1 m for the pump pressure and 0 dB re 1 μPa for the signal pressure at the receiver. The theoretical curve for the sound pressure level was plotted using Equation (3.46) for θ=0.

The amplitude of the measured sound pressure was corrected to take into account the finite distance to the position of the low frequency source. This correction was predicted by Berktay and Shooter.[65] Taking into account the spherical nature of the low frequency wavefront, the second-order sound pressure for θ=0 is

$$p = \frac{(\omega_1 \pm \omega_2)(1 + \frac{B}{2A})}{2\rho_o c_o^3} P_{11} P_{12} \exp[-(\alpha_\pm)x_o] \frac{\ln(\frac{R}{R-L})}{(\frac{L}{R})} \quad ,$$

where R is the range of the low frequency source from the receiving transducer. For our experiment, the range correction was 0.63 dB. Berktay and Shooter also demonstrated that the discrepancies in beam patterns would be negligible if $\frac{R}{L} > 4$ and the array was rotated about its center. In our case, $\frac{R}{L}$ was approximately 7. For the computation of the sound pressure level, we used a value of 3.5 for $(1 + \frac{B}{2A})$ as predicted by Beyer, Coppens et al.,[66] for a water temperature of 70°F. Unfortunately, as was mentioned in Chapter V, the basic experimental error could be as large

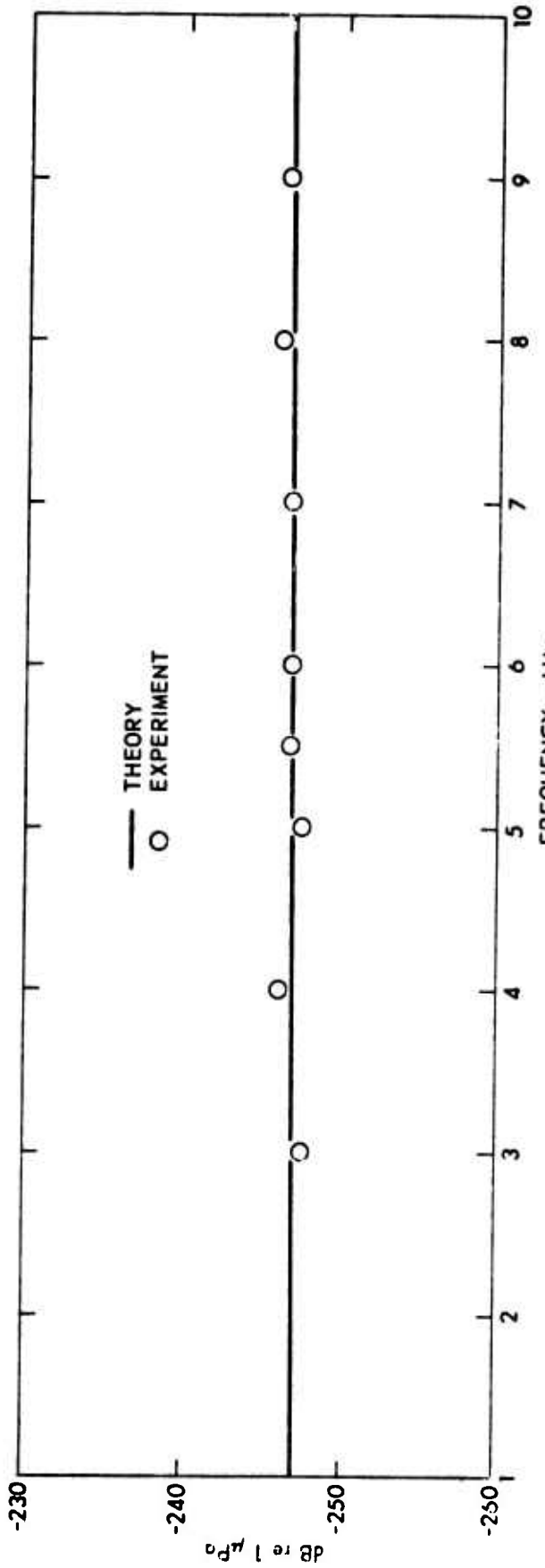

FIGURE 6.3
SUM FREQUENCY SOUND PRESSURE LEVEL FOR
AN OMNIDIRECTIONAL PUMP TRANSDUCER

as 2 dB, were the number of pressure measurements made taken into account. However, since careful measurements were made at several frequencies, the overall accuracy could be improved somewhat. The frequency response of the sum pressure is seen to have a frequency dependence of $(\omega_1+\omega_2)$. Some deviation in this dependence at the higher frequencies occurred due to a lower signal to noise ratio for the measurement signal caused by characteristics of the low frequency signal source.

The difference frequency sound pressure level is shown in Fig. 6.4. Again, this normalized sound pressure level has been corrected for the finite range of the low frequency sound.

B. Experiments on a Parametric Receiving Array with a Line Source Pump

In the experiment described now, a rectangular source was used as an approximation to a line source to study the properties of the second-order sound field. This rectangular transducer was constructed with bizonal shading to reduce the side lobes. The velocity of this type of acoustical source is not uniform across the aperture. The center portion of the transducer moves with twice the velocity of the ends of the aperture for a given drive voltage. This discrepancy between the theoretical model and experiment configuration will be eliminated by modifying the theory in Chapter IV to include the effects of bizonal shading. The sum of the results of two rectangular apertures will be summed: one is the full width of the transducer, generating a given farfield sound pressure level referenced to 1 m, and the second transducer aperture is smaller and has the appropriate length and amplitude weighting to give the approximate side lobe reduction of the active beam pattern. The amplitude of the sum

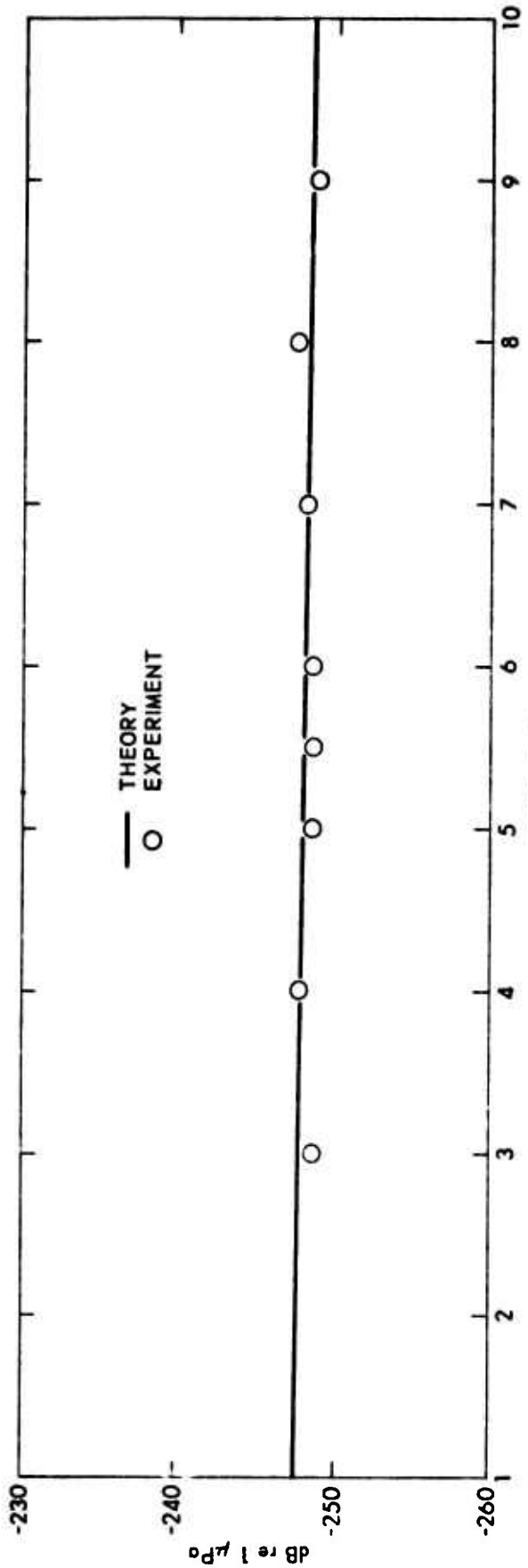

FIGURE 6.4
DIFFERENCE FREQUENCY SOUND PRESSURE LEVEL
FOR AN OMNIDIRECTIONAL PUMP TRANSDUCER

of the two sound pressures was adjusted to be P_1 referenced to 1 m, the value used in the theoretical result (Equations 4.14 and 4.17). The velocity amplitude of the center portion of the aperture was adjusted so that it had twice the velocity of the outer portion of the aperture. The fact that the correction for the shading can be easily made demonstrates the versatility of the theory that has been developed. The beam pattern for the narrowbeam pump transducer at 90 kHz is shown in Fig. 6.5. The results are plotted in rectangular coordinates to enhance the comparison between the theory and the experiment. The beam pattern was obtained by varying θ' and observing the pump signal. The bizonal shading of the transducer causes the usual beam pattern to be somewhat modified with a broader beam and lower side lobes for a given aperture. In this particular example, an outer aperture of 1.38 ft and an inner aperture of 0.78 ft was used.

An oscilloscope waveform of the sum and difference frequency side bands observed at the output of the second crystal filter is shown in Fig. 6.6(a). The signal frequency is 5 kHz and the pump frequency is 90 kHz. The pulse envelope of the difference frequency side band signal is shown in Fig. 6.6(b).

The sum and difference frequency sound pressure levels as a function of frequency are shown in Fig. 6.7 and Fig. 6.8. Again, the sound pressure level has been normalized for the sound pressure level of 0 dB re 1 μPa at 1 m for the pump pressure and 0 dB re 1 μPa for the signal pressure at the receiver. The correction for the finite range of the low frequency source was again incorporated in the result. The agreement between the theory and experiment was excellent. A value of 5

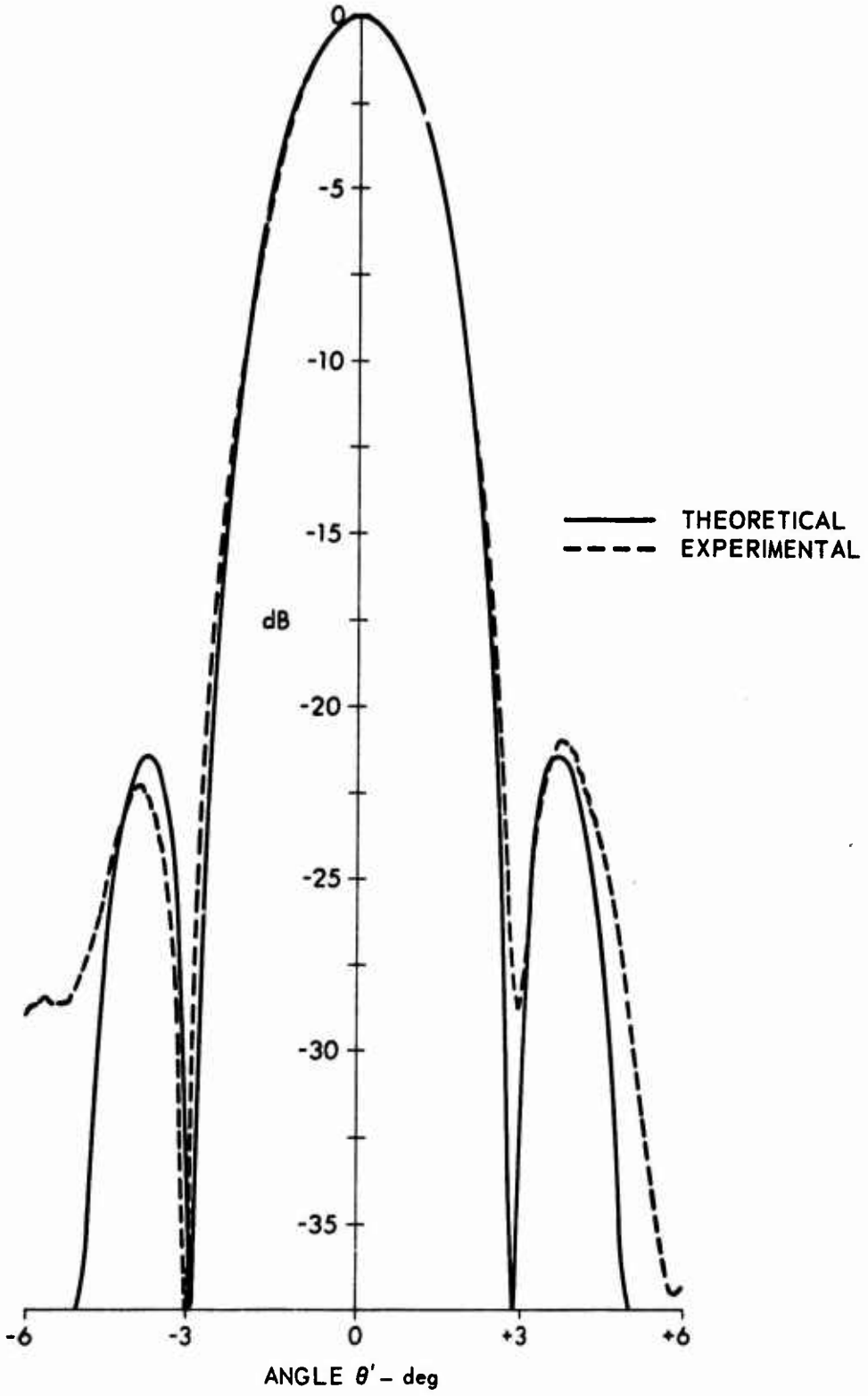

FIGURE 6.5
LINE SOURCE PUMP BEAM PATTERN

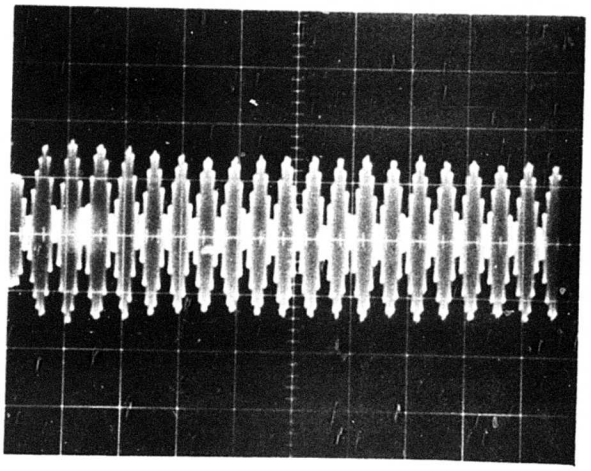

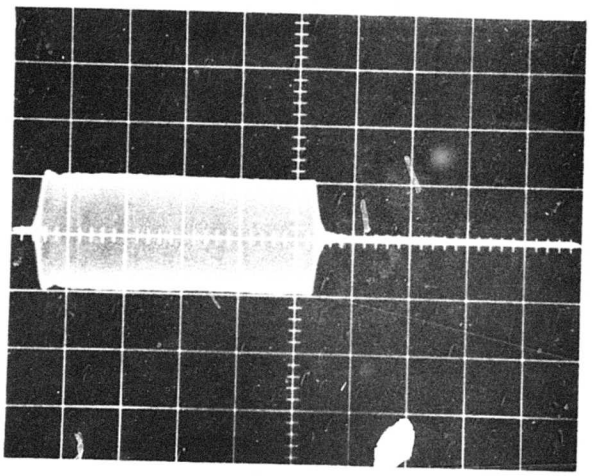

(b) DIFFERENCE FREQUENCY SIDEBAND

FIGURE 6.6
SIDEBAND SIGNALS AT THE OUTPUT OF THE CRYSTAL FILTERS

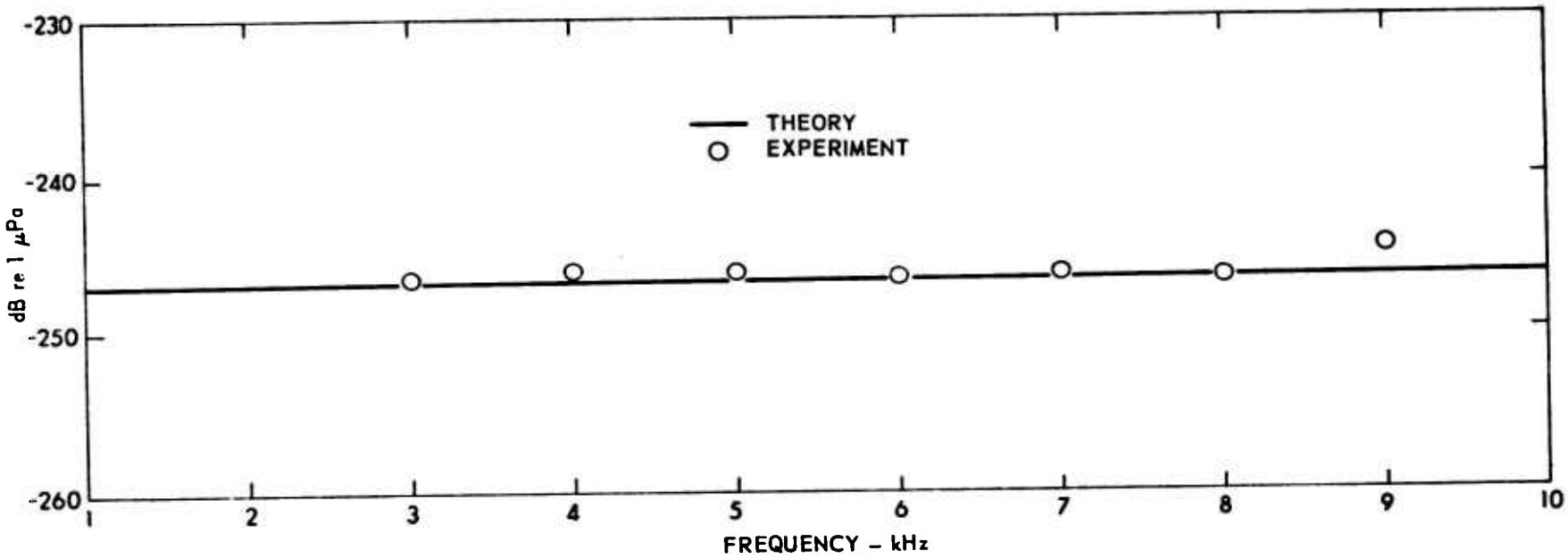

FIGURE 6.7
SUM FREQUENCY SOUND PRESSURE LEVEL
FOR A NARROW BEAM PUMP TRANSDUCER

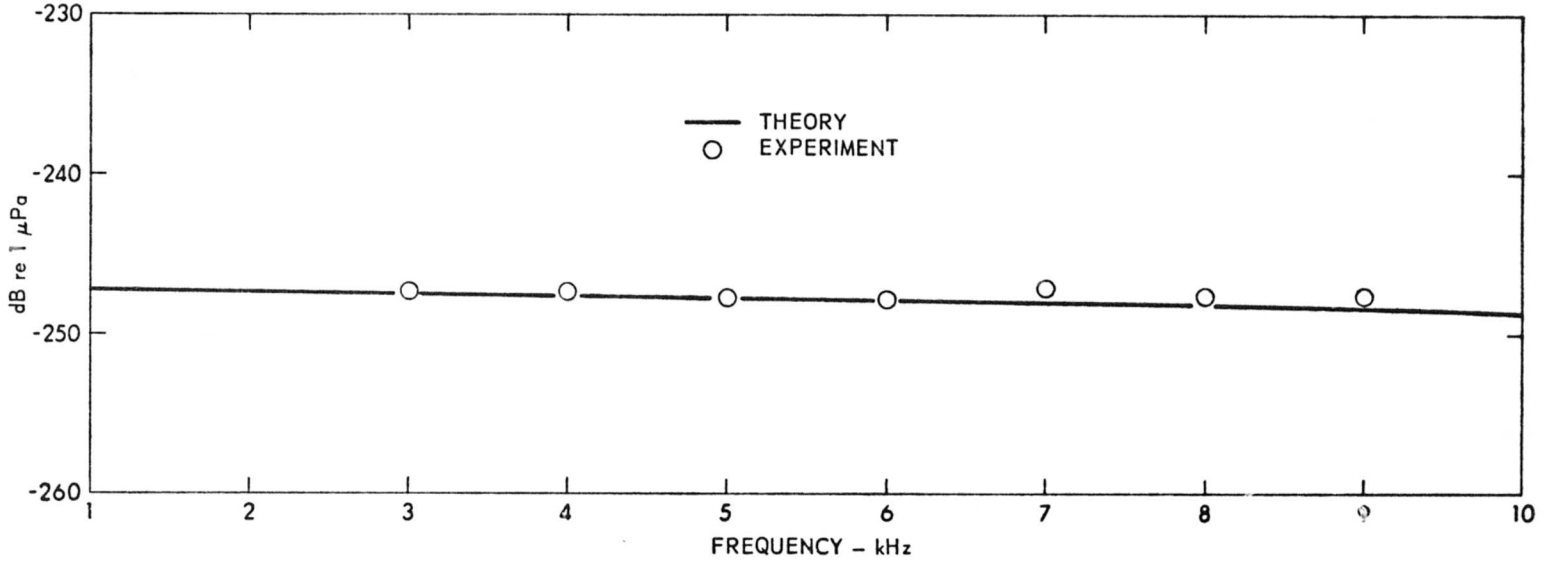

FIGURE 6.8
DIFFERENCE FREQUENCY SOUND PRESSURE LEVEL
FOR A NARROW BEAM PUMP TRANSDUCER

was used for B/A. Difference frequency beam patterns of the parametric receiving array at signal frequencies of 3 and 5 kHz are shown in Fig. 6.9. Sum frequency beam patterns were found to be very similar to the difference frequency beam patterns and therefore are not shown for signal frequencies of 3 and 5 kHz. A sum frequency beam pattern for a signal frequency of 9 kHz is shown in Fig. 6.9(c). The theoretical result from Equation (4.17) was used in an HP 9830 basic computer program; this program is given in Appendix C. Some inconsistency was observed in the experimental beam patterns, the side lobes and the symmetry being somewhat irregular in some cases. This irregularity is believed to be due to the presence of the support structure and the rotator. Even with this experimental difficulty, the agreement between the theory and the experiment is seen to be good.

Since the result given in Equation (4.14) is considerably simpler than that of Equation (4.17), a comparison between these two theoretical results is shown in Fig. 6.10 at three signal frequencies at $\theta=0$. The comparison between the two results indicates that for $\theta=0$ sufficient accuracy is achieved by using the simpler equation (Equation 4.14). The accuracy of Equation (4.14) will be examined further when the parametric array beam patterns with the pump transducer misaligned are considered.

The second-order sound pressure as a function of θ' for the sum and difference frequencies with a 5 kHz signal frequency is shown in Fig. 6.11. The experimental beam pattern was plotted carefully on rectangular chart paper with an angular scale of 3°/in. to ensure adequate angular resolution. The agreement between the theory and experiment was excellent. Equation (4.14) was used to generate the theoretical result. The experimental difference frequency beam pattern is compared to the

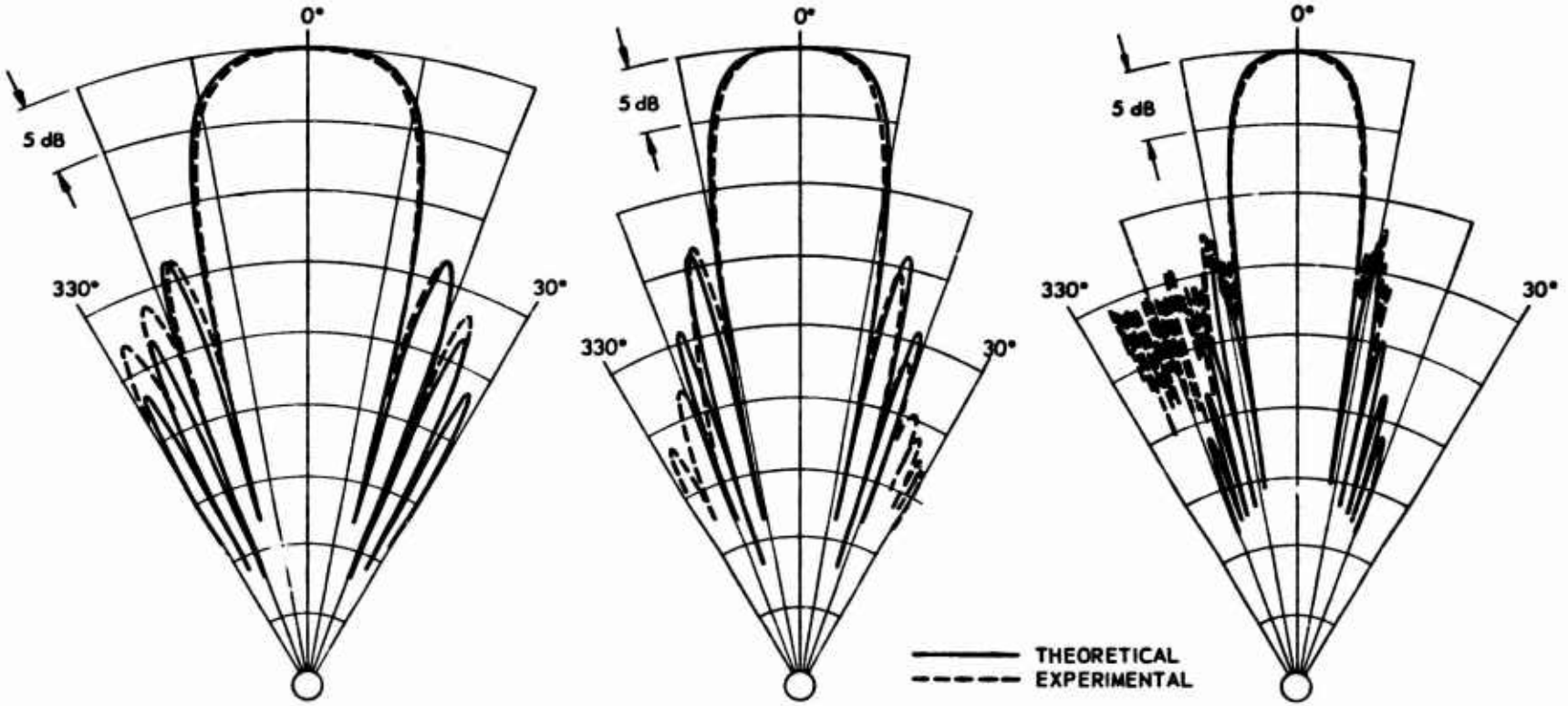

(a) 3 kHz (DIFFERENCE FREQUENCY) (b) 5 kHz (DIFFERENCE FREQUENCY) (c) 9 kHz (SUM FREQUENCY)

FIGURE 6.9
PARAMETRIC RECEIVING ARRAY BEAM PATTERNS
FOR A NARROW BEAM PUMP TRANSDUCER

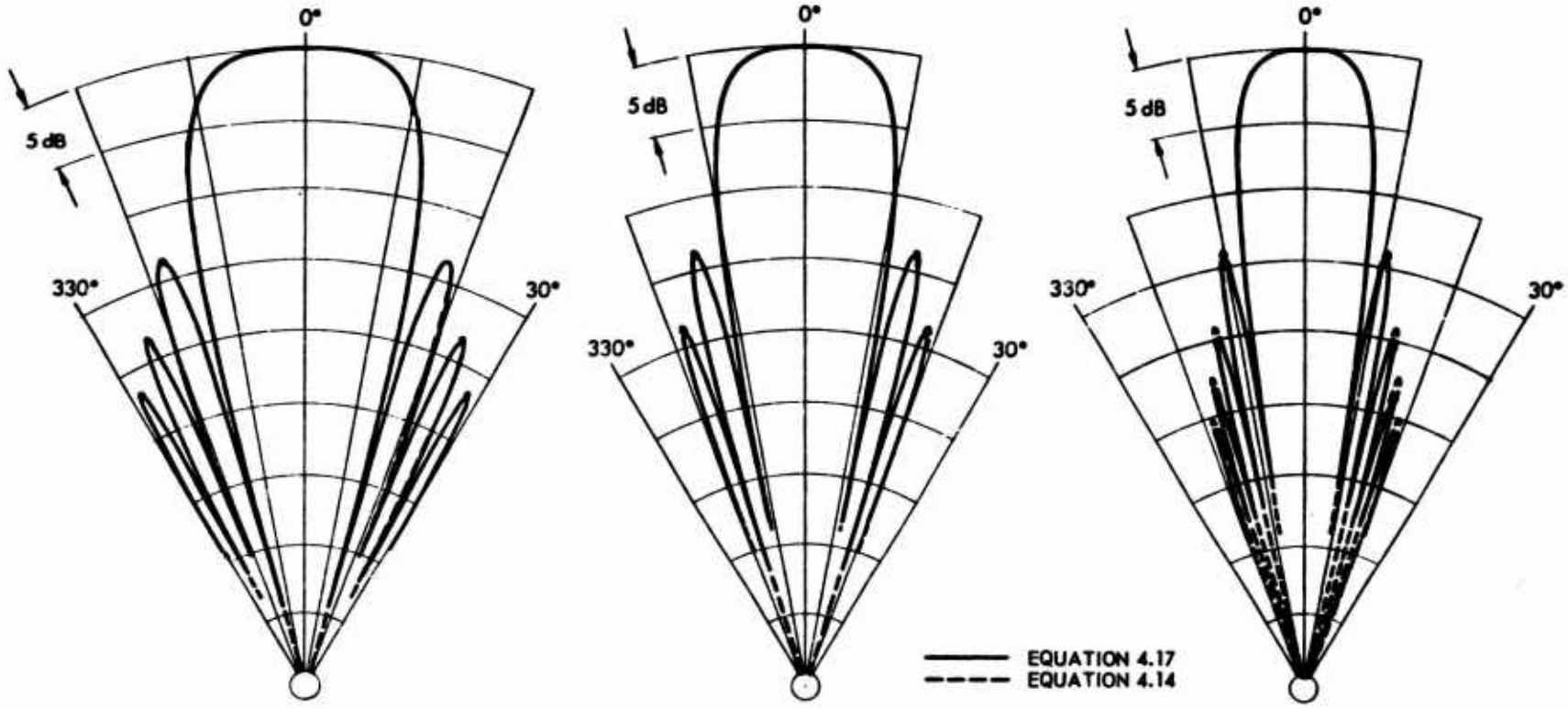

(a) 3 kHz (b) 5 kHz (c) 9 kHz

FIGURE 6.10
COMPARISON BETWEEN THE TWO THEORETICAL RESULTS

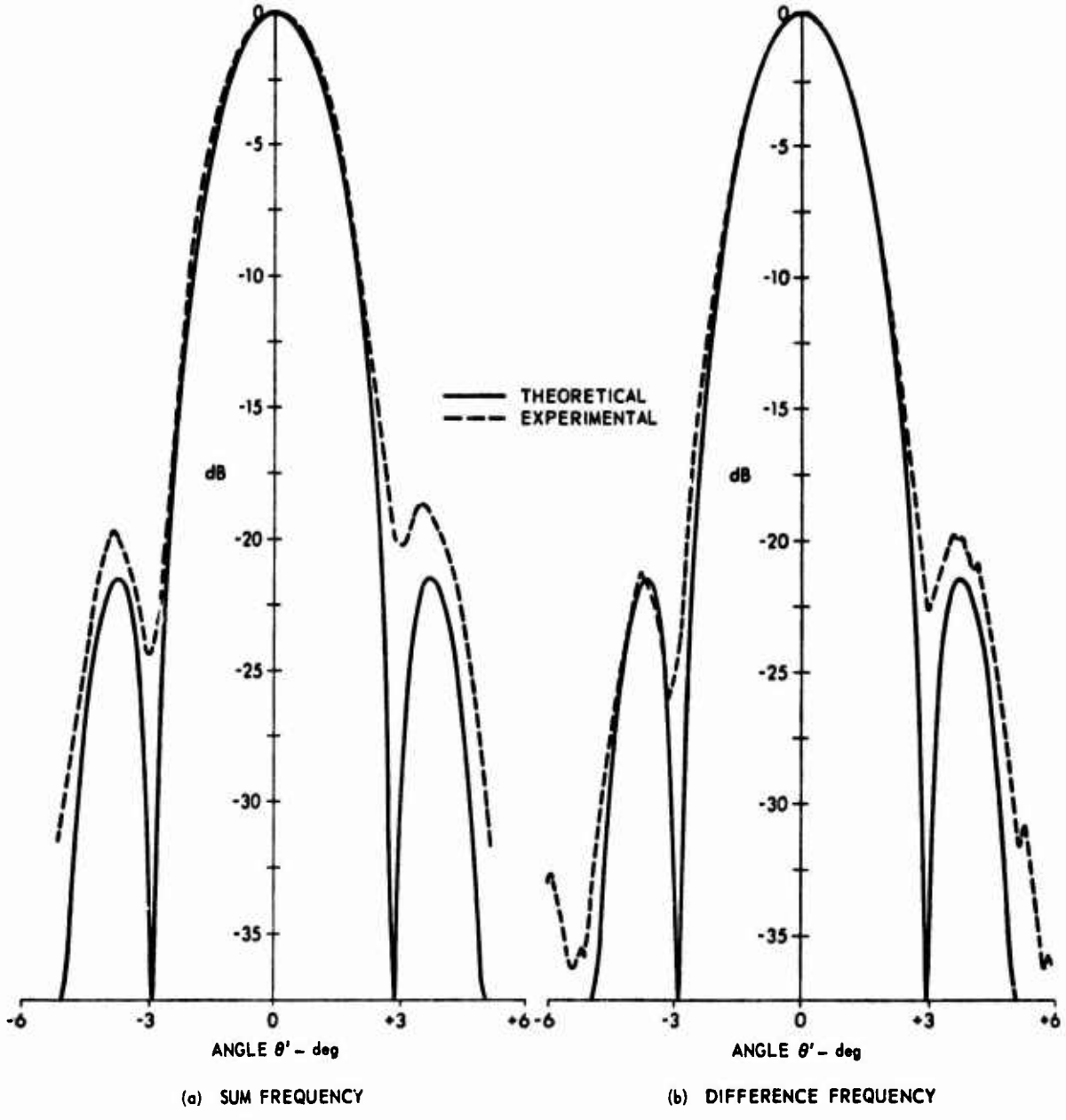

FIGURE 6.11
BEAM PATTERNS FOR THE SUM AND DIFFERENCE FREQUENCY
SOUND FIELDS AS PUMP ANGLE (θ') IS VARIED

experimental pump beam pattern in Fig. 6.12. The difference frequency beam pattern has the same beamwidth, within experimental error, as the pump beam pattern.

A series of measurements were taken with the pump misaligned. The pump bearing (θ') was adjusted to the 3, 6, or 10 dB downpoint on the pump beam pattern. The sum and difference frequency parametric array beam patterns for a signal frequency of 5 kHz with the pump misaligned to the -3 dB point ($\theta'=1.2$) are shown in Fig. 6.13. The sum and difference frequency beam patterns are no longer identical or symmetrical as they were for $\theta'=0$, nor is the maximum for the major lobe at $\theta=0$. One side lobe on each beam pattern was higher than the other side lobe. The theoretical beam patterns were computed using Equation (4.17). The sum and difference frequency beam patterns for the pump beam at -6 dB ($\theta'=-1.6$), and -10 dB ($\theta'=-2.0$) are shown in Figs. 6.14 and 6.15. Again, the two theoretical results (Equations 4.14 and 4.17) are compared for $\theta'=-1.6$ in Fig. 6.16. In each of these beam patterns we see that the angle θ, for which the array response is a maximum, is steered toward the direction θ' is rotated for the difference frequency and away from the direction θ' is rotated for the sum frequency. This property of the sum and difference frequency sound fields is related directly to the idea of "doppler" angles. These results indicate that the sum frequency sound field propagates in a slightly different direction than the original pump sound field, whereas the difference frequency sound field propagates in the same direction as the original pump wave. This result can be demonstrated more dramatically with an appropriate coordinate transformation. This will be done after discussing θ beam patterns with $\theta \neq 0$.

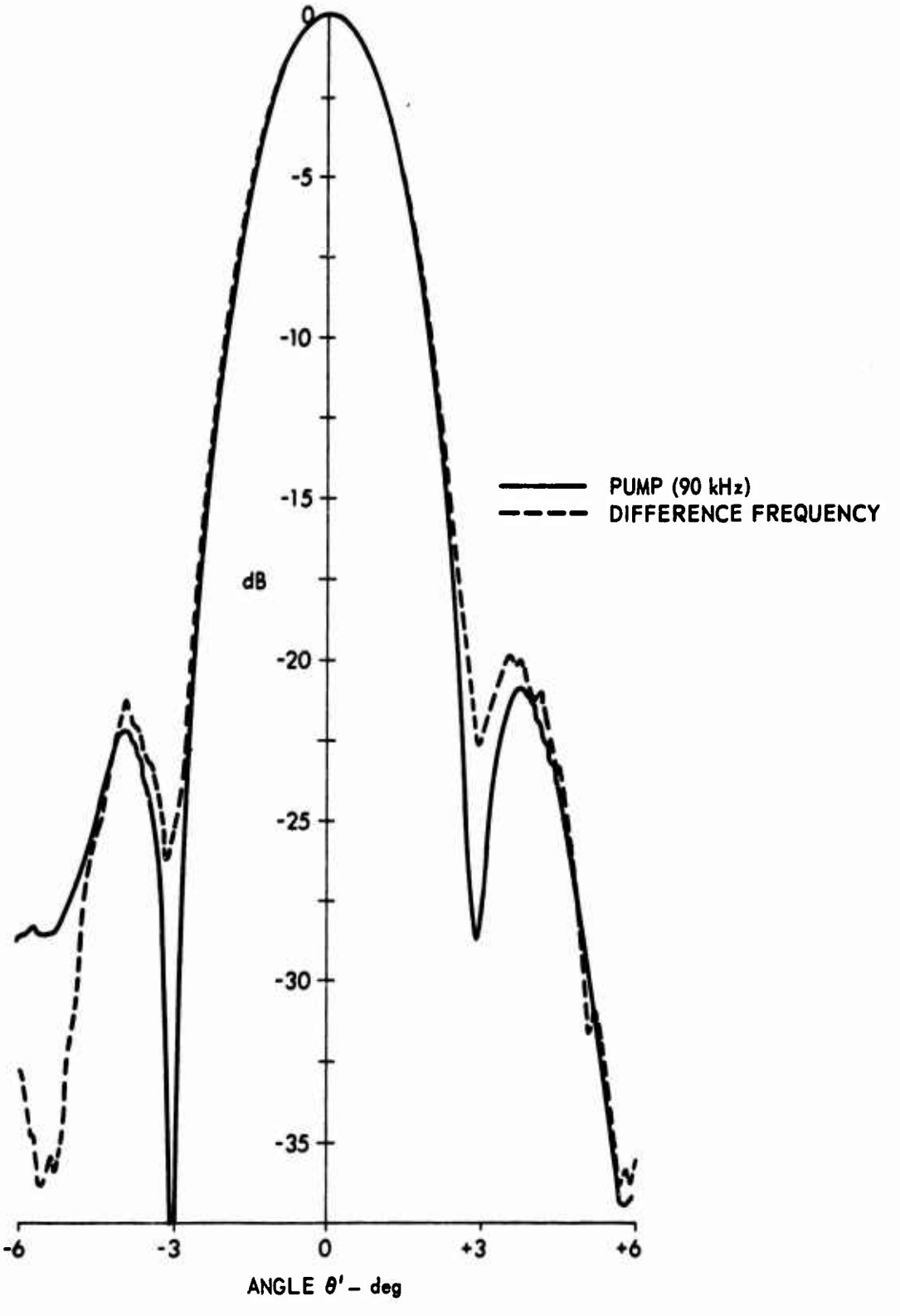

FIGURE 6.12
COMPARISON OF THE DIFFERENCE FREQUENCY SIDEBAND BEAM PATTERN WITH THE PUMP BEAM PATTERN AS THE ANGLE (θ') IS VARIED

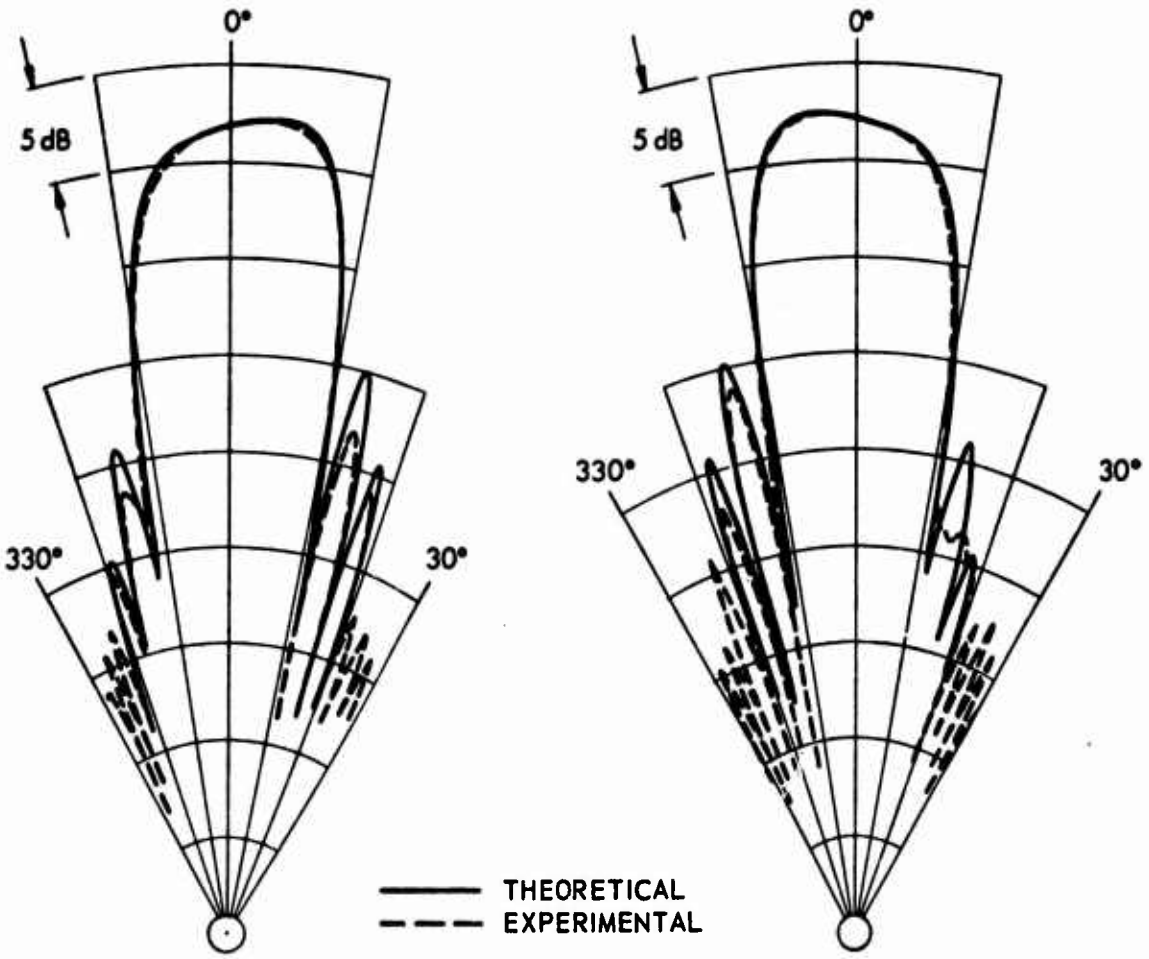

(a) SUM FREQUENCY (b) DIFFERENCE FREQUENCY

FIGURE 6.13
PARAMETRIC RECEIVING ARRAY BEAM PATTERNS
WITH PUMP MISALIGNED ($\theta' = 1.2°$)

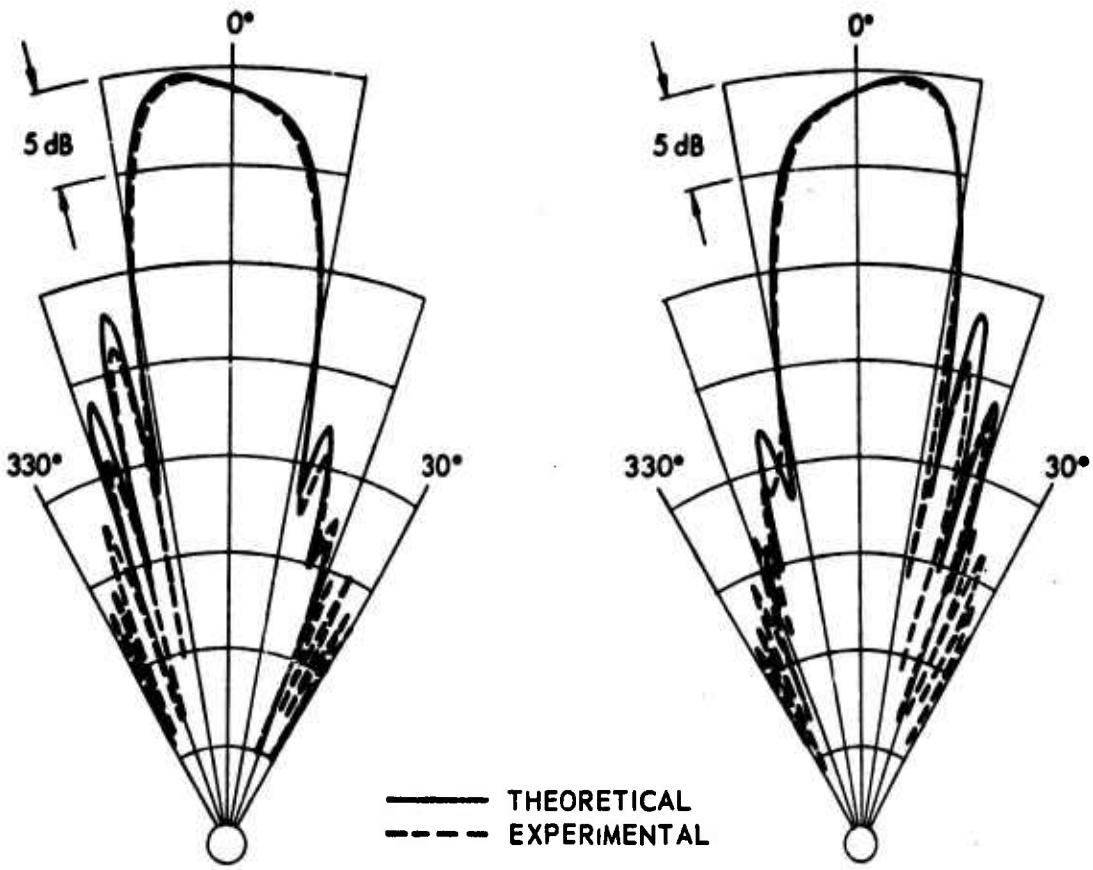

(a) SUM FREQUENCY (b) DIFFERENCE FREQUENCY

FIGURE 6.14
PARAMETRIC RECEIVING ARRAY BEAM PATTERNS
WITH PUMP MISALIGNED ($\theta' = -1.6°$)

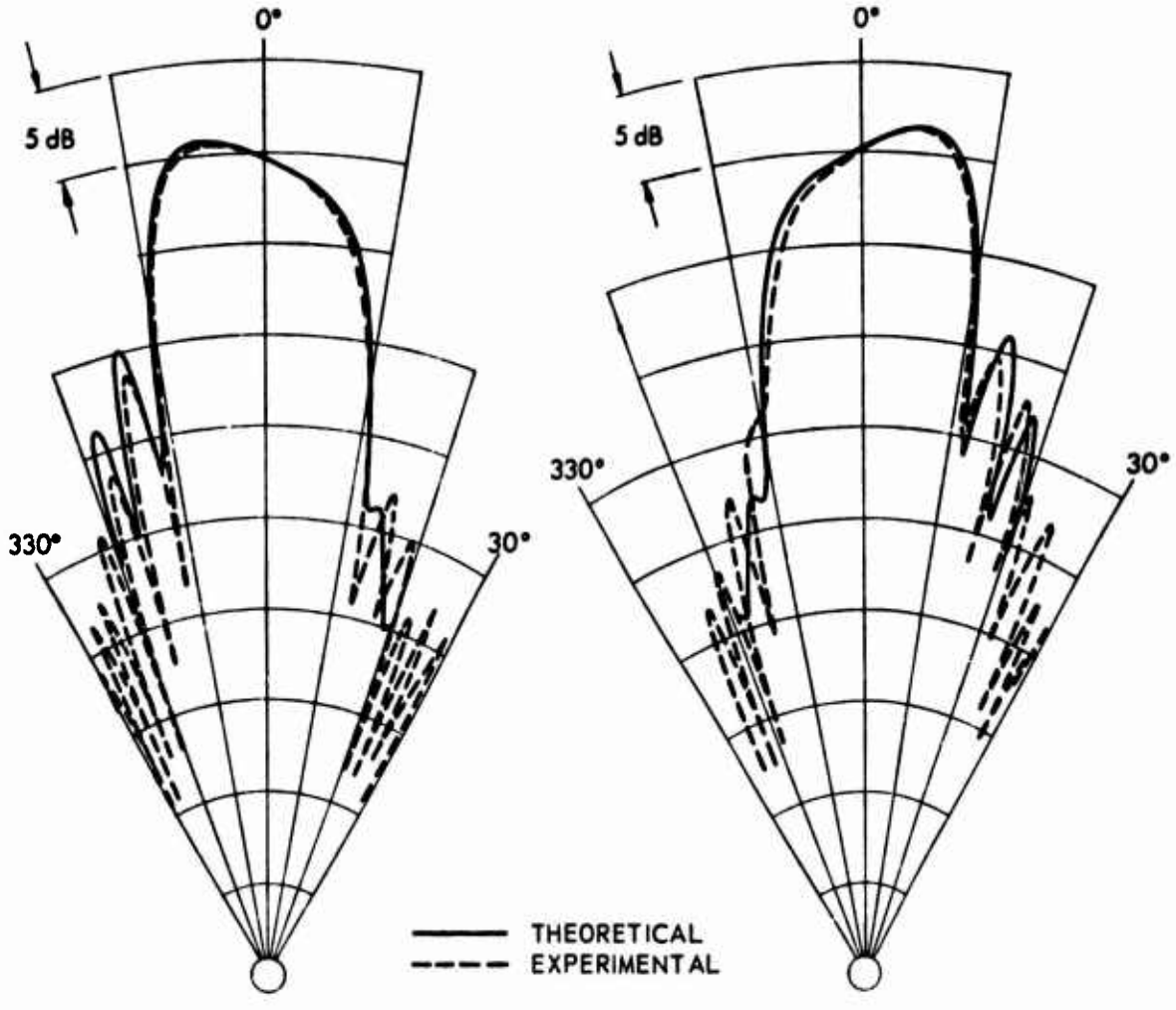

(a) SUM FREQUENCY (b) DIFFERENCE FREQUENCY

FIGURE 6.15
PARAMETRIC RECEIVING ARRAY BEAM PATTERNS
WITH PUMP MISALIGNED ($\theta' = -2.0°$)

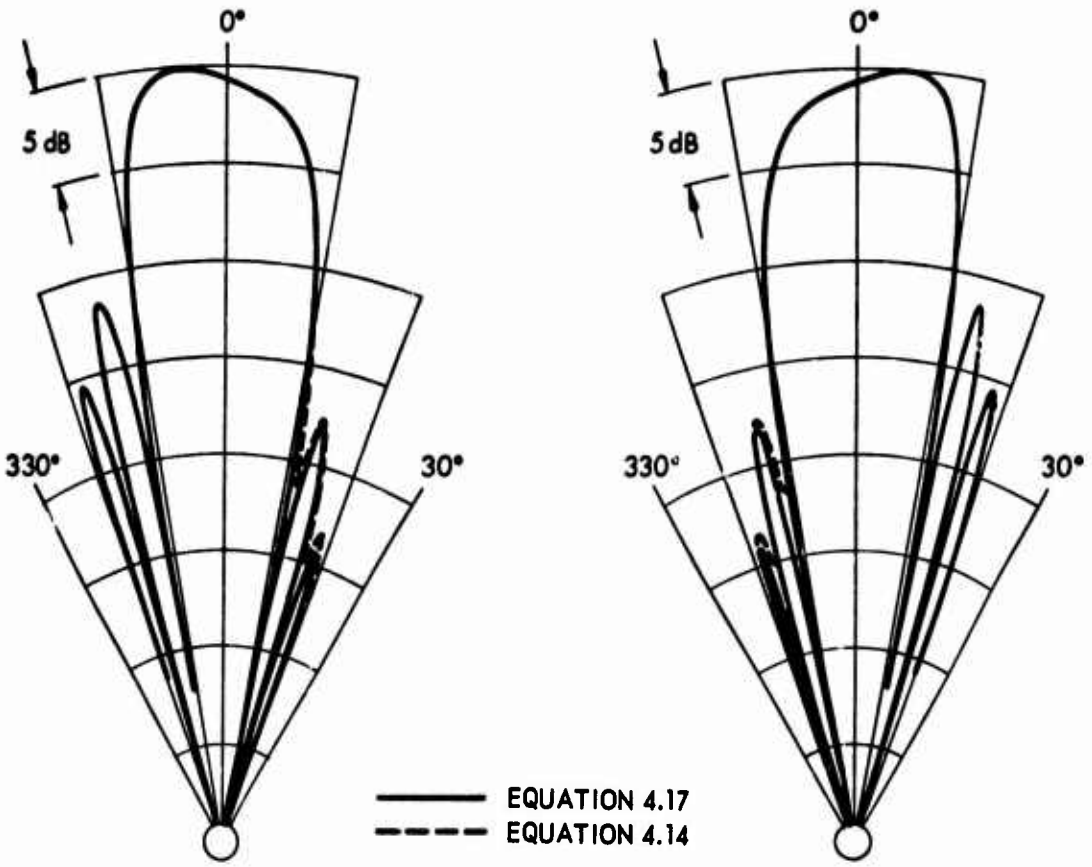

(a) SUM FREQUENCY (b) DIFFERENCE FREQUENCY

FIGURE 6.16
COMPARISON OF THE TWO THEORETICAL RESULTS FOR
PARAMETRIC RECEIVING ARRAY BEAM PATTERNS FOR $\theta' = -1.6°$

Beam patterns with varying θ' for $\theta=7°$, $10°$, and $13°$ for a 5 kHz signal frequency are shown in Figs. 6.17, 6.18, and 6.19. The value for the maximum sum and difference frequency sound pressures is seen to be slightly different than zero. For the sum frequency, the maxima were at $\theta'=0.25°$, $0.3°$, and $0.45°$ for $\theta=7°$, $10°$, and $13°$, respectively. For the difference frequency the maxima were at $\theta'=-0.25$, -0.3, and -0.45 for $\theta=7°$, $10°$, and $13°$, respectively. The angle $\theta=13°$ corresponded to the angle for the first side lobe. The value for the maximum response for $\theta=0$ is marked on each plot.

Doppler angles using the geometry shown in Fig. 6.20 will now be examined. The second-order sound field will be observed at a point (L,ϕ'). The angle of the low frequency plane vector with respect to the axis of the pump beam pattern is ϕ. Plots of the theoretical sound field for the sum and difference frequency components as a function of ϕ', with $\phi=5°$ and $\phi=7°$, are shown in Fig. 6.21. The signal frequency is 5 kHz and the pump frequency is 90 kHz. The sum frequency sound wave is seen to propagate with a maximum value at $\phi'=0$, as for $\phi=5°$ and $\phi'=0.4°$ for $\phi=7°$. The difference frequency sound wave propagates in the same direction as the pump wave.

In light of excellent agreement between the theoretical and experimental results, there is little doubt that any significant difference would be observed for an experiment done using the coordinate system shown in Fig. 6.20. We see that our theory and experiment is consistent with the idea of interaction occurring at nonzero angles between the direction of propagation of the two waves. Furthermore, we see that the "doppler" angles predicted by Pridmore-Brown and Ingard,[15] Dean,[49] and Lauvstad and Tjötta,[50] can indeed be observed.

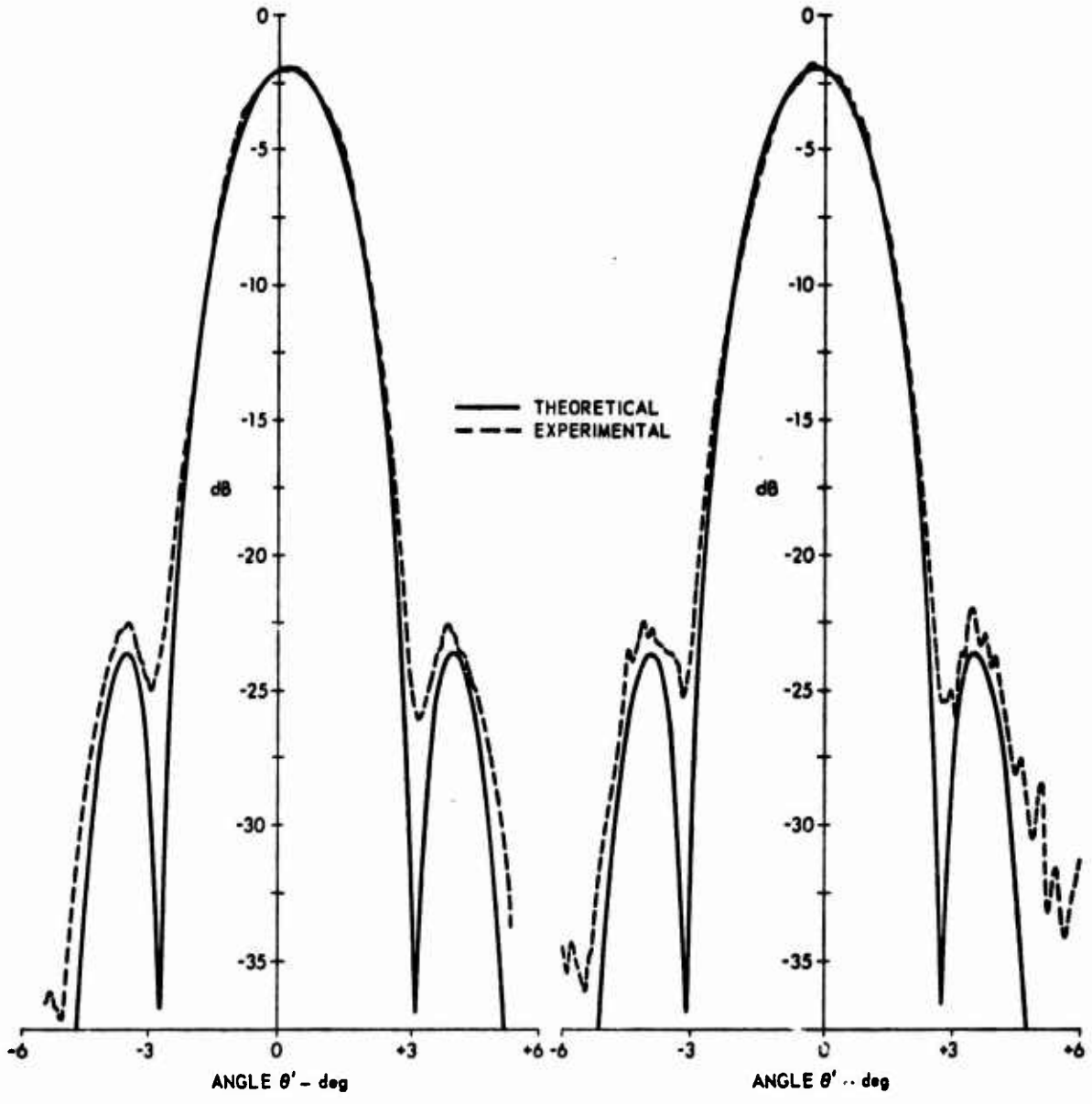

FIGURE 6.17
BEAM PATTERNS AT THE SIDEBAND FREQUENCIES FOR $\theta = 7°$ WITH VARYING θ'

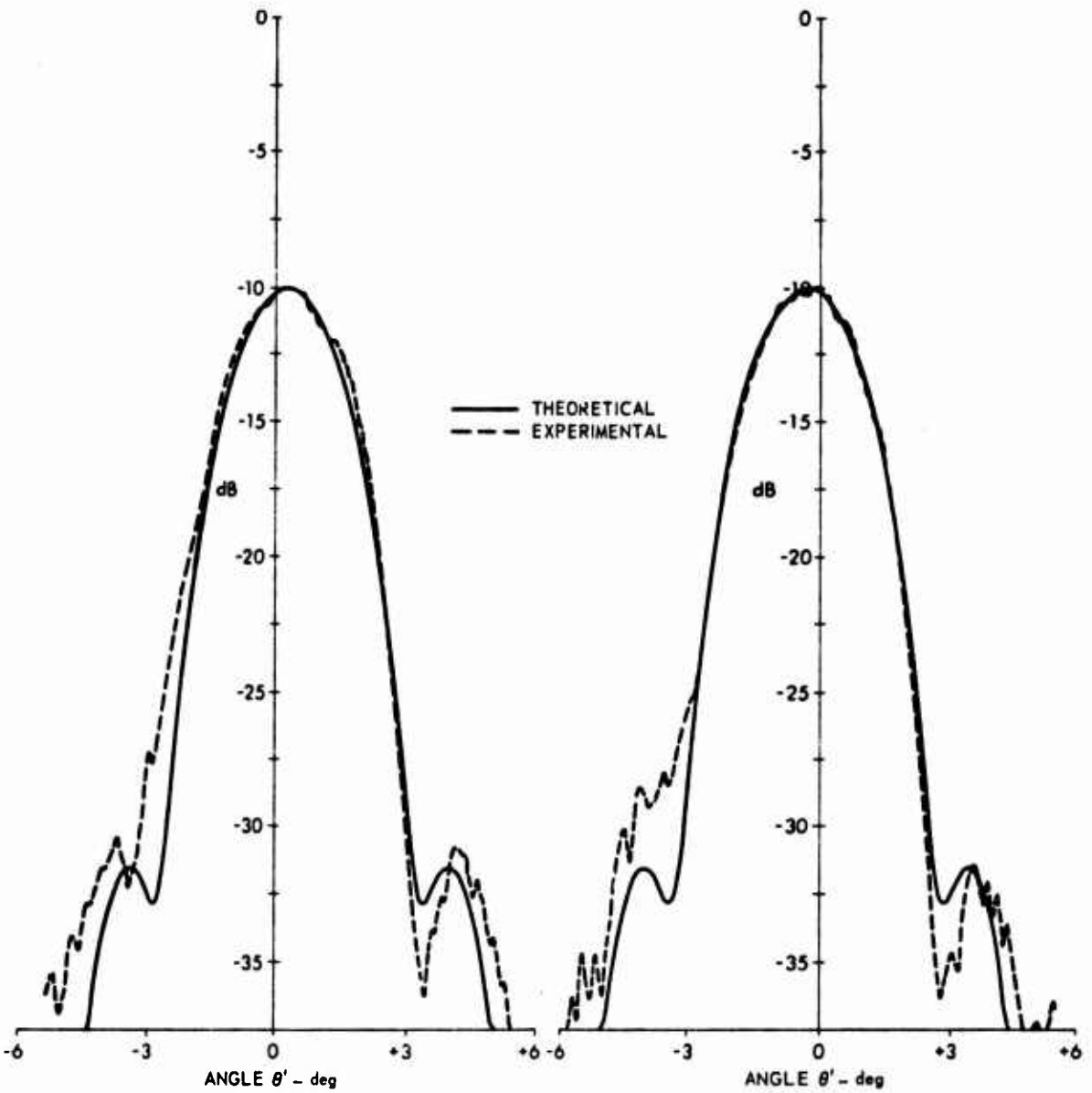

FIGURE 6.18
BEAM PATTERNS AT THE SIDEBAND FREQUENCIES FOR $\theta = 10°$ WITH VARYING θ'

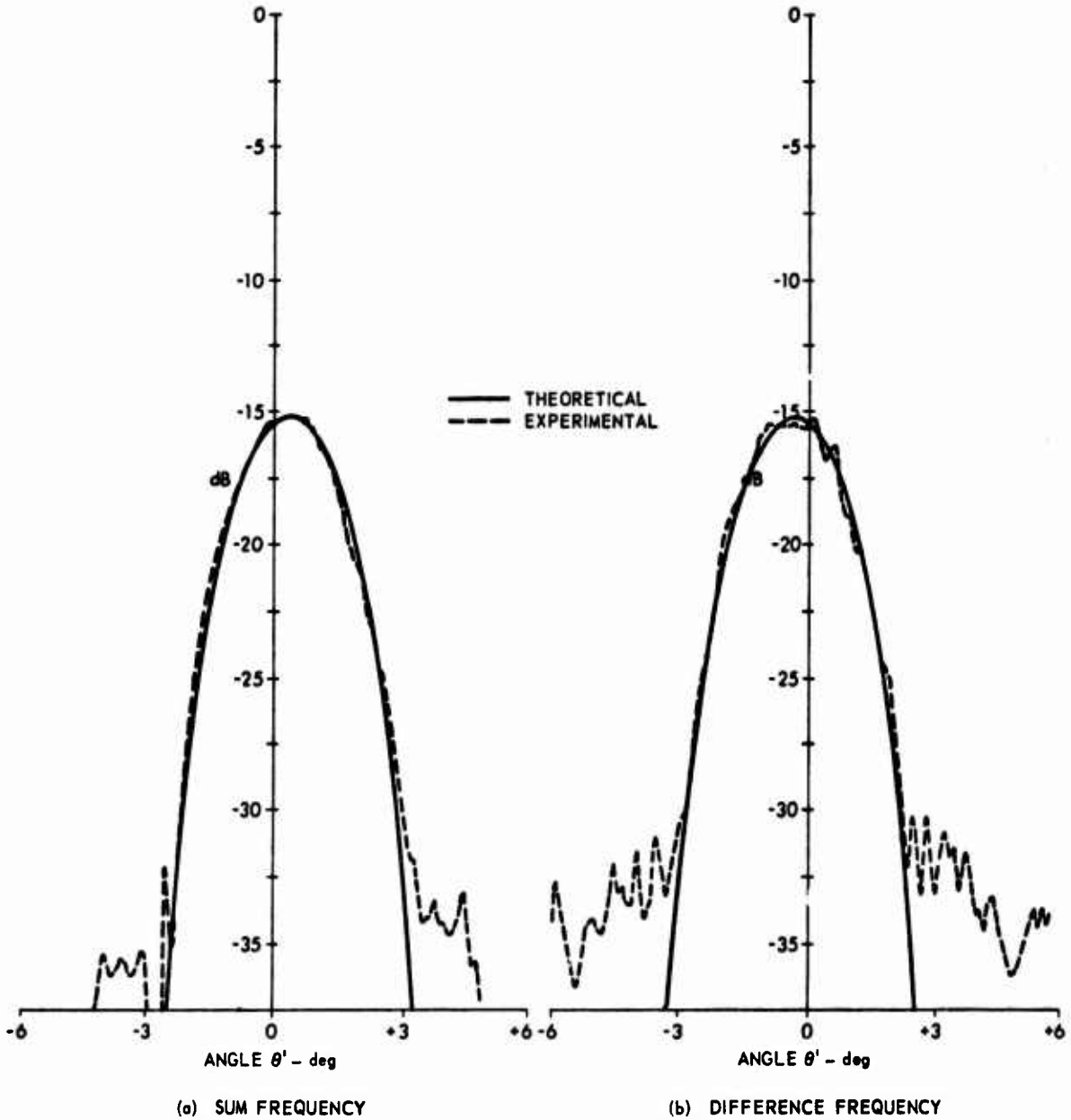

FIGURE 6.19
BEAM PATTERNS AT THE SIDEBAND FREQUENCIES FOR θ = 13° WITH VARYING θ'

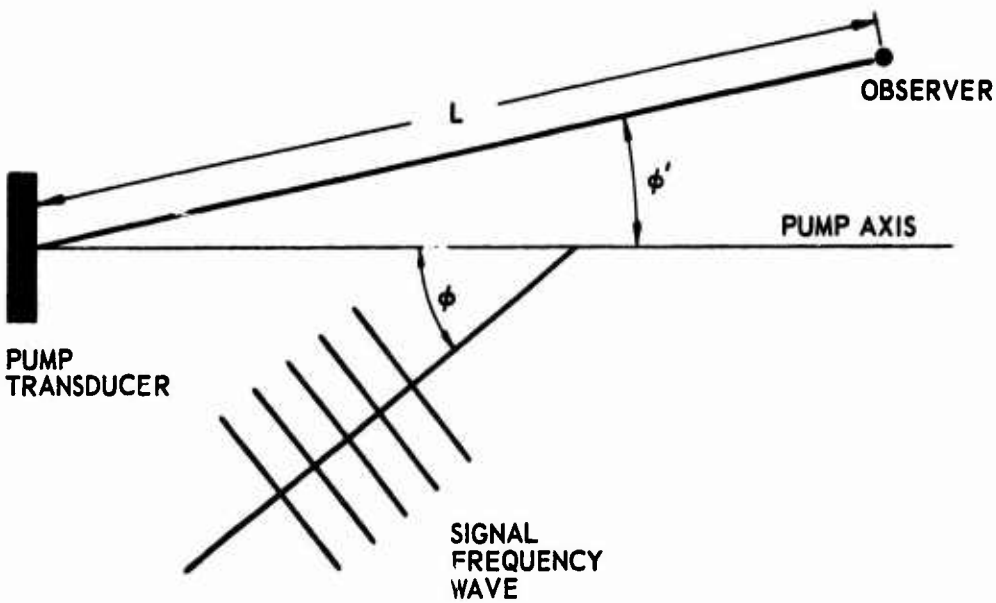

FIGURE 6.20
GEOMETRY FOR THE EXAMINATION OF THE DOPPLER ANGLES

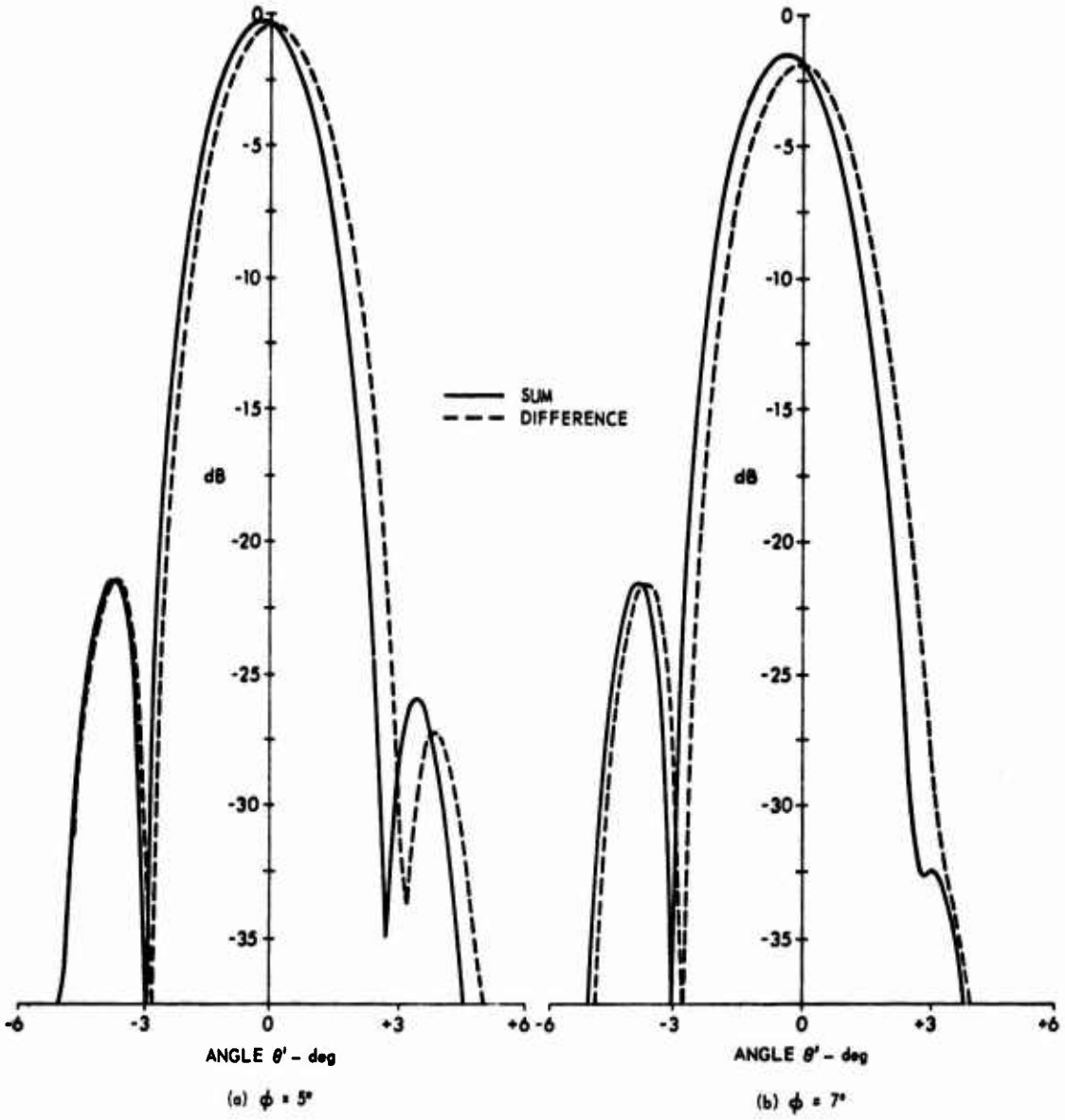

FIGURE 6.21
SECOND-ORDER SOUND FIELD FOR A RECTANGULAR PUMP

C. Experiments on the Parametric Receiving Array with an Omnidirectional Pump and a Line Receiver

We shall now reverse the high frequency transducers and examine the properties of a parametric receiving array with a narrowbeam receiver. We first examine sum frequency beam patterns for the parametric receiving array at $\theta'=0$. The beam patterns with signal frequencies of 5 and 9 kHz are shown in Fig. 6.22. These beam patterns are very similar to those for a narrowbeam pump. Equation (4.32) was used for calculating the theoretical beam patterns. The agreement with the theoretical results was excellent. The support for the omnidirectional transducer was a thin rod which did little to affect the low frequency sound field.

Difference frequency beam patterns with the receiver misaligned to the 3 dB ($\theta'=\pm1.3°$) and 6 dB ($\theta'=\pm1.7°$) points at a signal frequency of 5 kHz are shown in Figs. 6.23 and 6.24, respectively. These beam patterns resemble those found for the narrowbeam pump. The theoretical beam patterns were generated using Equation (4.32). The array beam pattern at the sum frequency for the narrowbeam receiver at -3 dB ($\theta'=1.1$) and at -6 dB ($\theta'=1.53$) are shown in Fig. 6.25.

Beam patterns obtained by varying θ' with $\theta=0$ are shown for the sum and difference frequencies in Fig. 6.26. There is an important difference in these beam patterns from the original pump beam patterns. The beamwidth of these patterns were found to be that of the receiver at the sum and difference frequencies rather than at the pump frequency, as was observed with the narrowbeam pump. The theoretical results were plotted using Equation (4.29).

Receiver beam patterns with varying θ' with an array angle of $\theta=7°$ and 13° are shown in Figs. 6.27 and 6.28, respectively. Again, a

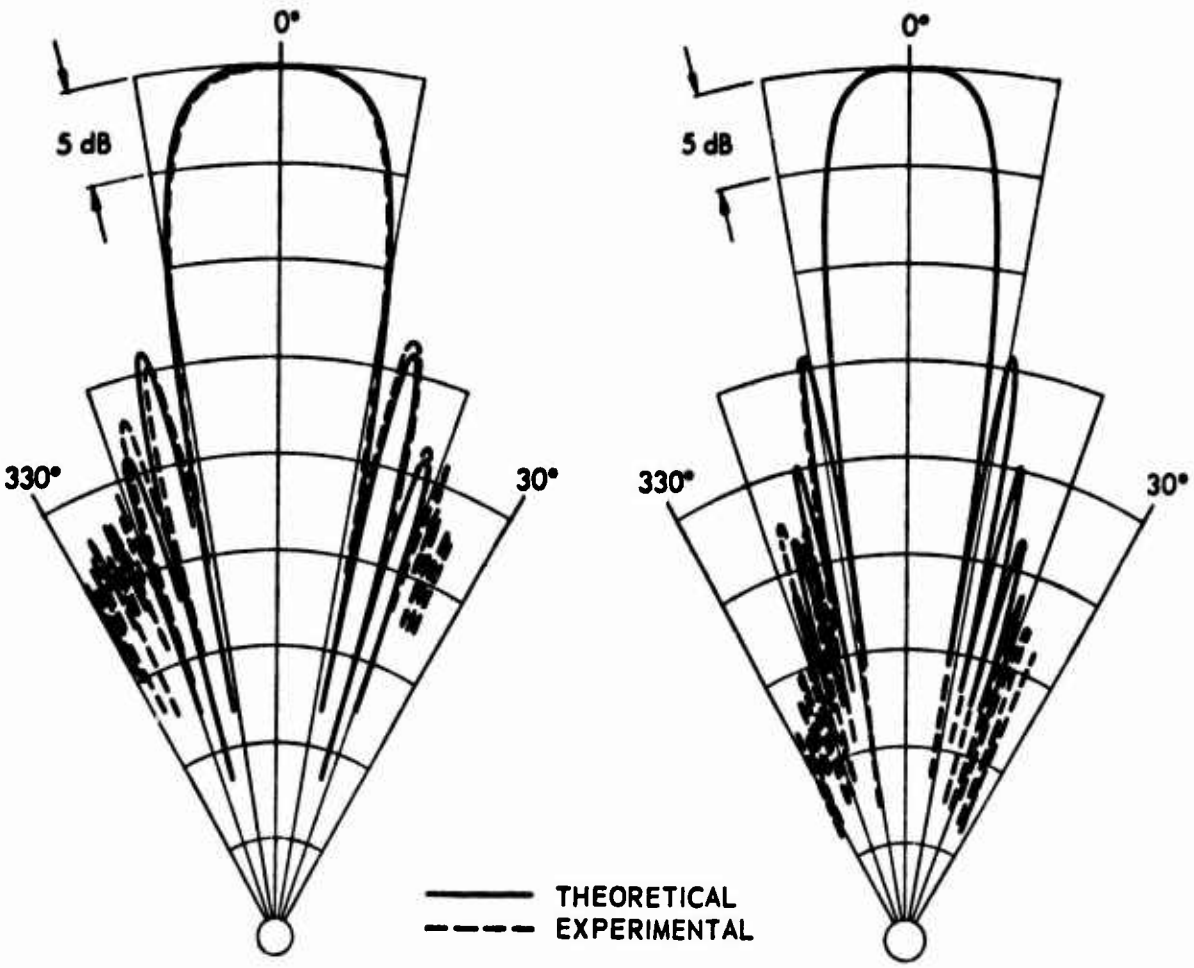

(a) 5 kHz SUM FREQUENCY

(b) 9 kHz SUM FREQUENCY

FIGURE 6.22
SUM FREQUENCY PARAMETRIC RECEIVING ARRAY BEAM PATTERNS

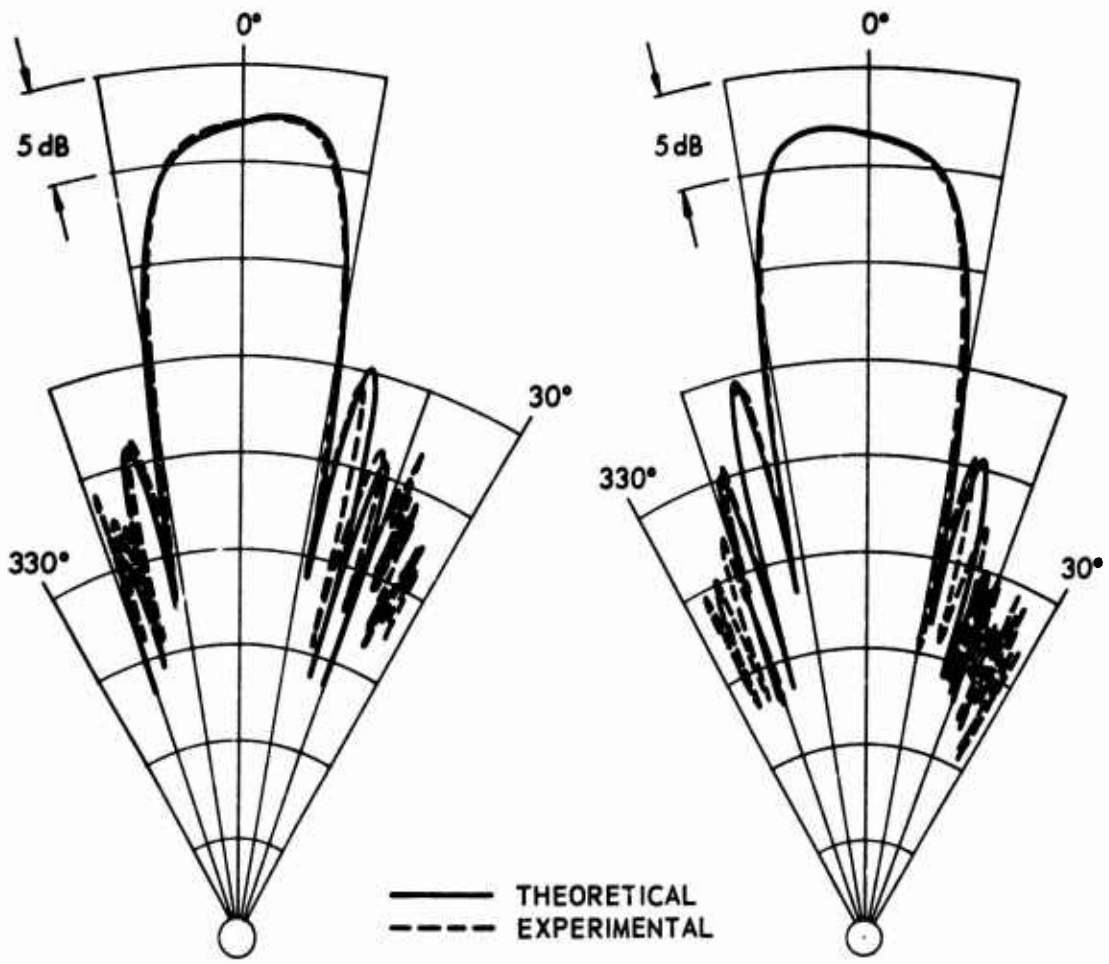

(a) $\theta' = 1.3°$ DIFFERENCE FREQUENCY (b) $\theta' = -1.3°$ DIFFERENCE FREQUENCY

FIGURE 6.23
DIFFERENCE FREQUENCY ARRAY BEAM PATTERNS
WITH THE RECEIVER MISALIGNED BY θ'

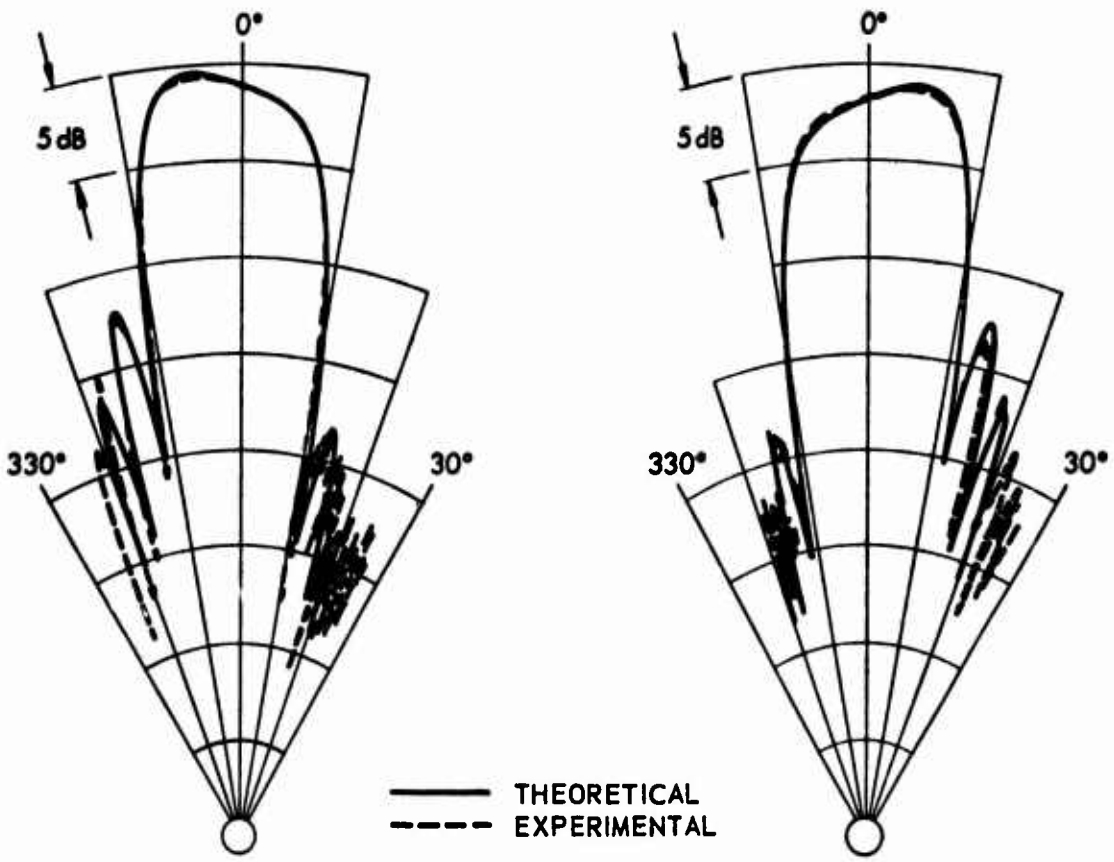

(a) $\theta' = 1.7°$ DIFFERENCE FREQUENCY (b) $\theta' = -1.7°$ DIFFERENCE FREQUENCY

FIGURE 6.24
DIFFERENCE FREQUENCY ARRAY BEAM PATTERNS
WITH THE RECEIVER MISALIGNED BY θ'

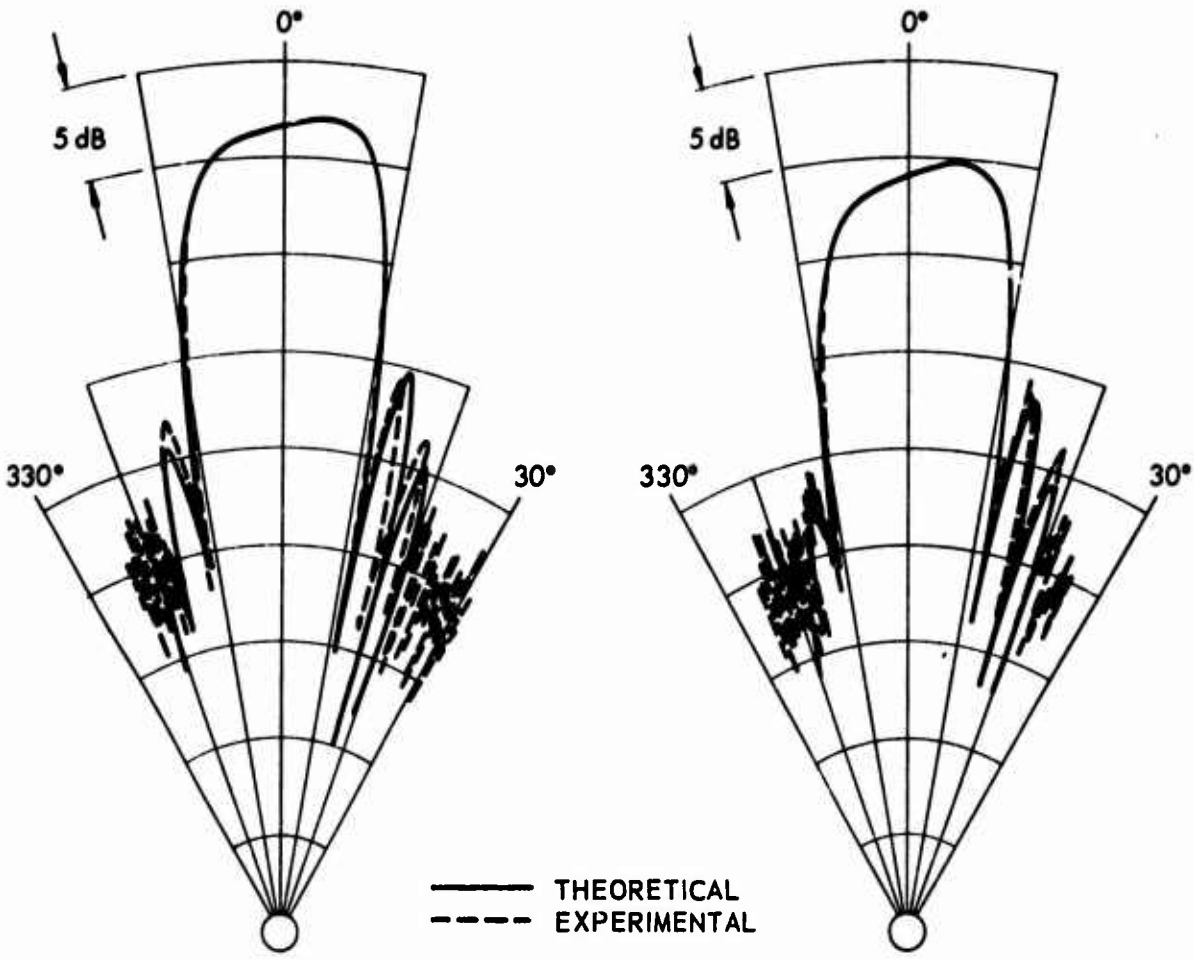

(a) $\theta' = 1.1°$ SUM FREQUENCY

(b) $\theta' = 1.53°$ SUM FREQUENCY

FIGURE 6.25
SUM FREQUENCY ARRAY BEAM PATTERNS
WITH THE RECEIVER MISALIGNED BY θ'

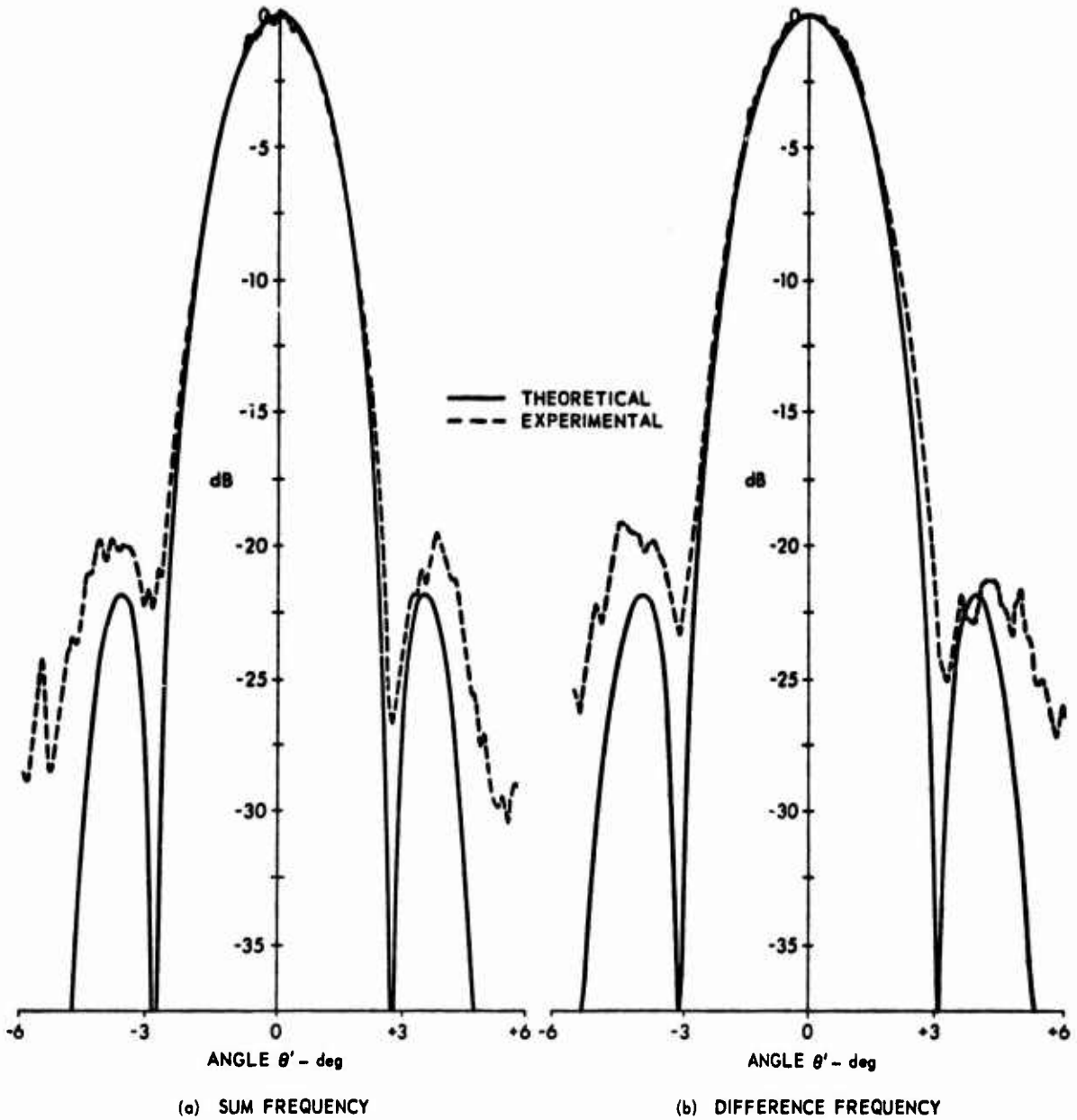

FIGURE 6.26
SIDEBAND RECEIVER BEAM PATTERNS FOR $\theta = 0°$

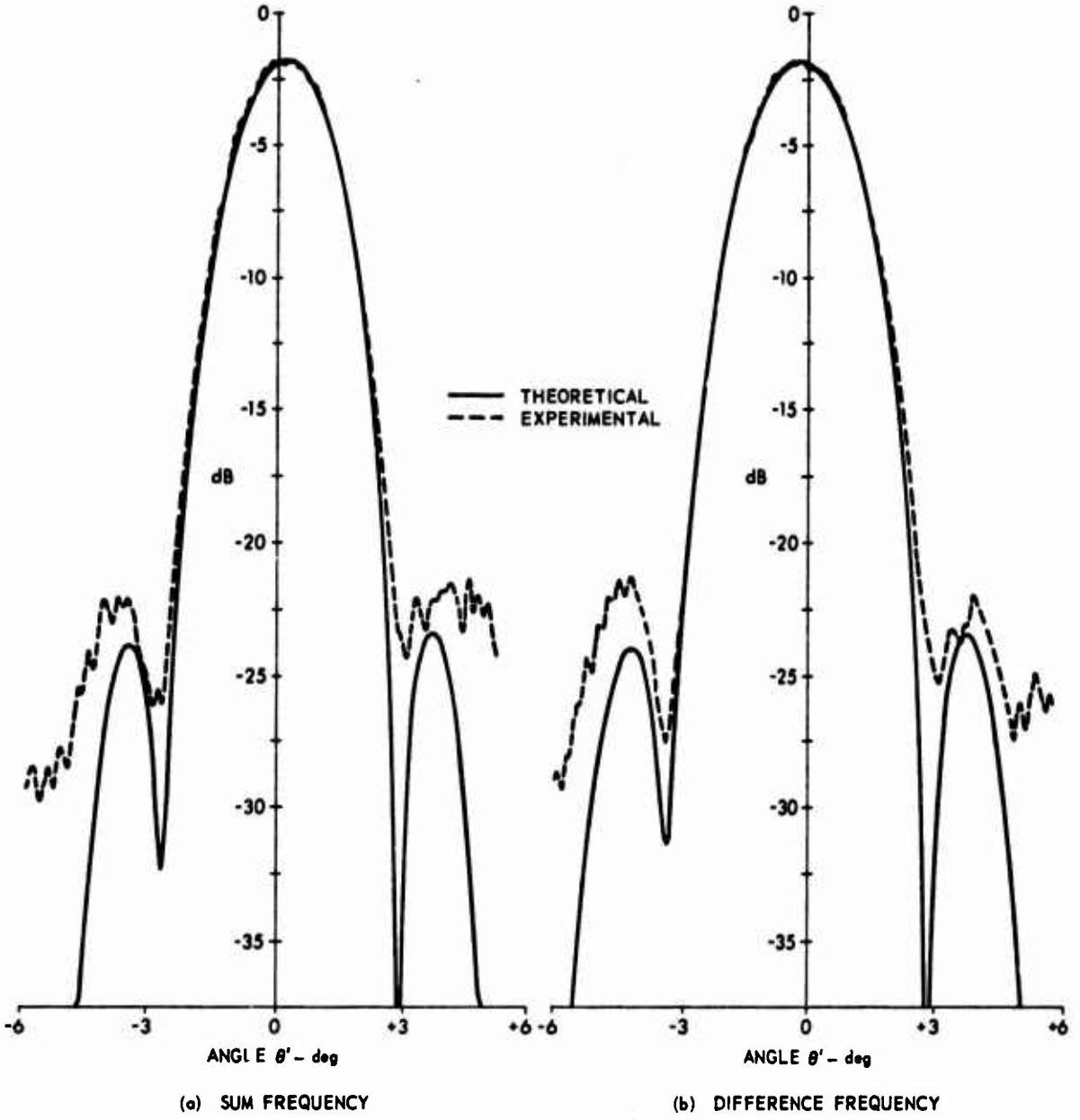

FIGURE 6.27
SIDEBAND RECEIVER BEAM PATTERNS FOR $\theta = 7°$

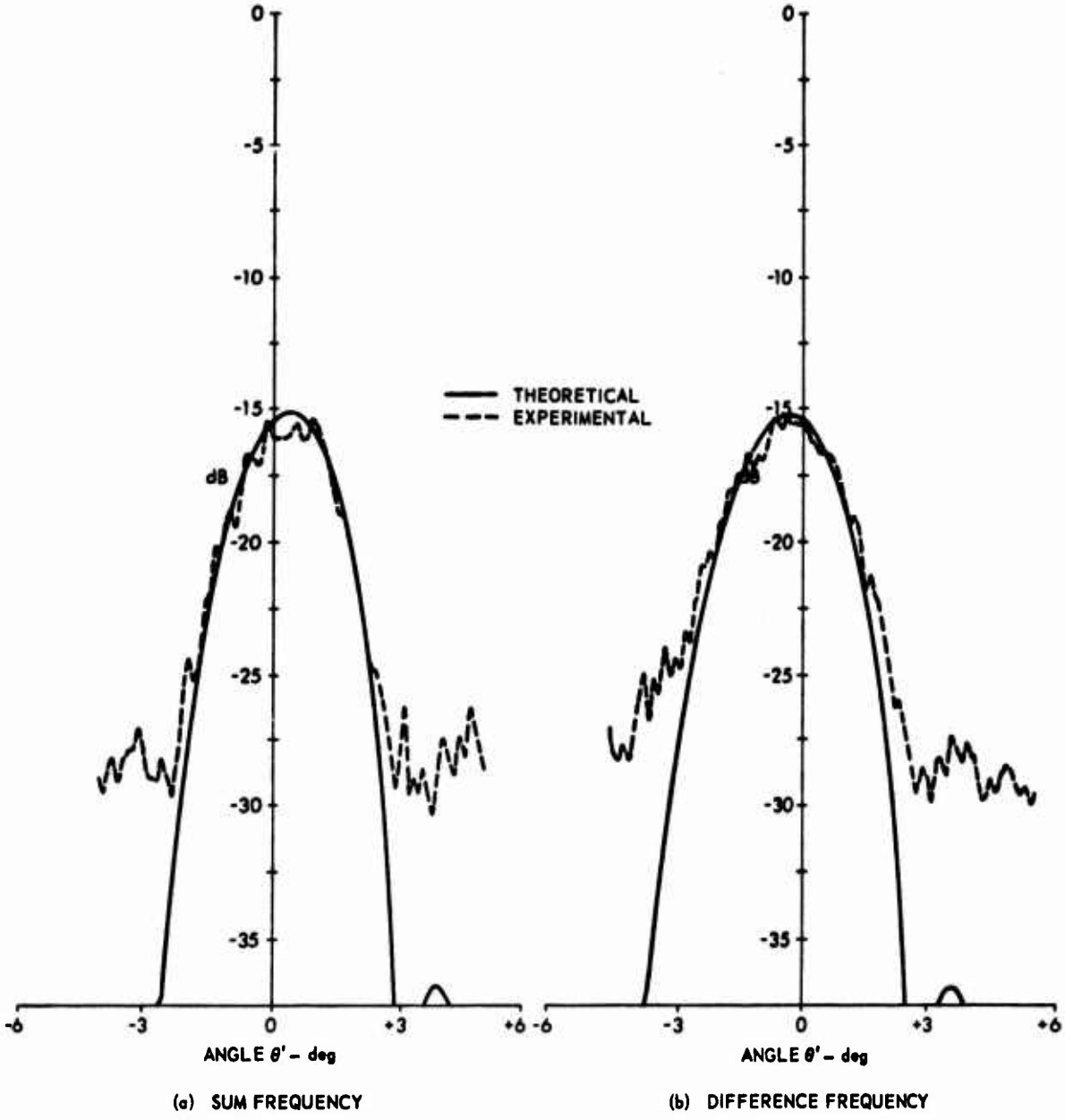

FIGURE 6.28
SIDEBAND RECEIVER BEAM PATTERNS FOR $\theta = 13°$

slight change in the angle θ' for the maximum was slightly different than zero.

D. Experiments on the Parametric Receiving Array with a Small Pump Transducer

A small transducer with a measured beam pattern at 90 kHz as shown in Fig. 6.29 was used for the pump transducer. The beam pattern for the transducer was found to be very similar to that of a 4 in. x 4 in. square aperture used for the theoretical result in Fig. 6.29. A beam pattern for the parametric array with a signal frequency of 5 kHz is shown in Fig. 6.30. As with the narrowbeam pump transducer, some irregularity in the beam pattern was observed. This irregularity is attributed to the presence of the rotator and mounting structure. Equation (4.29) was used to generate the theoretical beam pattern. The sum frequency beam pattern obtained by varying θ' with the array aligned with the signal wave is shown in Fig. 6.31. Again, Equation (4.29) was used to generate the theoretical result. The beam pattern closely resembles that of the pump transducer operated at 90 kHz as is predicted by the theory.

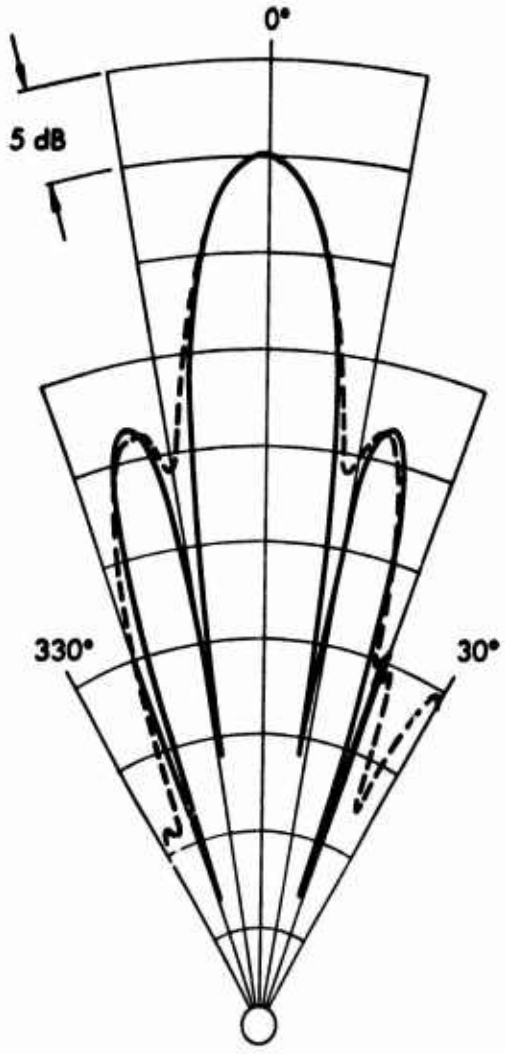

FIGURE 6.29
PUMP BEAM PATTERN

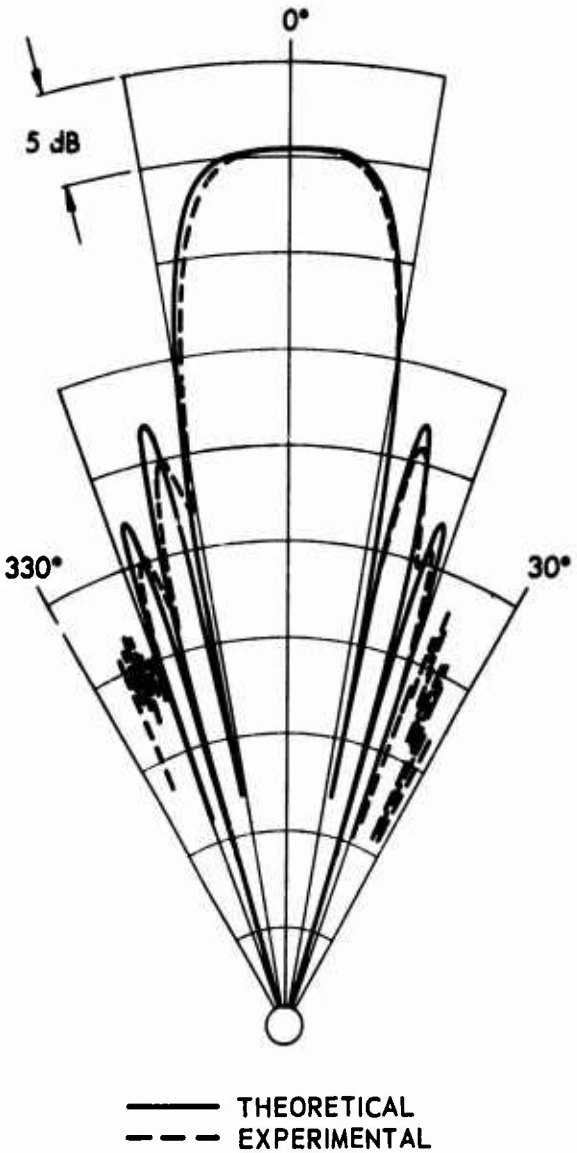

FIGURE 6.30
SUM FREQUENCY PARAMETRIC ARRAY BEAM PATTERN

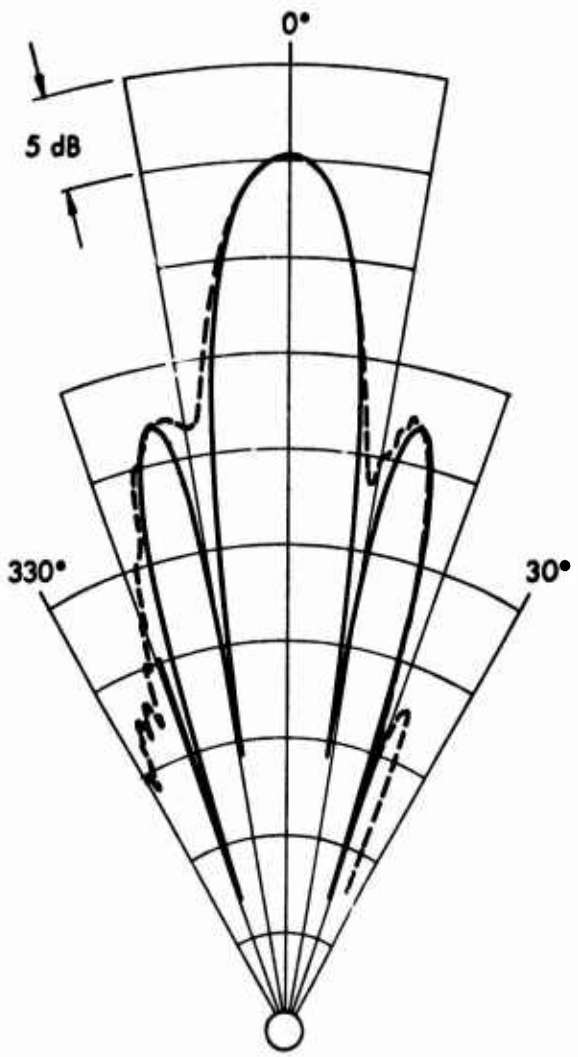

FIGURE 6.31
SUM FREQUENCY BEAM PATTERN WITH VARYING θ'

VII. SUMMARY AND CONCLUSIONS

Two objectives were undertaken in this study of the parametric receiving array. They were (1) to relate the parametric receiving array to the problem of interaction of sound by sound at nonzero angles, and (2) to find a solution for the second-order sound field for a parametric receiving array with pump sources which ranged from omnidirectional to very narrowbeam acoustic generators. Each of these objectives was accomplished using the perturbation solution developed by Westervelt. The second-order sound pressure was obtained by solving an inhomogeneous wave equation with a source function expressed in terms of a product of first-order sound field variables. In the derivation of the wave equation, the effects of viscosity and thermal conductivity were ignored. The effects of absorption were included in the expression of the first-order field variables.

The interaction of two plane waves over all space in a lossless medium was considered in Chapter III. Westervelt's 1957 result was reproduced. This result predicted an infinite sound pressure when the two plane waves are propagating in the same direction. When the sound waves are not propagating in the same directions, the second-order sound field was found to be a function of the local value for the first-order sound field. A more reasonable solution was then obtained by placing a boundary condition on one of the sound fields. For the parametric receiving array, the sound wave with the boundary condition was assumed to have a frequency f_1, such that f_1 was considerably greater than

f_2, the signal frequency. This case represented a parametric receiving array with an infinite planar piston source for a pump. The second-order sound pressure was found to be proportional to the distance of the observer from the planar boundary and had the directivity function of a truncated end-fire array. Berktay observed a similar result for the parametric receiving array with the receiving transducer in the nearfield of the pump transducer. The same end-fire function was predicted for an omnidirectional pump transducer in our study. The interaction of sound with sound was also considered in Chapter VI when we observed the properties of the second-order sound field at nonzero angles for the array. A modified form for the doppler angles was predicted by the theory and observed by the experiment. The form for the doppler angles was modified because the high frequency pump wave propagated as a spherical rather than a planar wave. In the present study, the observer was always in the region of interaction. It can be concluded that cumulative interaction of sound by sound at nonzero angles does occur within the zone of interaction. No conclusion about the presence of a second-order sound wave outside the region of interaction can be drawn since, strictly speaking, the observer was always in the zone of interaction.

An interesting special problem, the parametric receiving array with a point source pump, was solved in Chapter III. This solution is of particular significance for two reasons (1) this case represents a situation which can be modeled both theoretically and experimentally, and (2) the solution can be used to solve parametric receiving array problems with more complex pump source distributions. In our analysis, it has been assumed that the pump wave and signal wave amplitudes are small enough to

use a small-signal nonlinear acoustics or quasilinear solution to the problem. The point source solution was used as a starting point to obtain the solution for a line source pump. This summation was legitimate only because the amplitude of the pump wave was assumed to be small enough to preclude finite amplitude attenuation of the pump wave. The effects of absorption were included in the description of the first-order sound field. The solution for the point source pump wave was obtained using a two-dimensional stationary phase integral evaluation technique. This approach represents an interesting new means to solve three-dimensional nonlinear acoustics problems. To the author's knowledge, this application of the two-dimensional integral technique is the first for a nonlinear acoustics problem. The parametric receiving array with a point source pump was found to have a directivity function equal to that of an equivalent end-fire array. When the pump source was misaligned with respect to the receiver, the directivity function was dramatically changed. The beam patterns found by rotating the pump with the array aligned with the low frequency sound field was found to be almost identical to that of the pump operating at the pump frequency. These properties of the parametric receiving array with a line source pump were observed both theoretically and experimentally.

The line transducer was used as a receiver with an omnidirectional pump source. Again, the array beam patterns were found to be narrower with lower side lobes than the equivalent end-fire array. Beam patterns observed by rotating the receiver transducer were found to be the same as beam patterns made at the sum or difference frequency. Again, the theoretical and experimental results agreed closely.

When a transducer with dimensions small compared to a signal wavelength was used as a pump transducer, the properties of the parametric receiving array were only slightly different from those predicted by Berktay and Al Temimi,[32,33] Berktay and Shooter,[39] and Rogers et al.[40]

In this study of the parametric receiving array, only the cumulative contribution to the second-order pressure was considered. The second-order effects at the pump and at the receiver were ignored. Since the parametric receiver offers potential usefulness as a low frequency narrowbeam receiver, additional analysis of these local pressure terms is recommended since these terms could reduce the directivity of the parametric receiving array. The effects of noise at the side band frequency has not been considered in the present study. Side band noise will be generated by the electronics associated with both the pump and receiver. Furthermore, side band noise will be generated if the direct or reflected acoustic path length from the pump to the receiver varies with time. The amplitude of this side band noise needs to be determined under the actual conditions in which the parametric receiving array is considered for use.

The effects of inhomogeneities on the water medium likewise needs to be considered. Inhomogeneities in the region between the pump and receiver could reduce the amplitude of the desired side band pressure and also degrade the beam pattern of the parametric receiving array.

It is hoped that this study has laid a firm foundation for the understanding of the parametric receiving array with various pump and receiver transducers. Likewise, it is hoped that this work has shed some light on the problem of sound scattered by sound.

APPENDIX A

TWO-DIMENSIONAL STATIONARY PHASE SOLUTION OF THE SCATTERING INTEGRAL

In Section D of Chapter III, we had the Green's function integral solution

$$p = \frac{j(\omega_1 \pm \omega_2)^2}{4\Pi\rho_o c_o^4}\left(1 + \frac{B}{2A}\right) P_{11} P_{12}$$

$$\cdot \iiint_{\infty}^{\infty} \frac{1}{\sqrt{x^2 + y^2 + z^2}\sqrt{(x_o - x)^2 + y^2 + z^2}} \tag{A.1}$$

$$\cdot \exp\left[-\alpha_1\sqrt{x^2 + y^2 + z^2} - \alpha_2(x_o \cos\theta + y \sin\theta) - \alpha_{\pm}\sqrt{(x_o - x)^2 + y^2 + z^2}\right]$$

$$\cdot \exp\left[j(k_1\sqrt{x^2 + y^2 + z^2} \pm k_2 x \cos\theta \pm k_2 y \sin\theta)\right]$$

$$\cdot \exp\left[j(k_1 \pm k_2)\sqrt{(x_o - x)^2 + y^2 + z^2} - j(\omega_1 \pm \omega_2)t\right] dxdydz \quad .$$

For a given value of x, the integrand amplitude term is a slowly varying function of y and z. On the other hand, the phase varies rapidly with y and z. These properties of the integrand suggest the use of the method of stationary phase.

Double integrals of the form[59,67,68]

$$\iint S(y,z)e^{jkf(y,z)}\, dydz \tag{A.2}$$

can be evaluated by the method of stationary phase provided S(y,z) is a slowly varying function of y and z, and kf(y,z) is a rapidly varying function of y and z. The contributions to the asymtotic expansion of the

integral come only from regions in the vicinity of certain critical points. There are three types of critical points. The critical points of interest for our problem are those within the domain of integration at which

$$\frac{\partial f}{\partial y} = \frac{\partial f}{\partial z} = 0 \tag{A.3}$$

Then near the critical point (y_o, z_o) we can expand $f(y,z)$ in a Taylor series such that we have

$$f(y,z) = f(y_o,z_o) + \frac{1}{2}\alpha(y-y_o)^2 + \frac{1}{2}\beta(z-z_o)^2 + \gamma(y-y_o)(z-z_o) \quad , \tag{A.4}$$

where

$$\alpha = \frac{\partial^2 f}{\partial y^2} \quad , \quad \beta = \frac{\partial^2 f}{\partial z^2} \quad , \quad \gamma = \frac{\partial^2 f}{\partial y \partial z} \quad ,$$

the partial derivatives all being evaluated at (y_o, z_o). We can now choose new variables of integration such that

$$f(y,z) = f(y_o,z_o) + \frac{1}{2}\alpha^2 + \frac{1}{2}\beta\eta^2 + \gamma\xi\eta \tag{A.5}$$

The asymtotic approximation to Equation (A.1) is

$$S(y_o,z_o)e^{ikf(y_o,z_o)} \cdot \int_{\infty}^{\infty}\int_{\infty}^{\infty} \exp\left[\frac{1}{2} ik(\alpha^2+\beta\eta^2+2\gamma\eta\xi)\right] d\xi d\eta = \tag{A.6}$$

$$\frac{2\Pi j\ \sigma\ S(y_o,z_o)e^{ikf(y_o,z_o)}}{\sqrt{|\alpha\beta-\gamma^2|}\ k}$$

where the positive root is taken and σ=+1, -1, or -j according to whether

$$\alpha\beta>\gamma^2, \alpha>0 \ ; \quad \alpha\beta>\gamma^2, \alpha<0 \ ; \tag{A.7}$$

or $\alpha\beta<\gamma^2$.

Then the functions f(y,z) and S(y,z) are given by

$$f(y,z) = \frac{k_1}{k_1 \pm k_2}\sqrt{x^2 + y^2 + z^2} \pm \frac{k_2 y}{k_1 \pm k_2}\sin\theta + \sqrt{(x_o - x)^2 + y^2 + z^2}$$

and

$$S(y,z) = \frac{j(\omega_1 \pm \omega_2)^2\,(1+B/2A)\,P_{11}P_{12}}{4\Pi\rho_o c_o^4} \tag{A.8}$$

$$\cdot \exp\Big[-\alpha_2(x\cos\theta + y\sin\theta) - \alpha_1\sqrt{x^2 + y^2 + z^2}$$

$$- \alpha_\pm\sqrt{(x_o - x)^2 + y^2 + z^2} \pm k_2 x\cos\theta\Big] \quad .$$

It can be seen that f(y,z) is a rapidly varying function of y and z while S(y,z) is a slowly varying function of y and z.

To find the critical point, we must find the point at which

$$\frac{\partial f}{\partial y} = \frac{\partial f}{\partial z} = 0 \quad .$$

For the z derivative we have

$$\frac{\partial f}{\partial z} = \frac{\partial\left[\dfrac{k_1}{k_1 \pm k_2}\sqrt{x^2 + y^2 + z^2} \dfrac{\pm k_2 y\sin\theta}{k_1 \pm k_2} + \sqrt{(x_o - x)^2 + y^2 + z^2}\right]}{\partial z} \tag{A.9}$$

$$= \frac{k_1 z}{(k_1 \pm k_2)\sqrt{x^2 + y^2 + z^2}} + 0 + \frac{z}{\sqrt{(x_o - x)^2 + y^2 + z^2}}$$

$$= 0 \text{ if } z = 0$$

and for the y derivative we have

$$\frac{\partial f}{\partial y} = \frac{k_1 y}{k_1 \pm k_2\sqrt{x^2 + y^2 + z^2}} \pm \frac{k_2}{k_1 \pm k_2}\sin\theta + \frac{y}{\sqrt{(x_o - x)^2 + y^2 + z^2}} = 0 \; . \tag{A.10}$$

Solving for y we have

$$y \cong \frac{\mp k_2 \sin\theta}{\frac{k_1}{(k_1 \pm k_2)x} + \frac{1}{(x_o - x)}} = \mp \frac{k_2 \sin\theta\,(x)\,(x_o - x)}{k_1(x_o - x) + x(k_1 \pm k_2)} = \mp \frac{k_2 \sin\theta\,(x)\,(x_o - x)}{k_1(x_o) \pm k_2\,(x_o - x)} \tag{A.11}$$

We now can obtain the values of the second derivatives of f evaluated at the critical point. We have

$$\frac{\partial f}{\partial y \partial z} = - \frac{k_1 yz}{(k_1 \pm k_2)\,(x^2+y^2+z^2)^{3/2}} - \frac{2yz}{((x_o - x)^2+y^2+z^2)^{3/2}} = 0 \text{ for } z = 0, \tag{A.12}$$

$$\begin{aligned} \frac{\partial^2 f}{\partial y^2} &= - \frac{k_1 y^2}{(k_1 \pm k_2)\,(x^2+y^2+z^2)^{3/2}} - \frac{y^2}{((x_o - x)^2+y^2+z^2)^{3/2}} \\ &\quad + \frac{k_1}{(k_1 \pm k_2)\;x^2 + y^2 + z^2} + \frac{1}{\sqrt{(x_o - x)^2 + y^2 + z^2}} \\ &\cong \frac{k_1}{(k_1 \pm k_2)\,x} + \frac{1}{(x_o - x)} \quad \text{at } (y_o, z_o) \quad . \end{aligned} \tag{A.13}$$

Also we have

$$\begin{aligned} \frac{\partial^2 f}{\partial z^2} &= \frac{k_1}{(k_1 \pm k_2)\sqrt{x^2 + y^2 + z^2}} + \frac{1}{\sqrt{(x_o - x)^2 + y^2 + z^2}} \\ &\quad \cdot \frac{-k_1 z^2}{(k_1 \pm k_2)\,(x^2+y^2+z^2)^{3/2}} - \frac{z^2}{\sqrt{(x_o - x)^2 + y^2 + z^2}} \\ &\cong \frac{k_1}{k_1 \pm k_2\,x} + \frac{1}{(x_o - x)} \quad \text{at } (y_o, z_o) \quad . \end{aligned} \tag{A.14}$$

The function f evaluated at the critical point is

$$f(y_o,z_o) = \frac{k_1}{k_1 \pm k_2}\sqrt{x^2 + y_o^2} \pm \frac{k_2}{k_1 \pm k_2} y \sin\theta + \sqrt{(x-x_o)^2 + y^2}$$

$$\cong \frac{k_1}{k_1 \pm k_2} x + x_o - x + \frac{1}{2}\frac{k_2^2 x^2 \sin^2\theta}{(k_1 \pm k_2)^2 x_o} - \frac{1}{2}\frac{k_2^2 x \sin^2\theta}{(k_1 \pm k_2)^2} \qquad (A.15)$$

The second-order pressure is then

$$P_s = \frac{-(\omega_1 \pm \omega_2)^2 (1+B/2A) P_{11} P_{12} (2\Pi)}{4\Pi\rho_o c_o^4} \qquad (A.16)$$

$$\cdot \int_{-\infty}^{\infty} \frac{\exp\left\{-\alpha_1 x - \alpha_2 (x\cos\theta) - \alpha_{\pm}(x-x_o)\right\}}{x(x_o-x)\left[\frac{k_1}{(k_1 \pm k_2)x} + 1/x_o - x\right](k_1 \pm k_2)}$$

$$\cdot \exp\left[j\, k_1 x + (k_1 \pm k_2)\, x_o - k_1 x \mp k_2 x \pm k_2 x \cos\theta\right]$$

$$\cdot \exp\left[\frac{k_2^2 \sin\theta}{(k_1 \pm k_2)}\left(\frac{x^2}{x_o} - x\right) - j(\omega_{\pm} t)\right] dx \qquad (A.17)$$

APPENDIX B
TRANSDUCERS

The five transducers used for the parametric receiving array experiments are described in the following paragraphs.

A. Rectangular Transducer

This transducer was constructed using elements for use as a narrowbeam receiver. In our experiments, the transducer was used as both a projector and as a hydrophone. The dimensions of the active face were 17.5 in. by 2.75 in. The end elements are reduced in amplitude to provide amplitude shading to reduce the side lobes. Beam patterns for this transducer at 90 kHz are shown in Fig. 6.4.

B. Small Standard Transducer

This is a U. S. Navy standard TR-129 transducer designed as a small general purpose transducer. It was constructed of small ceramic cylinders designed to radiate omnidirectionally in the plane perpendicular to the axis of the cylinders. The cylinders have a circumferential resonance at 90 kHz.

C. Standard Hydrophone

This is a U. S. Navy standard TR-225 transducer developed by the Naval Research Laboratory, Underwater Sound Reference Division, Orlando, Florida. It is constructed with lead-zirconate/lead-titanate cylinders. Like the previous transducer, it is designed to be omnidirectional in the plane perpendicular to the axis of the cylinders. The transducer has a nominal freefield open circuit voltage sensitivity of -203 dB re 1 V/1 μPa and has a flat response (±1 dB) over the frequency range from 1 to 20 kHz.

D. Transducer

This transducer was used as a pump and as a receiver. This transducer was constructed at the Applied Research Laboratories and has been assigned the number DRL-123. It was constructed as a mosaic of Channelite 5400 ceramic cubes. The transducer had a resonant frequency of 90 kHz.

E. Hydrophone

This is a U. S. Navy standard H-23 hydrophone developed and supplied by the Naval Research Laboratory, Underwater Sound Reference Division, Orlando, Florida. It was constructed using eight lithium sulfate crystals. It has a follower amplifier to drive the cable. It has a nominal sensitivity of -188 dB re 1 V/1 μPa at 90 kHz.

APPENDIX C
COMPUTER PROGRAM

A computer program was written by J. Kodosky and W. C. Nowlin for use on the Hewlett-Packard 9830 Programmable Calculator in BASIC language. The program was designed to plot θ or θ' beam patterns using Equations (4.14), (4.17), (4.29), or (4.32). The choice of equation calculated was input selectable. The program allowed rotation of the zero for θ and θ' for alignment of the theoretical beam patterns with the experimental beam pattern. The amplitude of the theoretical beam pattern could also be adjusted to account for amplitude variations in the experimental results.

```
5 COM I0,B0,B1,A0,A1,A2,S0,N0,T,T2,S,F1,F2,R9,L,B$[201]
10 DSCALE 0,10,0,10,10,10
15 DIM J$[80]
20 FOR J=1 TO 30
25 DISP "ARRAY LENGTH=";
30 INPUT L
35 DISP "A1=";
40 INPUT A1
45 DISP "A2=";
50 INPUT A2
55 DISP "THETA (0) OR THETA' (1) PATTERN";
60 INPUT T
65 DISP "FIXED ANGLE (DEG)=";
70 INPUT T2
75 DISP "SUM (1) OR DIFF (-1) PATTERN";
80 INPUT S
85 DISP "F1=(MHZ)";
90 INPUT F1
95 DISP "F2 (MHZ)=";
100 INPUT F2
105 DISP "SWEEP (DEC)=";
110 INPUT S0
115 DISP "INCREMENT (DEG)=";
120 INPUT A0
125 DISP "LONG (1) OR SHORT (0) CALC";
130 INPUT N0
135 DISP "NORM RE 1.0=";
140 INPUT Z0
145 DISP "PUMP (0) OR RECEIVER (1)";
150 INPUT R9
155 T2=T2*PI/180
160 S0=S0*PI/180
165 A0=A0*PI/180
170 STORE  DATA J+1
175 DISP "ANY MORE";
180 INPUT J$
185 IF J$="NO" THEN 195
190 NEXT J
195 J0=J
200 FOR J=1 TO J0
205 LOAD  DATA J+1
210 T9=0
```

```
215 IF T <= 1 THEN 230
220 T=T9=1
225 T2=T2-A0-S0
230 T1=-S0-A0+2*T9*(A0+S0)
235 FØR I=1 TØ 2*S0/A0+1
240 BEEP
245 T1=T1+A0*(1-2*T9)
250 T2=T2+T9*A0
255 M=PI*F2*L*(1-CØS(T*T2-T*T1+T1))/4.92
260 C=PI*F2*(SIN(T1+T2+R9*2*(T2*(T-1)-T*T1))-SIN(T*T1-T*T2+T2))/4.92
265 A=PI*2*F1*SIN(T*T1-T*T2+T2)/4.92-S*C
270 A3=A1
275 Y0=X0=0
280 Y1=(A+C)*(M-A3*C)
285 Y2=(A+C)*(M+A3*C)
290 Y3=(A-C)*(M-A3*C)
295 Y4=(A-C)*(M+A3*C)
300 C5=C6=1
305 IF ABS(Y1)<ABS(Y4) THEN 330
310 Y5=Y1
315 Y1=Y4
320 Y4=Y5
325 C5=-1
330 IF ABS(Y2)<ABS(Y3) THEN 355
335 Y5=Y2
340 Y2=Y3
345 Y3=Y5
350 C6=-1
355 IF C#0 AND N0#0 THEN 420
360 Y=1
365 IF A=0 THEN 375
370 Y=SIN(A*A3)/(A*A3)
375 IF M=0 THEN 385
380 Y=Y*SIN(M)/M
385 Y=Y*A3/A1+Y0
390 IF A2=0 ØR A3=A2 THEN 410
395 Y0=Y
400 A3=A2
405 GØTØ 280
410 B[I]=ABS(Y)/(1+A2/A1)
415 CØTØ 480
420 IF Y1*Y2=0 THEN 470
```

```
425 Y=FNZ(1)+FNZ(2)+Y0+LØG(ABS(Y2*Y3/(Y1*Y4)))
430 X=-FNS(Y1/C)+FNS(Y2/C)+FNS(Y3/C)-FNS(Y4/C)+X0
435 IF A2=0 ØR A3=A2 THEN 460
440 Y0=Y
445 X0=X
450 A3=A2
455 GØTØ 280
460 B[I]=SQR(X^2+Y^2)/((A1+A2)*4*ABS(C))
465 GØTØ 480
470 Y=LØG(ABS(Y3*(M+C6*A3*C)/(Y4*(M-C5*A3*C))))+FNZ(2)+Y0
475 GØTØ 430
480 NEXT I
485 B1=B[1]
490 FØR I=2 TØ 2*S0/A0+1
495 IF B[I]<B1 THEN 510
500 B1=B[I]
505 I0=I
510 NEXT I
515 IF B0>0 THEN 525
520 B0=B1
525 T=T+T9
530 T2=T2-T9*S0
535 STØRE  DATA J+1
540 NEXT J
545 LINK 1,5,5
550 STØP
555 DEF FNZ(P)
560 IF P=2 THEN 590
565 Z8=ABS(Y1/C)
570 IF Z8<ABS(Y2/C) THEN 580
575 Z8=ABS(Y2/C)
580 Y5=-FNC(Y1/C)+FNC(Y2/C)
585 RETURN Y5
590 Z8=ABS(Y3/C)
595 IF Z8<ABS(Y4/C) THEN 605
600 Z8=ABS(Y4/C)
605 Y5=FNC(Y3/C)-FNC(Y4/C)
610 RETURN Y5
615 STØP
620 DEF FNC(P)
625 Z=P
630 Z9=1
```

```
635 GØSUB 665
640 RETURN Z0
645 STØP
650 DEF FNS(P)
655 Z=P
660 Z8=ABS(Z)
665 Z9=0
670 GØSUB 685
675 RETURN Z0
680 STØP
685 Z0=0
690 IF Z8>2 THEN 845
695 IF Z9=0 THEN 710
700 IF Z9=1 THEN 745
705 RETURN
710 Z5=-SGN(Z)
715 IF Z5 <= 0 THEN 730
720 GØSUB 925
725 Z=ABS(Z)
730 Z3=-1
735 IF Z#0 THEN 790
740 RETURN
745 IF Z>0 THEN 780
750 IF Z<0 THEN 770
755 Z0=-1E+99
760 Z9=10
765 RETURN
770 Z=-Z
775 Z9=11
780 Z3=0
785 Z5=1
790 FØR Z1=1 TØ 100
795 Z3=Z3+2
800 Z2=(-1)^Z1*Z^Z3/Z3
805 FØR Z4=2 TØ Z3
810 Z2=Z2/Z4
815 NEXT Z4
820 IF ABS(Z2)<1E-08*ABS(Z0) THEN 835
825 Z0=Z0+Z2
830 NEXT Z1
835 Z0=Z5*Z0
840 RETURN
```

```
845 IF Z9=0 THEN 860
850 IF Z9=1 THEN 860
855 RETURN
860 Z5=SGN(Z)
865 Z=Z5*Z
870 Z1=(Z^8+38.027264*Z^6+265.187033*Z^4+335.67732*Z^2+38.102495)/Z
875 Z1=Z1/(Z^8+40.021433*Z^6+322.624911*Z^4+570.23628*Z^2+157.105423)
880 Z2=(Z^8+42.242855*Z^6+302.757865*Z^4+352.018498*Z^2+21.821899)/Z^2
885 Z2=Z2/(Z^8+48.196927*Z^6+482.485984*Z^4+1114.978885*Z^2+449.690326)
890 IF Z9=0 THEN 915
895 IF Z5>0 THEN 905
900 Z9=11
905 Z0=Z1*SIN(Z)-Z2*COS(Z)-LOG(Z)
910 RETURN
915 Z0=(PI/2-Z1*COS(Z)-Z2*SIN(Z))*Z5
920 IF Z5>0 THEN 930
925 Z9=5
930 RETURN
```

```
5 COM I0,B0,B1,A0,A1,A2,S0,N0,T,T2,S,F1,F2,R9,L,BS[201]
10 Q0=1
15 Q1=Q2=Q3=0
20 DSCALE 0,10,0,10,10,10
25 DØFFST 0,-11
30 DPLOT 0,0,1
35 DISP "HIT CONTINUE WHEN READY";
40 STOP
45 FOR J=1 TO J0
50 LOAD  DATA J+1
55 GOSUB 490
60 IF R0=0 THEN 145
65 DØFFST 4.25,2.5
70 DPLØT 0,0,1
75 DPLØT 0,8,2
80 T1=-S0-A0
85 I9=3
90 FØR I=1 TØ 2*S0/A0+1
95 T1=T1+A0
100 P0=4*LGT(B[I]/30)+H
105 IF P0 >= 0 THEN 115
110 P0=0
115 IF P0>8.5 THEN 130
120 DPLØT 180*T1/(3*PI),P0,I9
125 I9=2
130 NEXT I
135 DØFFST -4.25,-2.5
140 GØTØ 220
145 DØFFST 4.25,5.5
150 DPLØT 0,0,1
155 DPLØT 0,5,2
160 T1=-S0-A0
165 I9=3
170 FØR I=1 TØ 2*S0/A0+1
175 T1=T1+A0
180 P0=2*LGT(B[I]/30)+H
185 IF P0 >= 0 THEN 195
190 P0=0
195 IF P0>5.5 THEN 210
200 DPLØT P0*SIN(T1+R1),P0*CØS(T1+R1),I9
205 I9=2
210 NEXT I
```

```
215 DATFST -4.25,-5.5
220 DPLØT 0.5,2.12,3
225 IF T=0 THEN 255
230 IF T>1 THEN 245
235 DLABEL (*,0.08,0.12,0)"THETA PRIME PATTERN";
240 GØTØ 260
245 DLABEL (*,0.08,0.12,0)"SØUND FIELD PATTERN";
250 GØTØ 260
255 DLABEL (*,0.08,0.12,0)"THETA PATTERN";
260 DPLØT 3.75,2.12,3
265 DLABEL (270)F1,F2
270 FØRMAT "PUMP=",F5.0," KHZ   SIGNAL=",F4.0," KHZ"
275 DLABEL (280)A1,A2
280 FØRMAT "A=",F6.3," FT      A'=",F6.3," FT"
285 DLABEL (290)20*LGT(B1/B0),(-S0-A0+10*A0)*180/PI
290 FØRMAT "MAX IS ",F5.1," DB  AT ",F6.2," DEG"
295 IF R1=0 THEN 310
300 DLABEL (305)R1*180/PI
305 FØRMAT "PLØT SHIFTED ",F6.2," DEG"
310 DPLØT 0.5,1.94,3
315 IF S=1 THEN 330
320 DLABEL (*)"DIFFERENCE FREQUENCY"
325 GØTØ 335
330 DLABEL (*)"SUM FREQUENCY"
335 IF T >= 1 THEN 350
340 DLABEL (*)"THETA PRIME="T2*180/PI"DEG"
345 GØTØ 355
350 DLABEL (*)"THETA="T2*180/PI"DEG"
355 IF N0=0 THEN 370
360 DLABEL (*)"LØNG CALCULATIØN"
365 GØTØ 375
370 DLABEL (*)"SHØRT CALCULATIØN"
375 IF R9=0 THEN 385
380 DLABEL (*)"RECEIVER"
385 DLABEL (*)"ARRAY LENGTH="L
390 DISP "TYPE IN ANY ADDITIØNAL LABEL    ";
395 INPUT J$
400 IF J$="STØP" THEN 415
405 DLABEL (*)J$
410 GØTØ 390
415 DISP "RE-PLØT";
420 INPUT J
```

```
425 IF J$="YES" THEN 460
430 IF J$="NØ" THEN 440
435 GØTØ 415
440 DØFFST 3.5,0
445 DPLØT 0,0,1
450 NEXT J
455 STØP
460 Q1=Q2=Q3=Q0=0
465 GØSUB 490
470 DØFFST 3.5,0
475 DPLØT 0,0,1
480 GØTØ 60
485 STØP
490 IF Q1=1 THEN 540
495 DISP "R ØR P PLØT";
500 INPUT J$
505 IF J$[1,1]#"F" THEN 520
510 Q1=1
515 J$[1]=J$[2]
520 IF J$="R" THEN 535
525 R0=0
530 GØTØ 540
535 R0=1
540 IF Q2=1 THEN 575
545 DISP "PLØT HEIGHT (INCHES)=";
550 INPUT J$
555 IF J$[1,1]#"F" THEN 570
560 Q2=1
565 J$[1]=J$[2]
570 H=VAL(J$)
575 IF Q3=1 THEN 610
580 DISP "PLØT RØTATED (DEG)=";
585 INPUT J$
590 IF J$[1,1]#"F" THEN 605
595 Q3=1
600 J$[1]=J$[2]
605 R1=VAL(J$)*PI/180
610 IF Q0=1 THEN 645
615 DISP "NØRM (RE 1.0)=";
620 INPUT J$
625 IF J$[1,1]#"F" THEN 640
630 Q0=1
```

```
635 J$[1]=J$[2]
640 B0=VAL(J$)
645 RETURN
```

BIBLIOGRAPHY

1. G. G. Stokes, "On a Difficulty in the Theory of Sound," Phil. Mag., (Series 3), 33, 349-356 (1848).

2. G. B. Airy, Phil. Mag. (Series 3), 34, 401-405 (1849).

3. R. D. Fay, "Plane Sound Waves of Finite Amplitude," J. Acoust. Soc. Am. 3, 222 (1931).

4. A. L. Thuras, R. T. Jenkins, and H. T. O'Neil, "Extraneous Frequencies Generated in Air Carrying Intense Sound Waves," J. Acoust. Soc. Am. 6, 173-180 (1935).

5. Ghiron E. Fubini, "Anomalies in the Propagation of Waves of Great Amplitude," Alta Frequenze 4, 530 (1935).

6. D. T. Blackstock, "Propagation of Plane Sound Waves of Finite Amplitude in Nondissipative Fluids," J. Acoust. Soc. Am. 34, 9-30 (1962).

7. D. T. Blackstock, "Thermoviscous Attenuation of Plane, Periodic, Finite-Amplitude Sound Waves," J. Acoust. Soc. Am. 36, 534 (1964).

8. D. T. Blackstock, "On Plane, Spherical, and Cylindrical Sound Waves of Finite Amplitude in Lossless Fluids," J. Acoust. Soc. Am. 36, 217-219(L) (1964).

9. D. C. Miller, An Anecdotal History of the Science of Sound to the Beginning of the 20th Century (The MacMillan Co., Inc., London, 1935).

10. H. L. F. Helmholtz, On the Sensations of Tone, (trans. by A. J. Ellis) (Longmans, London, 1875).

11. Rücker and Edser, Phil. Mag. (5) Vol. XXXIX (1895).

12. J. W. S. Rayleigh, "The Theory of Sound," 2nd Edition (Dover Press, New York, 1945).

13. H. Lamb, The Dynamical Theory of Sound, (Arnold, London, 1910). Also (Dover Press, New York, 1960).

14. Y. Rocard, Sur la propagation des ondes sonores d'amplitude finie, Comptes rendus 196, 161 (1933).

15. U. Ingard, and D. C. Pridmore-Brown, "Scattering of Sound by Sound," J. Acoust. Soc. Am. 28, 367-369 (1956).

16. P. J. Westervelt, "Scattering of Sound by Sound," J. Acoust. Soc. Am. 48, 199-203 (1957).

17. P. J. Westervelt, "Scattering of Sound by Sound," J. Acoust. Soc. Am. 29, 934-935 (1957).

18. P. J. Westervelt, "Parametric Acoustic Array," J. Acoust. Soc. Am. 35, 535 (1963).

19. J. L. S. Bellin, and R. T. Beyer, "Experimental Investigation of an End-Fire Array," J. Acoust. Soc. Am. 34, 1051 (1962).

20. H. Hobaek, "Experimental Investigation of an Acoustical End Fired Array," J. Sound Vib. 6, 460 (1967).

21. V. A. Zverev, and A. I. Kalachev, "Measurements of the Scattering of Sound by Sound in the Superposition of Parallel Beams," Soviet Phys. Acoust. 14, 173 (1968). (English Translation).

22. T. G. Muir, and J. E. Blue, "Experiments on the Acoustic Modulation of Large Amplitude Waves," J. Acoust. Soc. Am. 46, 227 (1969).

23. B. V. Smith, "An Experimental Study of a Parametric End-Fire Array," J. Sound Vib. 14, 7-21 (1971).

24. H. M. Merklinger, "High Intensity Effects in the Non-Linear Acoustic Parametric Array," A Thesis submitted to the Faculty of Science, University of Birmingham.

25. J. J. Truchard, and J. G. Willette, "The Receive Calibration of a Large Sonar Array Using a Parametric Transmitting Array," Paper presented at the 84th Meeting of the Acoustical Society of America (November 1972).

26. R. H. Mellen, D. G. Browning, and W. L. Konrad, "Parametric Sonar Transmitting Array Measurements," Paper N2, presented at the 80th Meeting of the Acoustical Society of America, Houston, Texas (November 1970).

27. T. G. Muir, "An Analysis of the Parametric Acoustic Array for Spherical Wave Fields," Applied Research Laboratories Technical Report No. 71-1 (ARL-TR-71-1) May 1971 (AD 723241). (Dissertation).

28. T. G. Muir, and J. G. Willette, "Parametric Acoustic Transmitting Arrays," J. Acoust. Soc. Am. 52(5) Part 2 (November 1972).

29. H. O. Berktay, "Parametric Amplification by the Use of Acoustic Non-Linearities and Some Possible Applications," J. Sound Vib. 2, 462 (1965).

30. H. O. Berktay, "A Study of the Traveling-Wave Parametric Amplification Mechanism in Nonlinear Acoustics," J. Sound Vib. 5, 155-163 (1967).

31. S. Tjötta, "Some Nonlinear Effects in Sound Fields," J. Sound Vib. 6(2), 255 (1967).

32. H. O. Berktay, and C. A. Al-Temimi, "Virtual Arrays for Underwater Reception," J. Sound Vib. 9, 295-307 (1969).

33. H. O. Berktay, and C. A. Al-Temimi, "Up-Converter Parametric Amplifications of Acoustic Waves in Liquids," J. Sound Vib. 13(1), 67-88 (1970).

34. G. R. Barnard, J. G. Willette, J. J. Truchard, and J. A. Shooter, "Parametric Acoustic Receiving Array," J. Acoust. Soc. Am. 52(2), 1437-1441 (1972).

35. W. L. Konrad, R. H. Mellen, and M. B. Moffett, "Parametric Sonar Receiving Experiments," Naval Underwater Systems Center, Technical Memorandum PA4-304-71 (9 December 1971).

36. H. O. Berktay, and T. G. Muir, "Arrays of Parametric Receiving Arrays," J. Acoust. Soc. Am. 50, 1056-1061 (1973).

37. V. A. Zverev, and A. I. Kalachev, "Modulation of Sound by Sound in the Intersection of Sound Waves," Soviet Phys. Acoust. 16, 204-208 (1970).

38. Hikaru Date, and Yoshiroi Tozuka, "Parametric Directional Microphone," The 6th International Congress on Acoustics, Tokyo, Japan (1968).

39. H. O. Berktay, and J. A. Shooter, "Parametric Receivers with Spherically Spreading Pump Waves," J. Acoust. Soc. Am. 54(4), 1056-1061 (1973).

40. P. H. Rogers, A. L. Van Buren, A. O. Williams, Jr., and J. M. Barber, "Parametric Detection of Low-Frequency Acoustic Waves in the Near-field of an Arbitrary Directional Pump Transducer (to be published).

41. C. A. Al-Temimi, "Effects of Acoustic Shadows on the Performance of a Parametric Receiving System," J. Sound Vib. 13, 415-433 (1970).

42. D. G. Tucker, "The Exploitation of Non-Linearity in Underwater Acoustics," J. Sound Vib. 2(4), 429-434 (1965).

43. N. S. Stepanov, "A Parametric Effect in Acoustics," Soviet Phys. Acoust. 8, 104-105 (1962).

44. L. A. Ostrovskii, and I. A. Papilova, "Nonlinear Mode Interaction and Parametric Amplification in Acoustic Waveguides," Soviet Phys. Acoust. 19, 45 (1973) (English translation).

45. H. O. Berktay, and C. A. Al-Temimi, "Scattering of Sound by Sound," J. Acoust. Soc. Am. 50(1), 181-187 (1971).

46. J. L. S. Bellin, and R. T. Beyer, "Scattering of Sound by Sound," J. Acoust. Soc. Am. 32(3), 339-341 (1960).

47. C. A. Al-Temimi, "Interaction Between Two Sound Fields Propagating in Different Directions," J. Sound Vib. 8(1), 44-63 (1968).

48. J. P. Jones, and R. T. Beyer, "Scattering of Sound by Sound," J. Acoust. Soc. Am. 48, 398-402 (1970).

49. L. W. Dean (III), "Interactions Between Sound Waves," J. Acoust. Soc. Am. 43(8), 1039-1044 (1962).

50. V. Lauvstad, and S. Tjötta, "Problem of Sound Scattered by Sound," J. Acoust. Soc. Am. 34, 1045-1050 (1962).

51. P. J. Westervelt, "Absorption of Sound by Sound" (to be published).

52. C. Eckart, "Vortices and Streams Caused by Sound Waves," Phys. Rev. 73, 68-76 (1948).

53. M. J. Lighthill, "On Sound Generated Aerodynamically," Proc. Roy. Soc. A211, 564-587 (1952).

54. M. J. Lighthill, "On Sound Generated Aerodynamically," Proc. Roy. Soc. A222, 1-32 (1954).

55. F. V. Hunt, "Notes on the Exact Equations Governing the Propagation of Sound in Fluids," J. Acoust. Soc. Am. 27, 1019-1039 (1955).

56. R. Kline, "On the Acoustic Wave Equation in the Presence of Virtual Mass Sources and Force Densities," Department of Physics, Brown University, Ph.D. Thesis (1966).

57. P. J. Westervelt, "Virtual Sources in the Presence of Real Sources," Nonlinear Acoustics, Proceedings of the 1969 Symposium held at Applied Research Laboratories, The University of Texas at Austin (1970).

58. P. M. Morse, and U. Ingard, Theoretical Acoustics (McGraw-Hill Book Co., New York, 1968).

59. M. Born, and E. Wolf, Principles of Optics, 3rd Edition (Pergamon Press, Oxford, 1965).

60. H. Stenzel, Leitfaden Zur Berechnung Von Schallvorgangen (Springer, Berlin) (1939).

61. A. Freedman, "Soundfields of a Rectangular Piston," J. Acoust. Soc. Am. 32, 2 (1960).

62. E. J. Skudrzyk, The Foundations of Acoustics (Springer-Verlay, New York-Wein, 1971).

63. G. N. Watson, A Treatise on the Theory of Bessel Functions (University Press, Cambridge, 1952).

64. R. J. Bobber, Underwater Electroacoustics Measurements, Naval Research Laboratory, Underwater Sound Reference Division, Orlando, Florida, Government Printing Office (1970).

65. H. O. Berktay, and J. A. Shooter, "Nearfield Effects in End-Fire Line Arrays," J. Acoust. Soc. Am. 53(2), 550-556 (1965).

66. A. B. Coppens, R. T. Beyer, M. B. Seiden, J. Donohue, F. Gulpsin, R. H. Hodson, and C. Townsend, "Parameter of Nonlinearity in Fluids. II," J. Acoust. Soc. Am. 38, 797-804 (1965).

67. J. Focke, Asymptotische Entwicklungen mittels der Methode der Stationären Phase, Ber. Verhandl. Sächs. Akad. Wiss. Leipzig, 101, 1-48 (1954).

68. M. Kline, and I. W. Kay, Electromagnetic Theory and Geometrical Optics, (New York Interscience Publishers, 1965) Chpt. XII.